A FULL-SCALE AND MODEL STUDY OF CONVECTIVE HEAT TRANSFER FROM ROOF MOUNTED FLAT-PLATE SOLAR COLLECTORS

VOLUME ONE

INTRODUCTION, THEORY AND LITERATURE REVIEW

A thesis submitted to the Faculty of Architectural Studies, University of Sheffield, for the degree of Doctor of Philosophy

PETER S. CHARLESWORTH

Department of Building Science
University of Sheffield,
SHEFFIELD
S10 2TN

MARCH 1986.

TO MY MOTHER AND FATHER -

FOR THEIR CONTINUOUS SUPPORT

THROUGHOUT MY ACADEMIC CAREER

"The cooling of a hot body exposed to the air is effected partly by radiation, and partly by conduction from the surface of the body to the air in contact with it. The activity of surface conduction is greatly quickened by wind, which continually brings fresh portions of cold air into contact with the surface, in place of those which have been heated".

- Deschanels' Natural Philosophy

1888

SUMMARY

This study is concerned with the convective heat transfer, due to the action of the wind, from the upper surface of roof mounted flat plate solar collectors. The ability to predict the quantity of heat transferred from a collector, in this manner, is necessary in order to facilitate the evaluation of the overall efficiency of a collector panel.

Previous methods of determining this convection coefficient have generally relied upon extrapolations of small scale wind tunnel results to full-scale values. The validity of these methods is questionable, and it was found that there was a lack of full-scale data relating to the convection coefficient from the upper surface of a flat-plate collector. It was also found that no systematic attempt to relate model results to full-scale values had been made.

Full-scale experiments have been performed to evaluate the convective heat transfer coefficient, h, from the upper surface of a roof mounted flat plate. The convection coefficient was found to be dependent upon the wind speed as measured above the roof ridge line, V_{6R}, and to some extent upon the direction of the prevailing wind, Θ. Relationships between h and V_{6R} are presented, as are relationships between h and V_H (the wind speed measured at the mid-panel height) and h and V_{10} (the meteorological 10m wind speed).

Small scale wind tunnel experiments were also performed. This was in order to assess the potential of using wind tunnel model results to predict accurately full-scale convective heat losses. These experiments showed some qualitative agreement with the full-scale tests. However, extrapolation of these model results to full-scale values rendered heat transfer coefficients in excess of those found in the full-scale work. Therefore the use of previously derived full-scale results from wind tunnel studies must be treated with caution. It is suggested that the full-scale results, presented here, represent a more satisfactory means of evaluating the convective heat transfer from the upper surface of roof mounted flat plate solar collectors.

ACKNOWLEDGEMENTS

A thesis such as this could never be completed without the help and understanding of many people. I should like, first and foremost, to thank my supervisor Dr. Stephen Sharples for his invaluable help and advice during my time spent in the Department of Building Science.

The technical staff of the department suffered my, often capricious, requests for materials, models and site visits, etc. with humerous stoicism. I am therefore deeply indepted to Messrs. Roy Webster, Peter Williams, Lol Wildgoose and Roger Grace not only for their technical ability but also for making the department a pleasant place to spend one's time.

I also owe great thanks to Hazel Hall for turning my rather untidy original drafts of this thesis into a final form of excellent quality.

The SERC provided the funding for this research and I am grateful for its support.

Finally I should like to thank the Crewe crew for putting up with my ever changing moods especially in the writing up stage of the research.

CONTENTS

VOLUME ONE

CHAPTER ONE

INTRODUCTION

CHAPTER TWO

FUNDAMENTAL CONVECTIVE HEAT TRANSFER

CHAPTER THREE

REVIEW OF EXPERIMENTAL ANALYSIS OF FORCED CONVECTIVE HEAT TRANSFER

VOLUME TWO

CHAPTER FOUR

EXPERIMENTAL DETAILS OF THE FULL-SCALE MEASUREMENTS OF THE CONVECTIVE HEAT TRANSFER FROM A LARGE FLAT PLATE IN THE NATURAL ENVIRONMENT

CHAPTER FIVE

EXPERIMENTAL RESULTS OF THE FULL-SCALE MEASUREMENTS OF FORCED CONVECTIVE HEAT TRANSFER AT THE NORTON SITE

CHAPTER SIX

DETAILS OF THE WIND TUNNEL MODEL EXPERIMENTS

CHAPTER SEVEN

RESULTS OF WIND TUNNEL MODEL EXPERIMENTS

CHAPTER EIGHT

CONCLUSION

CHAPTER ONE

INTRODUCTION

1.1 Domestic Energy Consumption within the United Kingdom - The Importance of Hot Water Supplies

The consumers of all the primary energy produced within the UK can be placed into four broad categories. (Digest of UK Energy Statistics [1984])*. These are industry, transport, domestic and others. Table 1.1 shows the energy consumption of each of these four groups - expressed as a percentage of the total energy consumed within the UK during 1983.

Table 1.1 Energy Consumption within the UK during 1983

(Digest of UK Energy Statistics [1984])

Category of User	Percentage of Total Energy Consumed (Total Energy = 1.58×10^{12} kWh)
Industry	31%
Transport	26%
Domestic	29%
Others	14%

*References are given in alphabetical order at the end of this thesis.

Therefore, domestic sources consume almost one third of the primary energy produced within the UK. The major use of energy in a dwelling is to provide a comfortable thermal and visual environment for its inhabitants. This is done via the heating and lighting systems within the building. Estimates of the end use of delivered energy to the UK domestic sector are given in Table 1.2.

Table 1.2 End Use of the Domestic Energy Consumed within the UK

(Department of Energy (Energy Paper No. 39 [1979])

End Use	Percentage of Total Domestic Consumption
Space Heating	50-60%
Water Heating	15-20%
Cooking	10%
Lighting TV, etc.	10%

It can be assumed that the figures presented in Table 1.2, still give a reasonably accurate picture of the distribution of energy consumption in dwellings. Therefore in 1983 approximately 9×10^{10} Kwh of energy was expended in the UK domestic sector for the heating of hot water supplies.

The two main fuels currently used for water heating in the UK are natural gas and electricity. From 1970 to about 1974 the cost of these two fuels, to the consumer, remained reasonably constant. Since then, however, gas and electricity prices have increased rapidly. If, for example, 1974 prices are taken as a standard index of 100, then in

1983 the indices of gas and electricity prices were 374 and 492 respectively. These increases are high, even when compared to the general inflation rate over the same period. A general index encompassing all consumer purchases would be approximately 250.

These price increases, coupled with a general awareness of the finite nature of fossil fuels led to a greater interest in harnessing the natural environment to produce useful energy. This interest gave rise to the examination of such topics as the use of wind or waves to generate electrical power, and the utilisation of solar energy for heating domestic hot water supplies. Because of the vast amounts of energy used for water heating in dwellings, the economic implications of research in this field are, potentially enormous.

1.2 The Heating of Domestic Hot Water Supplies using Solar Energy

The installation and use of solar systems for the heating of domestic hot water is discussed in detail by many standard texts (e.g. Szokolay [1975], Wozniak [1979], Duffie and Beckman [1980]). Basically, the only novel feature of a solar hot water system is the solar collector (or panel) itself. This is the device which collects the radiant energy from the sun and converts it into a usable form. Figure 1.1* shows a cross-sectional view of a typical solar panel used for domestic hot water heating. The panel comprises of five main components:

*Figures relating to each chapter may be found at the end of each chapter.

(i) Absorber Plate

This is a blackened or otherwise treated metal plate (usually copper or aluminium); its function is to convert the incident solar radiation to heat. The process by which the radiant energy is converted to heat is a complex one involving photon absorption, acceleration and multiple collisions of electrons, with the actual mechanism of the process being dependent upon the absorber plate material. However, the end result is the same in each case i.e. an increase in the temperature of the absorber plate.

(ii) Fluid Passages

These passages allow the flow of a fluid through the absorber plate. Heat generated on the collector plate is transferred to the fluid which is therefore refered to as the "heat transfer fluid". In a "direct system", i.e. one in which the fluid which passes through the collector is ultimately drawn from the hot taps in the house, then the heat transfer fluid is invariably water. For "indirect" systems; (i.e. those in which the fluid which flows through the collector, transfers its heat to the hot water supply via another heat transfer device) a fluid other than water may be used. Oil-based fluids are often employed in these systems, these fluids have better heat transfer properties than water and are less likely to corrode the absorber plate.

(iii) Transparent Covers

Although some collectors are produced without these covers most designs incorporate 1 to 3 transparent covers over the absorber plate. Ideally the covers, usually made of glass or perspex, should be totally transparent to the shortwave radiation from the sun but opaque to the long wave radiation transmitted from the heated absorber plate, thus maximising the heat gained from the incident solar radiation. The covers also insulate the absorber plate from the cooler ambient air and provide weather proofing.

(iv) Insulation

The insulation material placed behind the absorber plate provides mechanical support for the whole collector panel and reduces heat loss from the back of the absorber plate. This back loss is often further reduced by placing a thin sheet of reflective metal foil between the plate and the insulation. Glass fibre and polystyrene foam are typical materials used for insulation.

(v) Enclosing Frame

This frame, usually constructed from weatherproofed metal or wood, holds the other components of the panel in their correct positions and protects the absorber plate and back insulation from the weather. The frame may also contain insulation material in order to minimise the edge loss from the collector.

Solar collectors may be placed anywhere they are effectively exposed to the incident radiation from the sun. In urban areas they are usually positioned on dwelling roofs. In new buildings the collector panels are often directly incorporated in the roof structure, the upper surface of the collector being flush with the rest of the roof. However, for existing buildings the collector panels are usually installed directly onto the roof pitch so that they stand proud of the roof surface. (Recommended methods for this type of mounting are given by Wozniak [1979]). This type of mounting is often refered to as retro-fit mounting.

Whilst roof mounting gives a solar panel excellent exposure to incident radiation, this position gives little shelter from the elements which will deteriorate its performance, e.g. wind, rain, etc. A measure of the performance of a solar panel under operating conditions is its "efficiency factor".

1.3 The Efficiency Factor of Flat Plate Solar Collectors

The simplest model of solar panel performance is one which neglects thermal capacitance effects and was first proposed by Hottel and Whiller [1958]. In this case the energy balance of the panel can be expressed as:

$$Q = A[I\tau\alpha - U_L(T_p - T_a)] \quad ,W \qquad (1.1)$$

where Q = Useful energy delivered by the panel, W

A = Area of panel, m^2

I = Incident solar radiation, Wm^{-2}

τ = Solar radiation transmission coefficient of the glass cover(s)

α = Solar absorption coefficient of the absorber plate

U_L = Overall heat loss coefficient for the panel, $Wm^{-2}K^{-1}$

T_p = The mean temperature of the absorber plate, K

T_a = The ambient air temperature, K.

The efficiency, η, of the panel can then be defined as:

$$\eta = \frac{\text{useful energy delivered by panel}}{\text{total energy falling on the panel}} \times 100\% \qquad (1.2)$$

hence:

$$\eta = \tau\alpha - U_L \frac{(T_p - T_a)}{I} \times 100\% \qquad (1.3)$$

If all the parameters on the right hand side of equation 1.3 are known then the efficiency of a solar collector can be predicted. The transmission coefficient of the glass covers, τ, and the solar absorptance, α, of the metal plate are both measurable quantities, as is the incoming radiation I. The mean plate temperature, T_p, however, is difficult to define and is often replaced by the temperature of the fluid at the inlet of the collector panel, T_i. If this is the case then equation 1.3 becomes:

$$\eta = F\tau\alpha - F U_L \frac{(T_i - T_a)}{I} \times 100\% \qquad (1.4)$$

where F is a modification factor which is a function of the fluid flow rate through the collector and the overall loss coefficient of the collector U_L (Klein [1975]). Therefore, the determination of U_L is of primary importance in the determination of the efficiency of flat plate solar collectors.

1.4 The Overall Heat Loss Coefficient of a Flat Plate Solar Collectors

The determination of the value of the overall loss coefficient, U_L, of a solar panel is difficult, due to the fact that it is a function of the operating conditions of the collector. U_L may be considered to be the sum of U_T, U_B and U_E (Klein [1975]) where:

U_T = The "Top Loss Coefficient", $Wm^{-2}K^{-1}$. This relates to the energy lost from the upper surface of the absorber plate by convection and radiation.

U_B = The "Back Loss Coefficient", $Wm^{-2}K^{-1}$. This relates to the energy lost from the back of the absorber plate, through the insulation material, by conduction.

U_E = The "Edge Loss Coefficient", $Wm^{-2}K^{-1}$. This relates to the energy lost from the sides of the collector, through its frame, by conduction.

U_B and U_E can be approximated from a knowledge of the thermal properties of the insulation material and the frame. (Duffie and Beckman [1980]). These losses are usually considered to be small, but not negligible, as compared to the top loss U_T.

It is the calculation of this top loss coefficient which presents a problem of some difficulty. The energy lost from the upper surface of the plate results from radiative and convective exchanges between the top of the absorber plate and the inner-most glass cover (if one is present) or between the absorber plate and the atmosphere in the case of an uncovered collector. This energy is transmitted through the glass covers and the air layers between them and finally from the top surface of the collector to the atmosphere.

Initial attempts to obtain values for U_T (e.g. Hottel and Woertz [1942]) involved the solving of a set of N-1 non linear equations, where N is the number of covers over the absorber plate, i.e.

$$U_T - \frac{\sigma A(T_p^4 - T_{gi}^4) - h_{c,1} A(T_p - T_{gi})}{1/\varepsilon_p + 1/\varepsilon_g - 1} = 0 \qquad (1.5a)$$

•

•

$$U_T - \frac{-\sigma A(T_{g,i-1}^4 - T_{gi}^4) - h_{c,i} A(T_{g,i-1} - T_{gi})}{2/\varepsilon_g - 1} = 0 \quad (1.5b)$$

$$U_T - \varepsilon_g \sigma A(T_{g,N}^4 - T_s^4) - h_w A(T_{g,N} - T_a) = 0 \quad (1.5c)$$

where σ = Stefan Boltzmann Constant, 5.67×10^{-8} Wm^2K^{-4}

T_{gi} = Temperature of the ith glass cover, K

$h_{c,i}$ = Convection coefficient between parallel plates $Wm^{-2}K^{-1}$

h_w = Convection coefficient due to the wind, from the upper most glass cover, $Wm^{-2}K^{-1}$

T_s = Effective temperature of the sky, K

ε_p = Thermal emissivity of plate

ε_g = Thermal emissivity of glass cover

The solution of these equations requires an iterative process which is necessarily time consuming, even with the aid of modern computers. Recognising this problem Hottel and Woertz proposed an empirical relation which could be easily solved to determine U_T. This equation has been modified by several authors to take into account recent experimental evidence especially concerning the convection coefficient through air layers between parallel plates.

The most recent of these empirical equations is due to Agarwal and Larson [1981] who proposed the following formula for U_T.

$$U_T = \left[\frac{N}{\frac{C}{T_p}\left[\frac{T_p - T_a}{N + f}\right]^{0.33}} + \frac{1}{h_w} \right]^{-1}$$

$$+ \frac{\sigma (T_p + T_a)(T_p^2 + T_a^2)}{\left[\varepsilon_p + 0.05N(1 - \varepsilon_p)\right]^{-1} + \frac{2N + f - 1}{\varepsilon_g} - N}, \quad Wm^{-1}K^{-1} \qquad (1.6)$$

where $f = (1 - 0.04h_w + 0.005h_w^2)(1 + 0.091N)$

$C = 250[1 - 0.0044(S - 90)]$

and N = Number of transparent covers

h_w = The convection heat transfer coefficient of the upper surface of the top glass cover - due to the wind, $Wm^{-2}K^{-1}$

σ = The Stefan Boltzmann constant, 5.67×10^{-8}, $Wm^{-2}K^{-4}$

ε_p = Thermal emissivity of the absorber plate

ε_g = Thermal emissivity of the cover plates

S = Collector tilt angle as measured from the horizontal

The f factor in the above expression was later amended by Agarwal and Larson [1983] to

$$f = (1 + 0.04\ h_w + 0.0005\ h_w^2)(1 + 0.091N) \qquad (1.7)$$

However, in the light of a recent personal communication with V.K. Agarwal (Texas Tech. University, Lubbock, Texas, USA) the correct form of the f factor should be

$$f = (1 - 0.04\ h_w + 0.0005\ h_w^2)(1 + 0.091N) \qquad (1.8)$$

As can be seen from equation 1.6 the value of U_T is dependent upon several parameters, which themselves may be inter-related. General trends, i.e. of increase or decrease in the value of U_T with these parameters, are not immediately obvious from equation 1.6. However, a closer examination of this formulation for U_T reveals the following:

(i) U_T increases with increasing mean plate temperature, T_p.

(ii) U_T increases with increasing air temperature, T_a, although not as rapidly as with plate temperature

(iii) U_T increases rapidly with increasing plate emittance, ε_p

(iv) U_T increases with increasing wind convection coefficient, h_w

(v) U_T decreases with increasing number of glass covers, N.

(vi) U_T decreases slightly with increasing angle of tilt from the horizontal, S.

Of the six parameters, listed above, which effect U_T, the convective heat transfer coefficient from the upper surface due to the wind, h_w, is the most difficult to evaluate. Klein [1975] gives an expression for h_w in terms of wind speed V. This expression is based on an experimental study of forced convection from a heated copper plate placed flush with the sides of a wind tunnel, due to Jurges [1924]. Such an experimental set up is not representative of a solar collector placed on a three-dimensional building roof in the outdoor environment.

Agawal and Larson [1981] in their paper are also dubious as to the validity of Jurges' work for this application and note later work of Sparrow [1977] which is in conflict with Jurges' results. Sparrow's results were also based on small scale experiments performed in a wind tunnel. Agarwal and Larson offer no formula from which h_w can be derived stating that their equation for U_T is valid for $h_w \leqslant 40$ $Wm^{-2}K^{-1}$ regardless of how this parameter is evaluated.

Duffie and Beckman [1980] also give several parametric equations for the convective heat transfer coefficient from various geometries. However, they arrive at no distinct conclusion as to which should be used for this particular application. If there is no acceptable method for evaluating h_w and the value of h_w has a significant effect on U_T - and therefore on the efficiency of a collector - then there is obviously scope for the examination of methods by which h_w may be accurately evaluated.

1.5 The Effect on Collector Efficiency of the Convective Heat Transfer Coefficient (due to the wind) from the Upper Surface of a Flat Plate Solar Collector

The first step towards examining the effect of h_w on the efficiency of a collector is to assess how the value of h_w effects the top loss coefficient U_T. This can easily be performed by substituting various values of h_w into equation 1.6, keeping the other parameters constant.

Figure 1.2 shows the variation of U_T with h_w (over the range $5 < h < 40$ $Wm^{-2}K^{-1}$) for a collector with a single cover.

This Figure is based on equation 1.6, with the following conditions being assumed.

$S = 45°$

$N = 1$

$\varepsilon_p = 0.95$

$\varepsilon_g = 0.88$

$T_p = 313$ K

$T_a = 283$ K

From Figure 1.2 it can be seen that h_w has a significant effect on U_T for a single cover collector, with U_T increasing from 4 to 7 $Wm^{-2}K^{-1}$ over the range of h_w considered. The effect of h_w on U_T diminishes for multi-cover collectors because the absorber plate is better insulated from the atmosphere.

It will be recalled from Section 1.3 that the efficiency of a collector is given by equation 1.3 i.e.

$$\eta = \tau\alpha - \frac{U_L(T_p - T_a)}{I} \times 100\% \qquad (1.9)$$

U_L is the sum of the top, back and edge loss coefficients. The back and edge loss coefficients are evaluated from a knowledge of the dimensions of the collector and the thermal properties of the insulating material (Duffie and Beckman [1980]). If the following conditions are assumed:

Back insulation thickness = 50mm

Side insulation thickness = 25mm

Collector length = 2m

Collector width = 1m

Collector thickness = 75mm

Insulation conductivity = 0.045 $Wm^{-1}K^{-1}$

Then $U_B = 0.90\ Wm^{-2}K^{-1}$

$U_E = 0.13\ Wm^{-2}K^{-1}$

Therefore $U_L = U_T + 1.2\ Wm^{-2}K^{-1}$ (1.10)

The value of the transmission absorptance product $\tau\alpha$ will vary with the plate and cover materials used and also the angle of inclination of the plate. Dickinson and Cheremisnoff [1980] show that for a single cover collector inclined at 45°, $\tau\alpha = 0.8$. The value of $(T_p - T_a)$ is already known for this case i.e. 313-283 K = 30 K. If $I = 600\ Wm^{-2}K$ (This is a realistic value for I in the UK - for example see Lacy [1977]). Then for a single cover collector with the properties previously described:

$$\eta = (0.8 - 0.07(U_T + 1.2)) \times 100\% \qquad (1.11)$$

Figure 1.3 presents the variation of the efficiency of this collector with the convective heat transfer coefficient due to the wind. From Figure 1.3 it can be seen that, for otherwise constant conditions, the value of the convective heat transfer coefficient from the upper surface of the collector glass cover has a significant effect on the efficiency of the collector. It is therefore essential that reliable design values of h_w are available for either assessing collector performance under operating conditions or for use in computer modelling of solar collector systems.

1.6 The Objectives of this Current Study

In this chapter the potential importance of the use of flat plate solar collectors, in the domestic sector, for the heating of hot water supplies has been discussed. In order to assess accurately this potential it is necessary to be able to evaluate an efficiency factor for a given collector under operating conditions. It has been shown that one parameter which effects the efficiency of solar collectors is the convective heat transfer coefficient from the upper glass cover due to the wind, h_w.

The current methods available for evaluating this parameter are based on small scale wind tunnel studies. These studies are of questionable validity when extrapolated to full-scale collector systems. The aim of this study is to perform full-scale and model measurements which will help validate or repudiate the use of these small scale extrapolations, and provide fundamental results from which design values of h_w can be obtained.

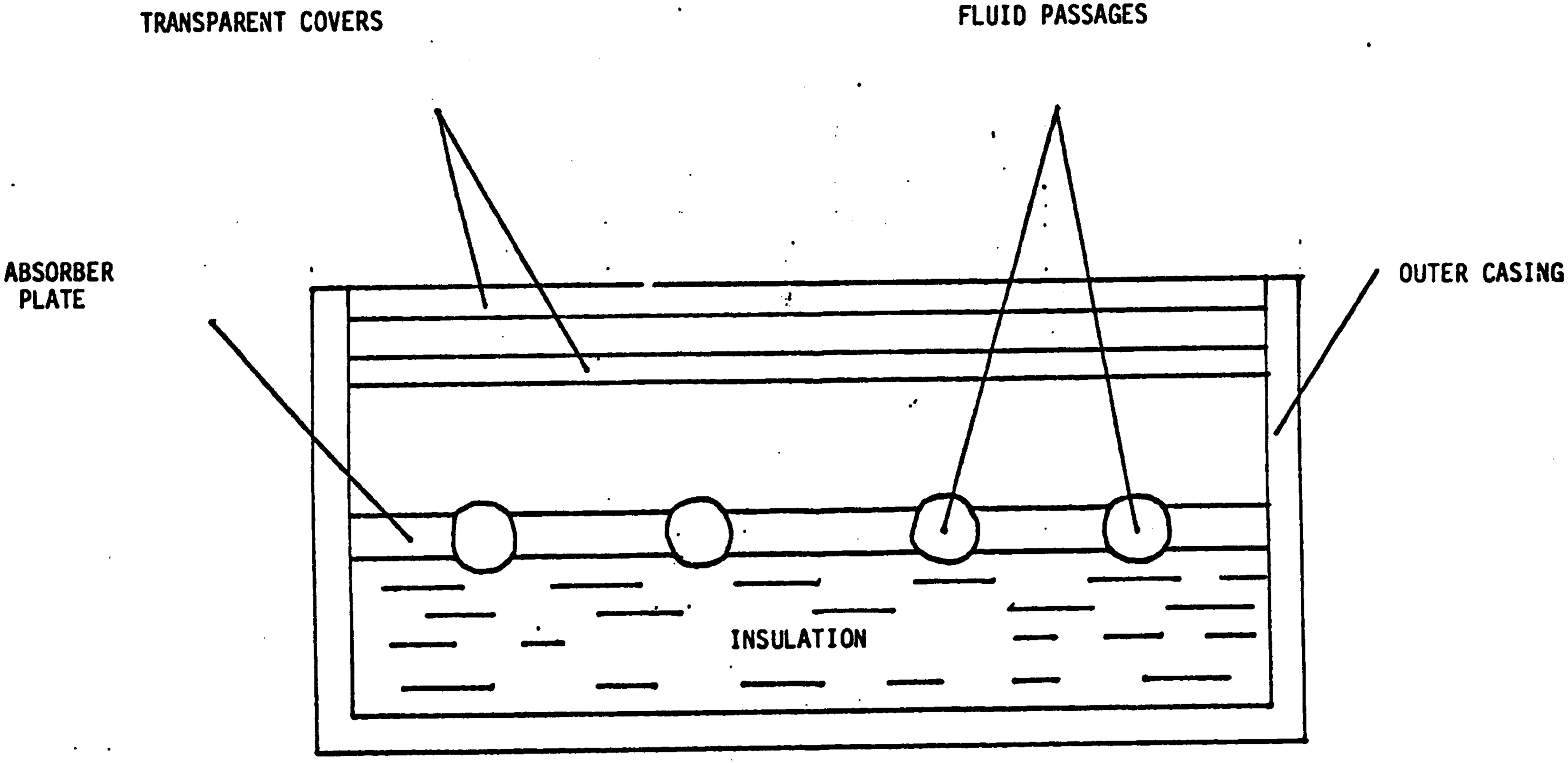

Figure 1.1 **Cross-section of a typical flat plate solar collector**

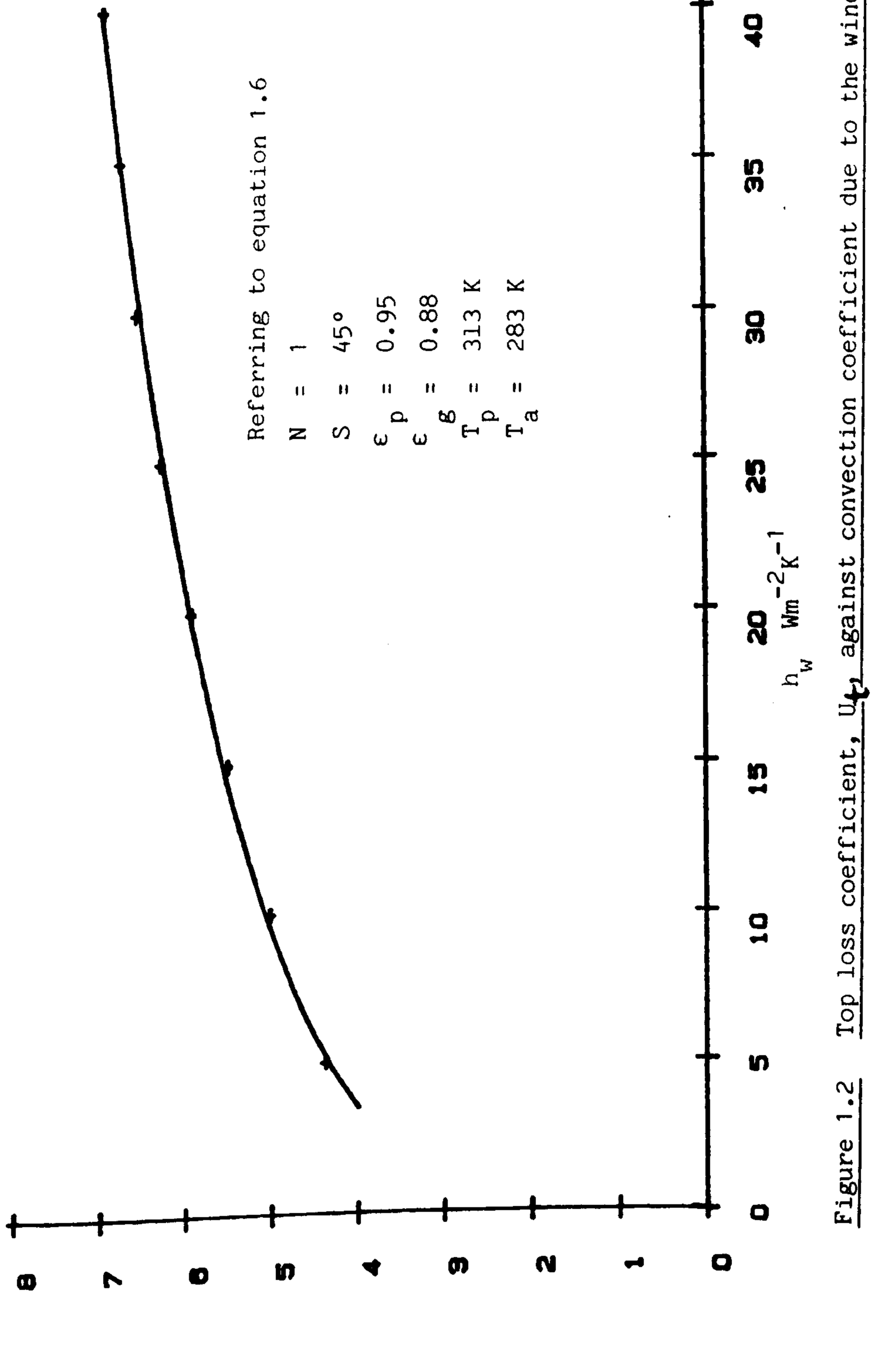

Figure 1.2 Top loss coefficient, U_t, against convection coefficient due to the wind, h_w

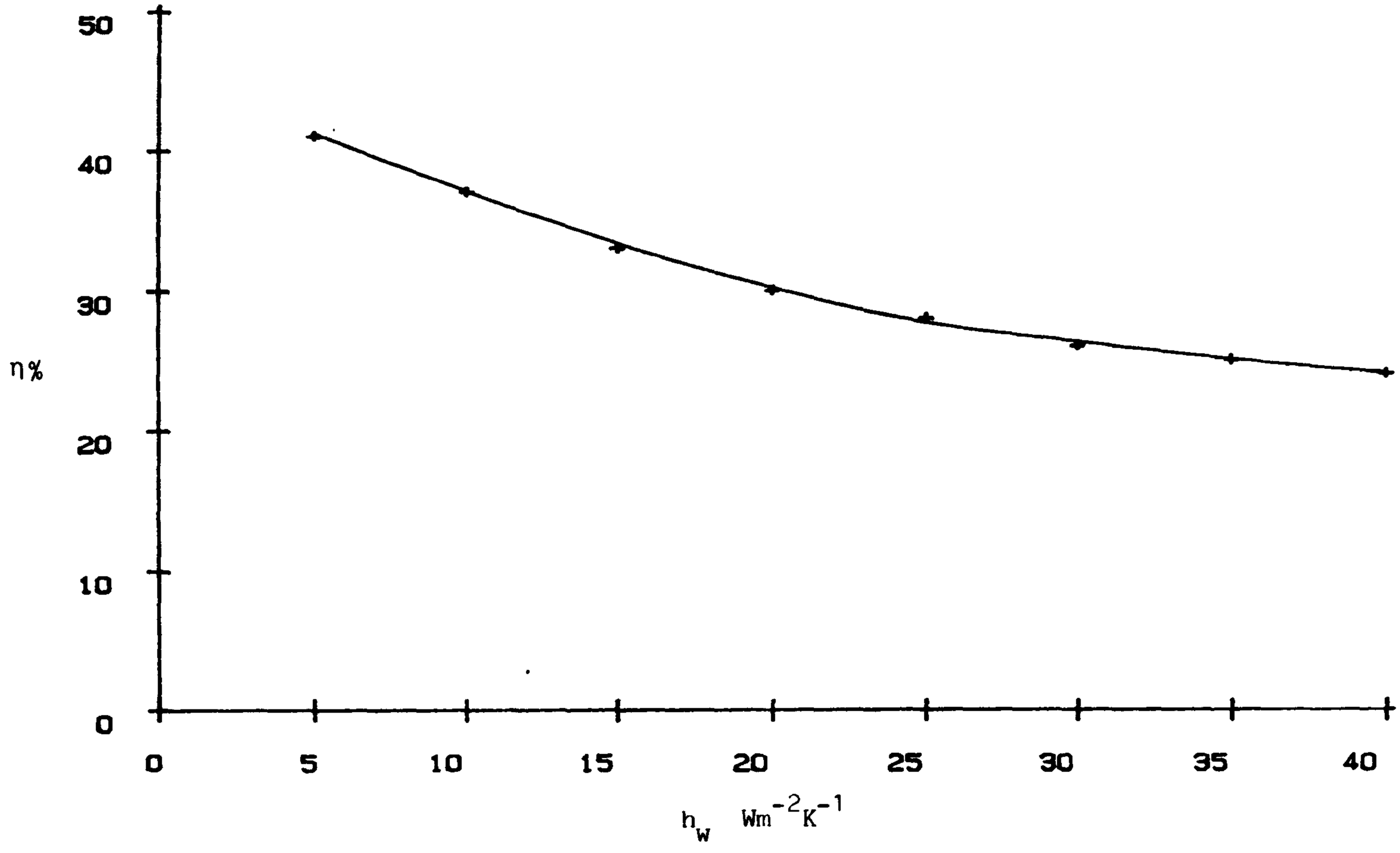

Figure 1.3 Collector efficiency, η%, against convection coefficient due to the wind, h_w (conditions as for Figure 1.2)

PAGE(S) MISSING
NOT AVAILABLE

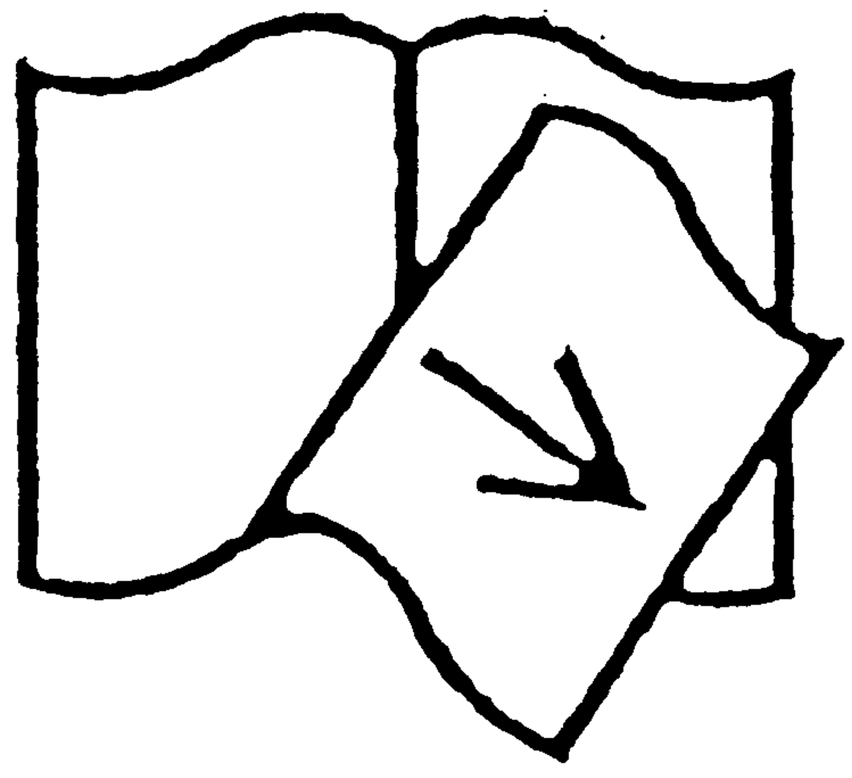

CHAPTER TWO

FUNDAMENTAL CONVECTIVE HEAT TRANSFER

Introduction

Many of the standard texts which deal with the efficiency of flat plate solar collectors (e.g. Meinel and Meinel [1976] or Duffie and Beckman [1980]) give correlations for calculating the wind induced energy losses from the upper surface of the collector. These correlations are often based on theoretical or experimental analysés of heat transfer from flat plates.

The purpose of this chapter is to explain the nature of convective heat transfer from flat plates, describe the parameters which effect it and review the fundamental formulae for predicting the quantity of energy lost from a flat plate by this process. These formulae will then be applied to a flat plate of dimensions similar to those of typical flat plate solar collectors.

2.1 Convective Heat Transfer Regimes

Convective heat transfer occurs when any solid surface is surrounded by a fluid, e.g. air, which is at a different bulk temperature than itself. Because of the practical situation under consideration, only heat transfer from a surface which is at a higher temperature than the surrounding fluid will be considered here. Dixon and Leslie [1979] show that the upper surface of a solar collector reaches temperatures approximately 15-20 K above that of the surrounding air under normal operating conditions. It is of interest to note, however, that warm fluid flowing over a cooler surface will induce conductive heat transfer into the solid surface.

Returning now to a surface immersed in a fluid which is at a lower temperature than itself. Energy will be transferred from this surface in several steps.

Initially heat will flow by conduction from the surface to adjacent particles of fluid. The energy thus transferred will increase the temperature and internal energy of these fluid particles. Then the fluid particles will move to a region of lower temperature in the fluid where they will mix with, and transfer energy to, other fluid particles. They themselves are replaced with particles of lower energy near the surface. Therefore, convection can be considered as the combined action of heat conduction, energy storage and mixing motion, with a flow of both mass (fluid) and energy (heat) away from the surface plane.

Natural or free convection occurs as a result of the temperature difference between the surface and the fluid and the action of gravity on the particles within the fluid. The motion of the fluid, and the transfer of energy, occurs solely due to buoyancy forces produced by density differences induced in the fluid by the temperature gradient within it, i.e. there is a downward flow of the heavier fluid and an upward flow of the lighter, thus there is a net transport of energy away from the surface.

Natural convection occurs under still conditions. If the motion of the fluid is also influenced by the presence of forces resulting from pressure gradients created by external means, e.g. a wind tunnel fan or the natural wind, then the convection regime is said to be forced.

In both convection regimes the energy is stored in the fluid particles and is transported as a result of their mass motion; so the effectiveness of the process depends directly upon the magnitude of the mixing motion. This means that as the motion is effected by external influences in forced convection systems this regime leads to generally higher rates of heat transfer than for natural regimes.

2.2 The Convective Heat Transfer Coefficient

Despite the fact that convection does not depend for its operation merely upon a temperature difference, the net effect is a transport of energy in the direction of a temperature gradient. It is therefore possible to define, from Newton's law of cooling, a gross parameter, the convective heat transfer coefficient h.

The convective heat flow per unit area is given by:

$$q = h(T_s - T_\infty) \quad Wm^{-2} \tag{2.1}$$

where q = Convective heat flow, Wm^{-2}

h = Convective heat transfer coefficient, $Wm^{-2}K^{-1}$

T_s = Surface temperature, K

T_∞ = Fluid temperature at some defined distance from the surface beyond which the fluid temperature does not vary with distance, K.

Equation 2.1 is a definition of h rather than a phenomenological law of convection. The convective heat transfer coefficient is actually a complicated function of the fluid flow, the thermal properties of the medium and the geometry of the system.

At the surface of a solid immersed in a fluid the heat flow at the surface is given by Fourier's conduction law.

$$q = -k_f \left[\frac{\partial T}{\partial n}\right]_s \quad Wm^{-2} \tag{2.2}$$

where k_f = Thermal conductivity of the fluid evaluated at the mean of the surface and fluid temperatures, $Wm^{-1}K^{-1}$.

and $(\frac{\partial T}{\partial n})_s$ = Temperature gradient in fluid, normal to surface, existing at the surface, Km^{-1}

Of course the heat flows in equations 2.1 and 2.2 are identical and so by comparison a definition of h is obtained, thus:

$$h = \frac{k_f}{(T_s - T_\infty)}\left[\frac{\partial T}{\partial n}\right]_s \quad Wm^{-2}K^{-1} \tag{2.3}$$

The actual analytical determination of h from equation 2.3 is highly complex. The major problem is finding the temperature gradient at the surface. Therefore the usual method for calculating h theoretically is to apply simplifying assumptions to the fluid and temperature fields within the system under consideration, such as assuming a uniform linear flow or that the surface is isothermal.

It should be noted at this stage that heat transfer data is often presented in terms of dimensionless groups. A full treatment of the derivation of these groups is given by Kreith [1976] and they will be presented here as and when required. Their importance lies in the fact that they enable data obtained from experiments using different surface lengths or fluid properties, for example, to be correlated - the only constraint being that the systems under consideration are geometrically similar.

The dimensionless form of the convective heat transfer coefficient is found by comparing it to the conduction coefficient of the fluid. Known as the Nusselt number Nu it is defined as:

$$Nu = \frac{hx}{k_f} \tag{2.4}$$

where Nu = Nusselt number

x = A characteristic dimension of the system under consideration, m

The characteristic dimension, x, is derived from the linear dimensions of the plate. For a simple square plate it is the length of the sides. For rectangular plates, (solar collectors often have this geometry) it is usually taken as length of the side parallel to the flow. However, if the plate is to be subjected to flows from any direction the characteristic dimension is calculated as the ratio of 4x the area of the plate to its perimeter (Sparrow [1979]). Hence for a rectangular plate of sides L_1 and L_2 the characteristic dimension x is given by:

$$x = \frac{4\ L_1\ L_2}{2(L_1 + L_2)} \qquad (2.5)$$

It can be seen that for a square plate i.e. $L_1 = L_2$ the above reduces to $x = L_1$.

2.3 Natural Convection

Because we are primarily concerned here with systems in the outdoor environment, pure natural convection occurs very rarely. Studies by Green et al [1980] suggest that the natural flow regime for solar collectors will break down at wind speeds as low as 2 ms^{-1} over the collector surface. Lacy [1977] shows that the annual average hourly mean wind speed in the UK at 10m above ground in open country based on four years data is always in excess of 4 ms^{-1}.

As solar collectors are most often mounted on buildings roofs it can be assumed that they are generally subjected to windloads in excess of 2 ms^{-1}. Hence forced convection will take a primary role in the heat loss from the upper surface. For these reasons natural convection will only be dealt with briefly here.

If the dimensional analysis, as mentioned in Section 2.2, (see Kreith [1976] for a full treatment) is carried out for natural convection it becomes apparent that the Nusselt number is a function of two other dimensionless groups known as the Prandtl number, Pr, and the Grashof number, Gr. These are defined as.

$$Pr = \frac{\nu}{\alpha} \tag{2.6}$$

where ν = kinematic viscosity, m^2s^{-1}

α = Thermal diffusivity of the fluid, m^2s^{-1}

and

$$Gr = \frac{g\beta(T_s - T_a)x^3}{\nu^2} \tag{2.7}$$

where

g = Acceleration due to gravity, ms^{-2}

β = Volume coefficient of expansion of the fluid, K^{-1}.

Physically interpreted, the Prandtl number represents the ratio of the relative rates at which velocity and temperature disturbances are propogated through the fluid. The Grashof number represents the ratio of the bouyancy forces to the viscous forces in the natural convection flow system.

The analytical solution for natural convection about vertical plates is well documented, see for example, Chapman [1974] or Kreith [1976]. Chapman recommends the following equation for calculating the average natural convection coefficient from a vertical surface of length L.

$$Nu_L = C(Gr\ Pr)^m \tag{2.8}$$

where Nu_L = Nusselt number based on the surface length L

and the constants C and m depend upon the product Gr Pr

For $10^4 < (Gr\ Pr) < 10^9$: C = 0.59, m = 0.25

and $10^9 < (Gr\ Pr) < 10^{12}$: C = 0.129, m = 0.33

A corresponding pair of values for C and m are given by McAdams [1954] for horizontal square plates. These are:

$10^5 < (Gr\ Pr) < 2 \times 10^7$: C = 0.54, m = 0.25

$2 \times 10^7 < (Gr\ Pr) < 3 \times 10^{10}$: C = 0.14, m = 0.33

Fussey and Warneford [1976] performed a refined analysis of natural convection from plates of an arbitrary angle of inclination. They present an equation similar in form to 2.8 only for the local Nusselt number, which relates to the heat transfer from a specific point on the surface. However, as the main interest here is the average heat transfer from a surface the most useful correlations found are those given by Holman [1981]. Here simplified equations for natural convection from plates to air at atmospheric pressure are presented.

For a horizontal heated plate facing upwards Holman gives the following equation based on the work of Fujii and Imura [1972]

$$h = 1.32 \left[\frac{T_s - T_\infty}{x}\right]^{0.25} \quad Wm^{-2}K^{-1} \qquad (2.9)$$

where x, the characteristic length of the plate, is given in metres.

So, for example, a plate of dimensions 1 x 2m would have an average natural convective heat transfer coefficient of 2.8 $Wm^{-2}K^{-1}$ if it was at a temperature of 25 K above that of the surrounding air.

For a vertical plate the corresponding equation is

$$h = 1.42 \left[\frac{T_s - T_\infty}{x}\right]^{0.25} \quad Wm^{-2}K^{-1} \qquad (2.10)$$

which, for the plate given above, gives a value of h = 3.0 $Wm^{-2}K^{-1}$ for the average heat transfer coefficient over the plate.

2.4 The Boundary Layer

2.4.1 The hydrodynamic boundary layer

By considering a fluid element flowing over a surface and the various forces acting upon it e.g. viscous forces due to friction, body forces due to gravity, inertia forces due to motion and pressure forces. It is possible by application of Newton's second law of motion, which states,

$$ma = \sum F \qquad (2.11)$$

where m = mass, Kg

a = acceleration, ms^{-2}

$\sum F$ = Summation of the acting forces, Newtons.

to derive equations which describe the fluid motion in the direction of the resultant force, in terms of those various forces. These equations are known as the Navier-Stokes equations, and although of fundamental importance their non-linearity makes them extremely difficult to solve for most practical situations.

The concept of the boundary layer, introduced by Prandtl in 1904, enables the Navier-Stokes equations to be reduced to a form in which they can be solved. This is done, effectively, by assuming that several of the terms in the equations can be treated as negligibly small.

Boundary layer theory for a flat plate essentially divides the flow field into two domains. A thin layer covering the surface of the plate where viscous forces are large and hence the velocity gradient (normal to the surface) is great, and a region outside this layer where the velocity is nearly equal to the free stream value. Beyond the boundary layer thickness, δ - usually taken as the distance away from the plate where the velocity has reached 99% of its free stream value, the flow assumes the properties of an inviscid fluid. δ is assumed to be thin as compared to the plate dimensions. Within the boundary layer there are two distinct sub-divisions of the flow regime. Firstly, developing from the leading edge of the plate there is laminar flow, in which the individual fluid particles travel smoothly along continuous paths. These are parallel to one another and to the flat surface over which they are flowing.

Secondly there is turbulent flow which may be pictured as a random churning action, with macroscopic chunks of fluid moving to and fro in all directions.

In between these two regions there is a transition zone, which for a flat plate with a streamlined leading edge and flow of zero incidence (parallel to the plate) occurs at the critical dimensionless Renolds number Re_{cr}, given by.

$$Re_{cr} = \frac{V_\infty X_{cr}}{\nu} \qquad (2.12)$$

where V_∞ = free stream velocity, ms^{-1}

X_{cr} = distance from leading edge to transition region, m

ν = kinematic viscosity of the fluid, m^2s^{-1}

The value of Re_{cr} is usually taken as 5×10^5 for most analytical purposes. In a practical situation its value depends upon surface roughness conditions and the turbulence intensity of the free stream flow; it may vary between 10^5 and 10^6. The physical concepts of the hydrodynamic boundary layer are shown in Figure 2.1. For air moving over a flat plate at a free stream speed of 10 ms^{-1} and a bulk temperature of 300 K, the transition point X_{cr} would be approximately 0.78m from the leading edge of the plate.

Although the flow in the region beyond $Re_x > Re_{cr}$ in effect becomes fully turbulent, the solid surface damps down the turbulence immediately adjacent to it. This gives rise to a laminar sublayer in the turbulent region, and because these two flow regimes are so different the transition from laminar sublayer to fully turbulent flow cannot occur at a precise point. Instead a buffer region is found to be present through which a gradual change in flow characteristics is found to exist. Figure 2.2 shows these three distinct regions.

2.4.2 The thermal boundary layer

By considering a volume element of the fluid as a thermodynamically "closed system", and applying the first law of thermodynamics , a complex partial differential equation called the energy equation of the fluid can be obtained. As with the Navier-Stokes equations of motion, solution for most practical cases are difficult.

Fortunately, the underlying concepts of the hydrodynamic boundary layer may also be applied to the thermal field. The thermal boundary layer is defined as that region where temperature gradients are present in the flow.

The thermal boundary layer has a thickness δ_T which is not necessarily the same as δ at any given point on the plate. Also the thermal and velocity boundary layers need not start at the same point on the plate as is the case if the plate has an unheated starting length, X_o. This is illustrated in Figure 2.3.

If δ_T can be assumed to be thin relative to the size of the plate then simplifications to the energy equation may be made, enabling it to be solved with less difficulty.

2.5 Laminar Forced Convective Heat Transfer from a Flat Plate

Within the laminar boundary layer i.e. where the influence of viscous forces is felt, the shear stress τ between the fluid layers is assumed to be proportional to the velocity gradient normal to the surface. The defining equation for the viscosity is:

$$\tau = \mu \frac{dV}{dy} \qquad (2.13)$$

where τ = shear stress

μ = dynamic viscosity, kg $m^{-1}s^{-1}$

$\frac{dV}{dy}$ = normal velocity gradient

The physical mechanism of viscosity is one of momentum exchange, with molecules moving from one laminar to another carrying with them a momentum corresponding to the velocity of the flow. Thus there is a net exchange, or flux, of momentum between regions of low velocity to regions of high velocity, creating a force in the direction of flow.

The flux of energy normal to the flat plate in laminar flow is by molecular conduction, so the heat flux q is given by Fourier's Law.

$$q = -k_f \frac{dT}{dy} \qquad (2.14)$$

The first solution to the boundary layer modified versions of the Navier-Stokes equations for laminar flow over a flat plate were obtained by Blasius [1908]. Blasius's solutions for the velocity distribution in the boundary layer were confirmed experimentally by Dhawan [1952].

Once the velocity distribution has been established it is possible to determine the boundary layer thickness δ at any point x along the plate, i.e.:

$$\frac{\delta}{x} = \frac{5.0}{Re_x^{0.5}} \qquad (2.15)$$

Considering the physical situation mentioned in Section 2.4.1, the thickness of the hydrodynamic boundary layer at the transition point i.e. 0.78m along the plate will be 0.0055m which is (as required) thin compared to the length of the plate.

By taking into account considerations of the thermal boundary layer Pohlhausen [1921] solved the energy equation for laminar heat flow from a flat plate. His solution enables the temperature distribution throughout the boundary layer to be found. More importantly, it enables the temperature gradient at the surface to be calculated, thus allowing h to be determined from equation 2.3 directly.

The method of obtaining the exact solutions to the laminar boundary layer equations is given in several standard heat transfer texts, for example Holman [1981].

The analysis shows that the forced convective heat transfer coefficient, in terms of the Nusselt number, is a function of the Reynolds number and the Prandtl number, as defined earlier.

The final result of this analysis is the non-dimensional Pohlhausen equation for laminar local forced convection from a flat plate in parallel flow.

$$Nu_x = 0.332\ Re_x^{0.5}\ Pr^{0.33} \qquad (2.16)$$

This represents the local heat transfer at a distance x from the leading edge of the plate. The average heat transfer from a plate is found by integration over its entire length, say L, so the average Nusselt number Nu_L is given by:

$$Nu_L = 0.664\ Re_L^{0.5}\ Pr^{0.33} \qquad (2.17)$$

Equations 2.16 and 2.17 assume that the plate is heated over its entire length. If however the plate has an unheated starting length x_o - as in Figure 2.3, then the thermal boundary layer will not start to grow until $x = x_o$, and this modifies the local and average Nusselt numbers to

$$Nu_x = 0.332\ Re_x^{0.5} Pr^{0.33}\left[1 - \left(\frac{x_o}{x}\right)^{0.75}\right]^{-0.33} \qquad (2.18)$$

and

$$Nu_L = 0.664\ Re_L^{0.5} Pr^{0.33}\left[1 - \left(\frac{x_o}{L}\right)^{0.75}\right]^{0.67} / \left(1 - \frac{x_o}{L}\right) \qquad (2.19)$$

2.6 Turbulent Forced Convective Heat Transfer from a Flat Plate

2.6.1 The turbulent transport equations

In the fully turbulent region of the turbulent boundary layer (see Figure 2.2) the main mechanism of momentum and heat exchange is one involving macroscopic lumps of fluid moving about in the flow. Here the eddy viscosity, ν_e, and eddy diffusivity, α_e, are considered,

The physical mechanism of heat transfer in turbulent flow is similar to that in laminar. However the main difficulty lies in that the analysis must deal with the eddy properties and these properties vary across the boundary layer.

The eddies arise from the time dependent fluctuation of the velocity, V', on the time independent mean velocity $\overline{V}$. So the actual velocity at any instant, V, is given by $V = \overline{V} + V'$.

These velocity fluctuations produce additional shear stresses in the flow, so that the total apparent shear stress in turbulent flow τ_t may be defined as.

$$\tau_t = \rho(\nu + \nu_e)\frac{\partial \overline{V}_x}{\partial y} \qquad (2.20)$$

where $\overline{V}_x$ = Velocity fluctuations parallel to the plate

ρ = fluid density, $Kg\ m^{-3}$

$\frac{\partial \overline{V}_x}{\partial y}$ = mean velocity gradient

By considering the energy equation for turbulent flow and introducing the eddy diffusivity, α_e, the total apparent heat flux in turbulent flow, q_t, may be defined as

$$q_t = -\rho C_p(\alpha + \alpha_e)\frac{\partial T}{\partial y} \qquad (2.21)$$

where C_p = specific heat of fluid at constant pressure $JKg^{-1}K^{-1}$

α = thermal diffusivity of fluid = $K_f/\rho C_p$, m^2s^{-1}

Comparison of equations 2.20 and 2.21 with equations 2.13 and 2.14 respectively shows the laminar flow type appearance given to the turbulent transport equations by the introduction of the eddy viscosity ν_e and the eddy diffusivity, α_e.

Analysis of turbulent flow must eventually rely on experimental data because there is no completely adequate theory to predict turbulent flow behaviour. A study of the analogy between heat transfer and momentum transfer (first suggested by Reynolds [1874]and modified later by Prandtl and then Von Karman [1939]) for turbulent flow, has realised useful theoretical results. This analogy is studied in the next section.

2.6.2 The analogy between heat and momentum transfer

Reynolds original analogy between heat and momentum transfer was for laminar flow over a flat plate with the fluid having identical values for kinematic viscosity, ν, and thermal diffusivity, α. This means, of course, that the velocity and temperature boundary layer profiles are identical in form. Hence the Prandtl number

$Pr = \nu / \alpha = 1.$

By considering the similarity of these profiles in their dimensionless form and introducing the shear stress at a laminar plane and the heat flux across that plane the mathematical expression of Reynolds analogy for laminar flow is obtained, thus:

$$\frac{\tau_r C_p}{V_\infty - V_{xr}} = \frac{q_r}{T_r - T_\infty} \qquad (2.22)$$

where τ_r = shear stress at plane r in flow

V_{xr} = fluid velocity parallel to layer r at r

q_r = heat flux across laminar plane r

T_r = temperature at laminar plane r

Prandtl modified the Reynolds analogy to deal with turbulent flow by assuming firstly that $\nu_e >> \nu$ and $\alpha_e >> \alpha$ and secondly that in the fully turbulent region $\nu_e = \alpha_e$. Using these assumptions a statement similar to equation 2.17 can be obtained for turbulent flow.

By taking a simple two-stage model of a laminar sublayer and a turbulent main flow, Prandtl obtained the following expression for the local heat transfer from a flat plate in parallel flow.

$$Nu = \frac{0.0292\ Re_x^{0.8}\ Pr}{1 + 2.12\ Re^{-0.1}\ (Pr - 1)} \qquad (2.23)$$

Von Karman further modified the analogy to take into account the buffer layer described in Section 2.3.1 and shown in Figure 2.2. In this zone it is assumed that the eddy coefficients are of the same order of magnitude as their molecular counterparts, and that the shear stress and heat flux are constant throughout the layer. The Von Karman expression for the local Nusselt number is:

$$Nu_x = \frac{0.0292\ Re^{0.8}\ Pr}{1 + 0.855\ Re^{-0.1}[(Pr - 1) + \ln[1 + 0.83(Pr - 1)]]} \qquad (2.24)$$

Colburn [1933] suggests, on the basis of empirical evidence, that the denominators of equations 2.23 and 2.24 are constant for gasses with a value of Pr close to unity. Air at a temperature of 300K has Pr = 0.708. In such cases Johnson and Rubensin [1949] state a simplified equation for the local Nusselt number in turbulent flow, i.e.

$$Nu_x = 0.0292\ Re_x^{0.8}\ Pr^{0.33} \qquad (2.25)$$

Therefore the average Nusselt number for turbulent flow over a plate of length L is found by integration and is given by:

$$Nu_L = 0.036\ Re_L^{0.8}\ Pr^{0.33} \qquad (2.26)$$

A semi-empirical analysis with experimental confirmation by Reynolds et al [1958 (a),(b) and (c)] showed that where an unheated starting length x_o exists, the average Nusselt number is modified to:

$$Nu_L = 0.036\ Re_L^{0.8}\ Pr^{0.33} \left[1 - \left(\frac{x_o}{L}\right)^{0.9}\right]^{0.89} / \left(1 - \frac{x_o}{L}\right) \qquad (2.27)$$

Even in turbulent flow over a plate there will always exist, up to the value of X_{cr} - when Re becomes critical - a laminar flow region near the leading edge of the plate.

So, a more accurate expression for the average turbulent heat transfer from a plate of length L should include a combination of equation 2.17 (integrated between x = 0 and x = x_{cr}) and equation 2.26 (integrated between x = x_{cr} and x = L). Performing these integrations gives the average Nusselt number for a flat plate in turbulent, parallel incompressible flow as

$$Nu_L = 0.036\ Pr^{0.33}(Re_L^{0.8} - Re_{cr}^{0.8} + 18.44\ Re_{cr}^{0.5}) \qquad (2.28)$$

2.7 Application of the Fundamental Forced Convective Heat Transfer Equations

In this section the fundamental equations as developed in Sections 2.5 and 2.6 will be applied to a 2 x 1m heated plate. These dimensions are typical of those of flat plate solar collectors.

It will be assumed that the plate is isothermal and at a temperature of 325 K. The ambient air temperature will be taken as 300 K. As the plate is rectangular the characteristic dimension is calculated from the expression given in Section 2.2, hence x = 1.33m. Air properties, taken at the relevant temperature, were obtained from tables given by Holman [1981].

Table 2.1 shows the dimensional relationships for the different flow regimes. Table 2.2 gives the correction factors which would be applied if various unheated starting lengths were present. Physically, in the case of solar collectors, the unheated starting length could be envisaged as the section of roof surrounding the collector or the frame of the actual collector itself. Finally, Figure 2.4 shows the relationship between the average convection coefficient and the free stream wind speed for each flow regime.

TABLE 2.1 Dimensionless and Dimensional Relationships for Fundamental Forced Convective Heat Transfer

Flow Regime	Dimensionless Relationship	Dimensional relationship for plate with characteristic dimension x = 1.33m
Laminar Equation 2.17	$Nu = 0.664\ Re^{0.5} Pr^{0.33}$	$h = 3.65\ V_\infty^{0.5}$, $Wm^{-2}\ K^{-1}$
Turbulent Equation 2.26	$Nu = 0.036\ Re^{0.8}\ Pr^{0.33}$	$h = 5.96\ V_\infty^{0.8}$, $Wm^{-2}\ K^{-1}$
Combined Equation 2.28	$Nu = 0.036\ Pr^{0.33}(Re_L^{0.8} - Re_{cr}^{0.8} + 18.44\ Re_{cr}^{0.5})$	$h = 2.11\ V_\infty^{0.8} + 2.79\ V_\infty^{0.5}$, $Wm^{-2}K^{-1}$

TABLE 2.2 The Unheated Starting Length Correction Factor for Laminar and Turbulent Flows

Flow Regime	Correction Factor to NU_L	L = 1.33m		
		x_o = 0.1m	x_o = 0.5m	x_o = 1m
Laminar	$[1 - (\frac{x_o}{L})^{0.75}]^{0.67} / (1 - \frac{x_o}{L})$	0.975	1.033	1.334
Turbulent	$[1 - (\frac{x_o}{L})^{0.9}]^{0.89} / (1 - \frac{x_o}{L})$	0.987	0.995	1.074

Conclusion

In this chapter the mechanisms of convection have been examined and the derivation of the fundamental formulae discussed. These formulae have been applied to a flat plate of similar dimensions to a solar collector.

It has been shown that the value of the heat transfer coefficient h depends on the type of flow regime surrounding the surface, the velocity of that flow and some of its physical properties.

Whilst the effect of these parameters is relatively well understood theoretically it is necessary to confirm these predictions with empirical evidence. Experimentally derived values of h for a variety of relevant situations are reported and discussed in the next chapter.

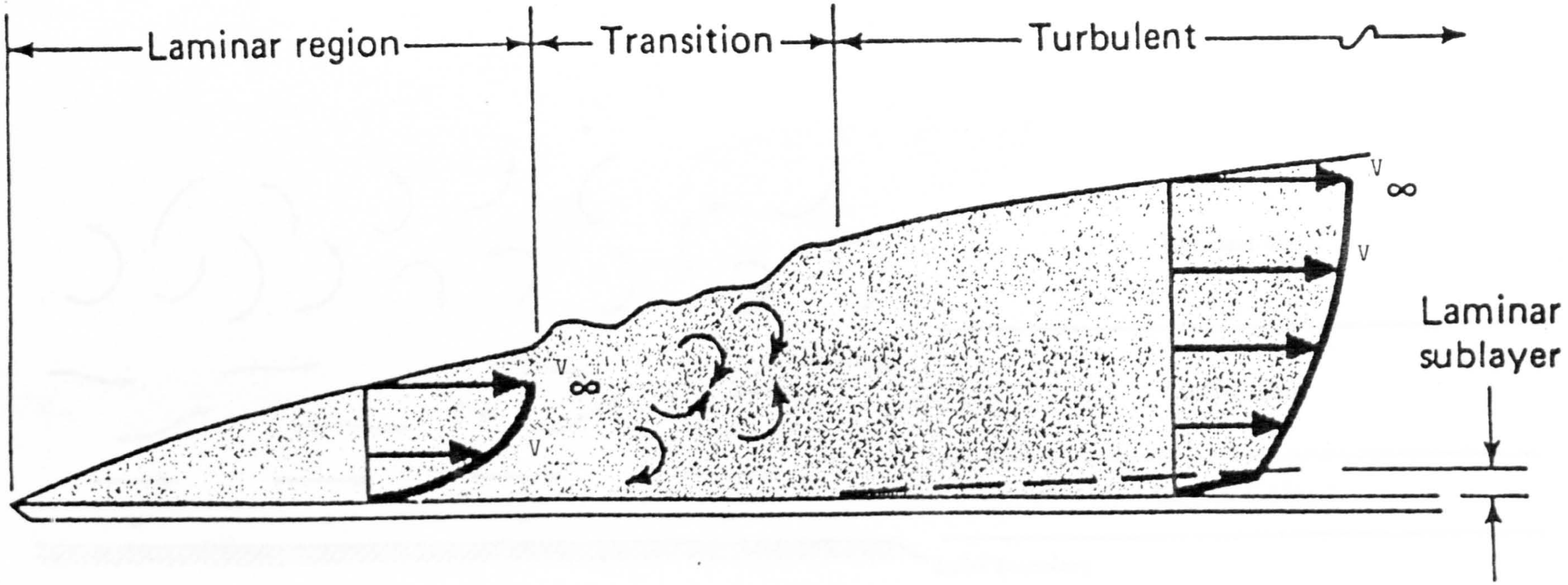

FIGURE 2.1 The Physical Concepts of the Hydrodynamic Boundary Layer

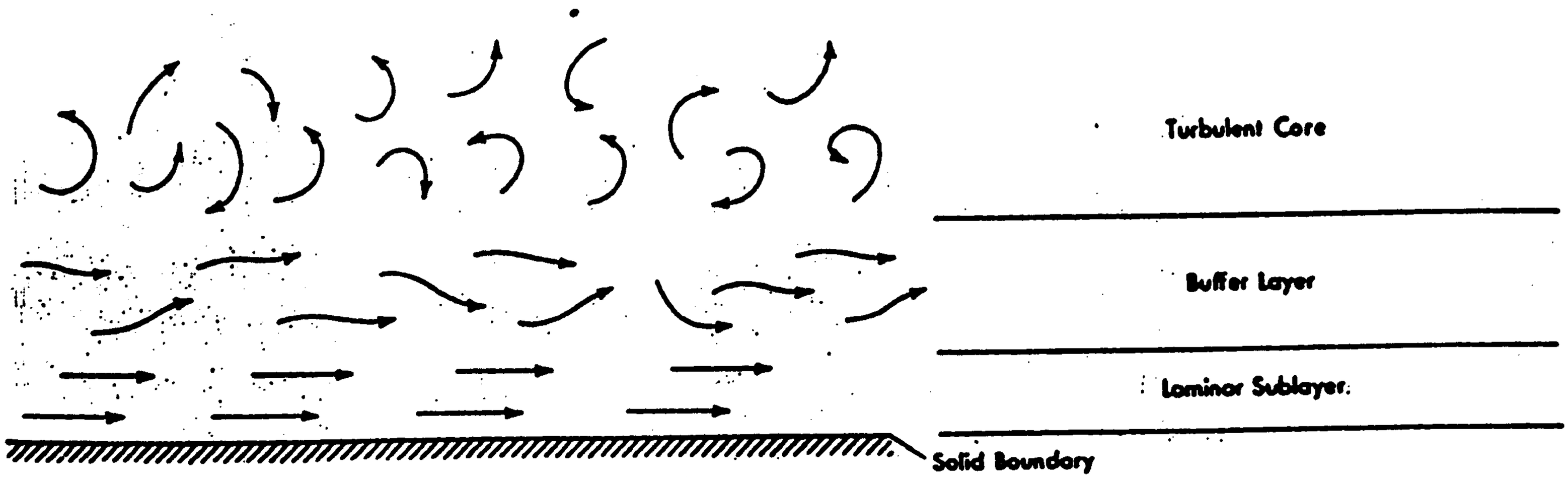

FIGURE 2.2 The Three Regions of the Turbulent Boundary Layer

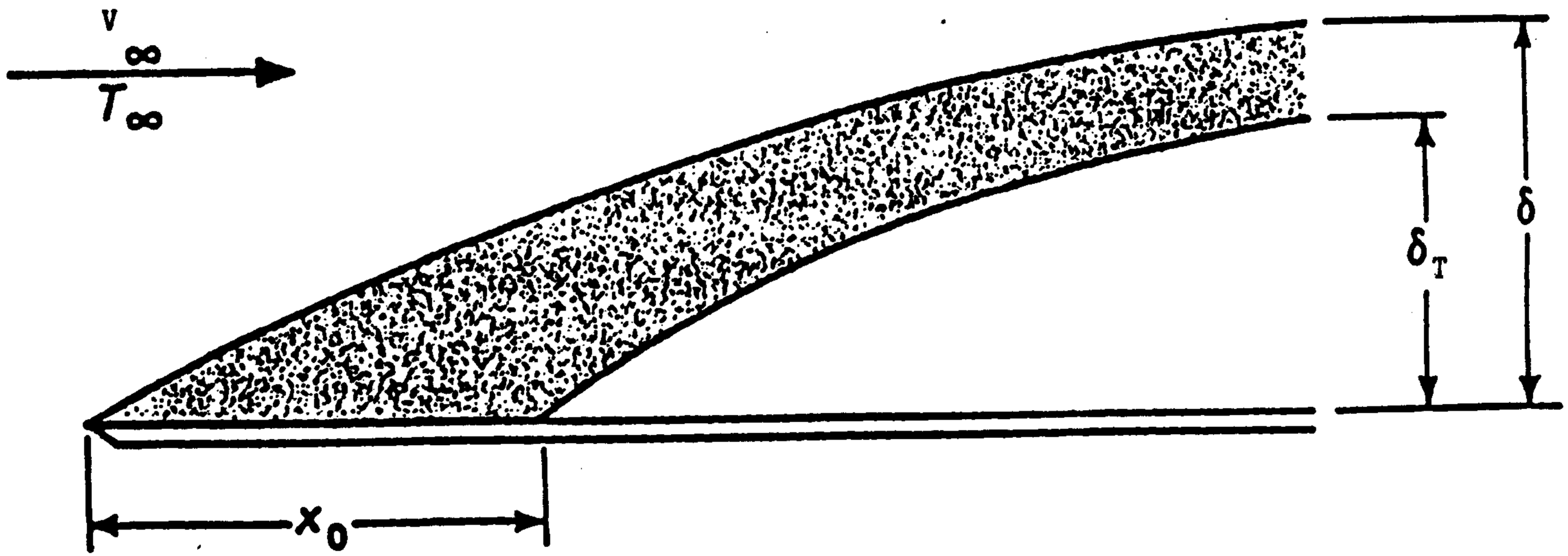

FIGURE 2.3 The Development of the Hydrodynamic and Thermal Boundary Layers for a Plate with a Unheated Starting Length x_o

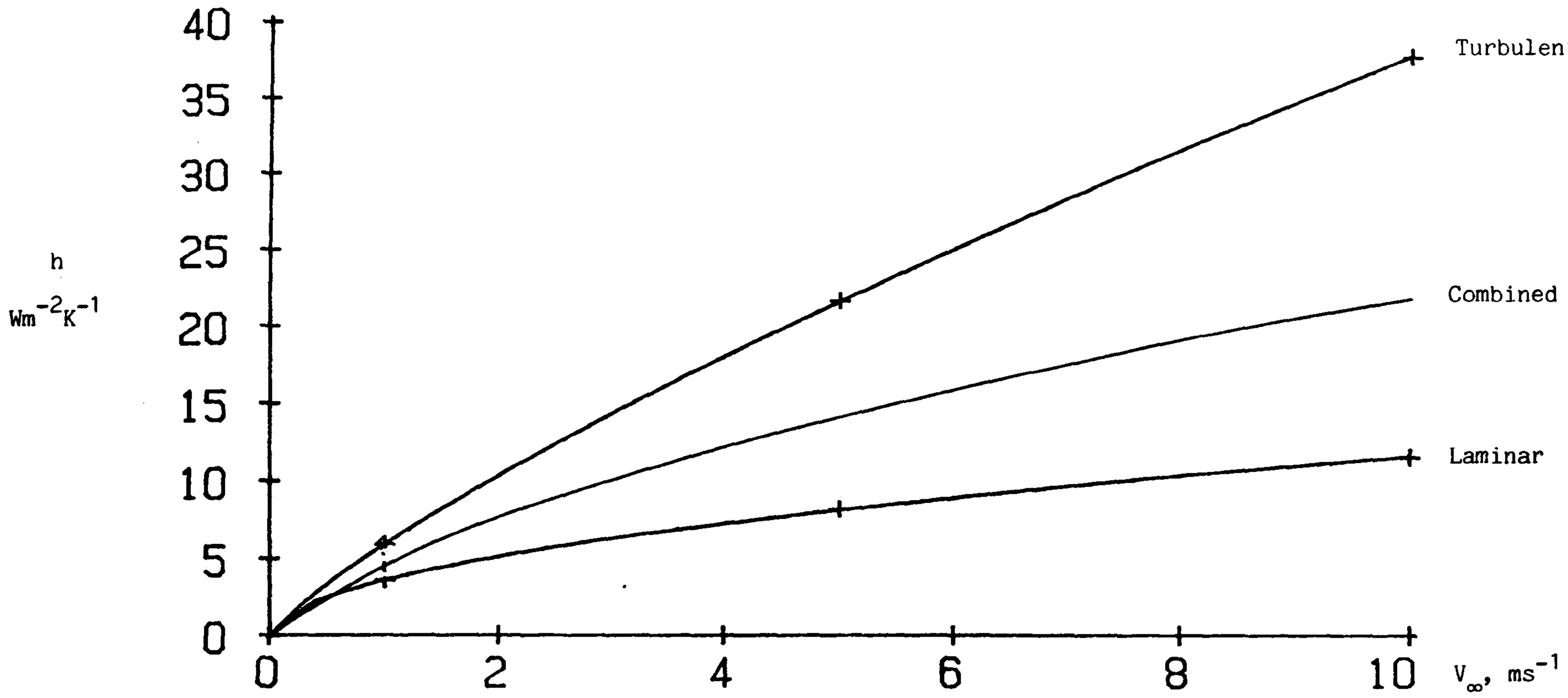

Figure 2.4 Convection coefficient, h, against free stream wind speed, V_∞ for the three theoretical flow regimes discussed in Section 2.7 (2 x 1m plate size)

CHAPTER THREE

REVIEW OF EXPERIMENTAL ANALYSIS OF FORCED CONVECTIVE HEAT TRANSFER

Introduction

Chapter Two examined the theoretical analysis of forced convective heat transfer from an isothermal flat plate, with a streamlined leading edge, in parallel flow. Whilst the upper surface of a flat plate solar collector can be considered essentially as a heated flat plate, it must be realised at this stage that it differs physically from the "ideal" case considered in Chapter Two.

The upper surface of the collector will not be isothermal and its average temperature will change with time. This is because the working fluid enters the absorber plate at a lower temperature than that at which it leaves. Therefore there is an increase in the absorber plate temperature with the fluid flow direction. This increase has been found by Dickinson and Cheremisinoff [1980] to be of the order of 10 K for liquid collectors and 30 K for a collector with air as the working fluid.

There will also be local span wise variations of the plate temperature. This is due to the fact that the cooling action on the plate of the working fluid is more prominent closer to tubes through which the fluid flows. How these temperature variations effect the temperature of the upper surface of the collector is less well understood, but it may be expected that they will produce a non-isothermal temperature profile on the upper glass cover.

The average temperature of the plate will vary with time, simply because of the variability of the incident solar radiation. For example Dixon and Leslie [1979] show the variation of the average glass temperature of an actual solar collector with time. This variation over a 20 min. period was 311.5 - 313.5 K.

A flat plate solar collector must then be thought of as a rectangular body and not a flat plate. This is because it usually has a thickness which cannot be considered negligible as compared to its length or width. Its thickness is due, primarily, to the layer of insulation placed at the back of the absorber plate. This is to prevent heat loss by conduction in this direction. Streed and Waksman [1981] measured 8 collectors and found their thicknesses to range from 60mm to 220mm. Of course the edges of solar collectors are not usually streamlined in any way, and so present a bluff front to the wind flow.

A basic parameter used for the description of a rectangular body is the aspect ratio. This is the ratio of the thickness of body to its stream wise length, or chord. Hence the aspect ratios of the solar collectors examined by Streed and Waksman ranged from 1:17 to 1:5, and their chord lengths were all approximately 1m.

Because solar collectors are primarily placed on the roofs of domestic dwellings, they are inclined to the horizontal. This is also of practical importance as it also leads generally to a greater utilisation of the incident solar radiation. The optimum angle of inclination for solar collectors is discussed in some depth by Deris [1961], but Duffie and Beckman [1980] state a general "rule of thumb" as follows. For maximum annual utilisation of solar energy a

collector should be tilted at an angle to the horizontal equivalent to the latitude of its position. For maximum summer only utilisation the slope should be 10° less than the latitude and for maximum winter utilisation, it should be 10° greater than the latitude.

There is also some evidence that the angle of inclination of a solar collector effects the value of the total heat loss from its upper surface. Cooper [1981] shows that this loss is less, by as much as 30%, for a collector in a vertical orientation, as compared to its value for a horizontal orientation.

A roof, although it will also absorb incident radiation, will not usually reach as high a temperature as the upper surface of the collector. So in effect a retrofit collector must be considered as a heated plate elevated above an unheated host surface.

The final difference between the theoretical case considered in Chapter Two and the physical situation under consideration here is probably the most important. A solar collector is mounted on a three-dimensional bluff body, i.e. a building, and is exposed to the natural environment. The main point being that the atmospheric wind is omni-directional, variable with height and has large levels of free-stream turbulence. An exhaustive account of the properties of the natural wind is given by Counihan [1975].

The purpose of the rest of this chapter is threefold. Firstly, it will examine experimental evidence which relates directly to the theoretical case described in Chapter Two, with the specific aim of comparing the experimental results with the theoretical predictions. Secondly it will describe and discuss experimental work which examines the convective heat transfer from plates or bodies which more closely resemble roof mounted flat plate solar collectors. Finally the use of these experimental results in predicting the convective heat transfer from the upper surface of a flat plate solar collector will be discussed.

3.1 Forced Convective Heat Transfer from a Flat Plate in Parallel Flow

In this section experimental work which most closely resembles the theoretical model given in Chapter Two will be examined. The problems encountered in making these measurements will be discussed and the results will be compared with each other and with the theoretical analysis.

3.1.1 The work of Jurges

One of the earliest experimental analyses of forced convective heat transfer from a flat plate was carried out by Jurges [1924]. His results have been presented by McAdams [1954].

Jurges used a heated copper plate approximately 0.5m square, mounted vertically and flush with the walls of a wind tunnel. The plate was maintained at 324.6 K while air at, initially, 293.6 K was blown over the plate. The air speed was measured at the centre of the tunnel.

Three surface textures (smooth, rolled, rough) were examined and expressions developed for two different wind speed ranges. For $V_\infty < 5.0\ ms^{-1}$, the convection coefficient was found to be a linear function of V_∞, where V_∞ is the free stream wind speed (i.e. at the centre of Jurges' tunnel).

$$h_{smooth} = 4.0\ V_\infty + 5.6 \quad Wm^{-2}K^{-1} \qquad (a)$$

$$h_{rolled} = 4.0\ V_\infty + 5.8 \quad Wm^{-2}K^{-1} \qquad (3.1) \qquad (b)$$

$$h_{rough} = 4.2\ V_\infty + 6.2 \quad Wm^{-2}K^{-1} \qquad (c)$$

for $V_\infty > 5.0\ ms^{-1}$ Jurges data was better fitted to a power relationship:

$$h_{smooth} = 7.1\ V_\infty^{0.78} \quad Wm^{-2}K^{-1} \qquad (a)$$

$$h_{rolled} = 7.1\ V_\infty^{0.78} \quad Wm^{-2}K^{-1} \qquad (3.2) \qquad (b)$$

$$h_{rough} = 7.5\ V_\infty^{0.78} \quad Wm^{-2}K^{-1} \qquad (c)$$

The analytically derived relationship for turbulent heat transfer from a smooth plate is given by equation 2.26, i.e.

$$Nu_L = 0.036\ Re_L^{0.8} Pr^{0.33} \qquad (3.3)$$

By dimensionalising the above equation using Jurges values for plate length, etc., the following is obtained:

$$h_{smooth} = 6.8\ V_\infty^{0.8} \quad Wm^{-2}K^{-1} \qquad (3.4)$$

In comparison with Jurges' equation 3.2(a) equation 3.4 shows good agreement. The breakdown of the comparison at $V_\infty < 5.0\ ms^{-1}$ is to be expected because at $V_\infty = 0\ ms^{-1}$ the right hand side of equations 3.2 and 3.4 reduce to zero and this does not take into account natural convection effects.

If however, Jurges' values are substituted into equation 2.9 (the simplified natural convection equation for a vertical flat plate in air) i.e.

$$h = 1.42\left[\frac{T_s - T_\infty}{x}\right]^{0.25} \quad Wm^{-2}K^{-1} \qquad (3.5)$$

then a value of $h = 4.0\ Wm^{-2}K^{-1}$ is obtained. Natural convection occurs under still conditions i.e. $V_\infty = 0\ ms^{-1}$. If this value of V is substituted into equation 3.1. then $h = 5.6 - 6.2\ Wm^{-2}K^{-1}$. These values are some 40-50% higher than that theoretically predicted. The reason for these discrepancies could be that Jurges took no account of radiative exchange between his heated metal plate and the walls of the wind tunnel.

Watmuff et al [1977] suggest that radiatively corrected form of Jurges' equation 3.1 would be

$$h = 3.0\ V_\infty + 2.8 \qquad Wm^{-2}K^{-1} \qquad (3.6)$$

However this correlation should be treated with caution because Watmuff does not make clear his method of evaluating the radiative component in Jurges' experiment.

3.1.2 The work of Rowley et al

During the 1930's Rowley and his co-workers conducted a series of experiments to determine the surface heat transfer coefficient from a flat plate in parallel flow (Rowley et al [1930 (a) and (b)]). It should be noted at this stage that the surface heat transfer coefficient also includes heat lost and gained from the surroundings by radiative exchange. The ASHRAE Handbook states that under the conditions of these experiments the radiative component was approximately equivalent to a loss of 4.0 $Wm^{-2}K^{-1}$.

Rowley's work was essentially similar to that of Jurges, in that he measured the heat transmission from a 0.3 x 0.3m vertical flat plate placed flush with the side of a wind tunnel. However, a more in depth study of Rowley's experiments is worthwhile not only because of the results he obtained but for the systematic approach he made to the problem.

By considering equation 2.3 i.e.

$$h = -k_f/(T_s - T_\infty)\left[\frac{\partial T}{\partial n}\right]_s \qquad Wm^{-2}K^{-1} \qquad (3.7)$$

it can be seen that any experimental determination of the heat transfer coefficient relies on the accurate measurement of the plate and air flow temperatures T_s and T_∞. The initial problem Rowley considered was the locations to be used for the determination of these temperatures.

Examining the surface temperature first; if a recording thermocouple was embedded in the surface there would be a danger that the temperature recorded would be that of the material below the surface and not of the surface itself, this would be an appreciable factor in materials of low conductivity. As Rowley intended to study, primarily, building materials, e.g. plaster, pine and brick (all of low conductivity) it was decided to place the thermocouples on the surface of the material and cover them with thin vellum paper, despite the fact that this method would leave them more susceptible to being effected by the air temperature.

The air temperature varied with distance from the heated surface, and hence the position of its determination would effect the value of the heat transfer coefficient, as evaluated by equation 3.7. Rowley calculated the surface conductance of the plate using values for T_∞ air temperatures measured at distances from the plate ranging from 1.3mm to 101.6mm. It was found that the value of the surface conductance was substantially insensitive to position of air temperature measurement, for distances greater than 12.7mm. Therefore 25mm away from the plate and above its centre was chosen to be the reference point for the air temperature measurements.

A further problem was highlighted by Houghten and McDermott [1931], but will be considered here because of its similarity to the problem of air temperature measurement. In addition to the temperature variation with distance from a heated surface, there also exists a velocity gradient due to the flow being retarded at the surface by friction. Therefore the velocity of the air flow, and hence the convective heat transfer coefficient correlation, will depend upon the distance away from the plate at which the velocity is measured.

Houghten and McDermott conducted tests which measured the wind velocity at increasing distances from a 3.05 x 1.84m flat plate in an unconstrained airflow. It was found that a constant velocity was reached 0.26m away from the surface for a 5 ms^{-1} wind speed. For a wind speed of 22 ms^{-1} a constant velocity was reached 0.36m from the surface.

In tests carried out in ducts it was shown that the velocity was always a maximum in the centre of the duct. This is to be expected as, if all four surfaces of the duct have the same roughness they will retard the flow equally. It was found, however, that for any wind speed measured in the centre of a duct the velocity gradient near the surface depended upon the size of duct. The velocity gradient in a 0.15 x 0.15m duct was steeper than that for a 0.3 x 0.3m duct; this in turn was greater than the velocity gradient found in free flow.

Therefore in any heat transfer experiment careful note must be made of the distance away from the surface at which the air velocity was measured. Any correlation found to exist between the heat transfer coefficient and the wind speed, may only apply to the specific distance, away from the test surface, at which the wind speed was measured.

Returning now to the work of Rowley et al. In addition to his consideration of the problems of temperature measurement, Rowley recognised four fundamental aspects to be regarded in developing an experimental technique for measuring the surface conductance of a material. These were:

(i) Accurately controlled air temperatures

(ii) Air moving over a test surface at various but constant velocities.

(iii) A test surface which could be supplied with a known amount of heat.

(iv) Instruments for measuring the free stream air velocity, the temperature of the air flowing over the test surface and the amount of heat passing through the test surface.

These four considerations still form the experimental basis for the determination of the convective heat transfer from flat plates. Rowley achieved these aims in the following manner. The air temperature was controlled using a refrigerator, from which the air was pushed, by a fan, along rectangular ducting measuring 0.15m x 0.3m in section. In order to minimise turbulence the air passed through 5.2m of ducting before reaching the 0.3m x 0.3m test surface. The air velocity was measured midway between the centre of the test surface and the opposing duct wall, using a pitot-static tube. Test surfaces were heated using a hot plate connected to a 110 volt D.C. supply and rheostat. The quantity of heat passing into the test surface was measured by a Nicholls-type heat meter sandwiched between the hot plate and the test surface. A full description of the manufacture and use of this type of meter is given by Nicholls [1924].

Because all temperatures were taken at the centre of the test surface, and the test plate was thin as compared to its area, (typically the test plate thickness was of the order of 10mm), no account was taken of edge losses from the plate. However, the edges of the hot plate, heat meter and test surface were insulated with heavy layers of felt in order to further reduce this heat loss.

Several types of surface were examined ranging in surface roughness from glass, the smoothest, to stucco, the roughest. Measurements of the surface conductance for each test plate was carried out under steady state conditions and for a range of wind velocities (0-16 ms^{-1}). The effect of the variation of the mean of the surface and air temperatures was also considered over the range 256-310 K.

Rowley found that there was an almost linear dependence of surface conductance on the wind speed in the range examined. By assuming this linearity two equations can be presented which represent the extremes of the type of surface considered, i.e.

$$h_{glass} = 2.7\ V_{\infty} + 8.5 \qquad Wm^{-2}K^{-1} \qquad (3.8)$$

$$h_{stucco} = 5.7\ V_{\infty} + 11.3 \qquad Wm^{-2}K^{-1} \qquad (3.9)$$

For a given wind speed the surface coefficient increases slowly with the mean of the plate and air temperatures. For instance, for a glass surface with an air velocity of 10 ms^{-1}, there is an increase in the surface conductance of approximately 10% over a range of mean surface to air temperatures of 270-310K. The effect of surface roughness on the coefficient, as can be seen from equations 3.8 and 3.9 was much greater. At an air velocity of 10 ms^{-1} the surface conductance of stucco is approximately twice that of glass.

The effect of surface roughness on the surface coefficient is of minimal importance as applied to solar collectors, the upper surface most often being a smooth glass cover. It is of interest to point out, however, that the variation is surface conductance with roughness, probably arises out of the fact that the rougher the surface the larger the area of actual exposed surface per superficial area of material. Also the uneven surface could induce local turbulence near the plate and this would lead to higher rates of heat transfer.

One case where this effect could be of importance in the study of heat loss from flat plate solar collectors would be for an unglazed collector. In these cases the absorber plate would be directly exposed to the wind flow. Absorber plates are usually made of metal and sometimes have tubes which sit slightly proud of the surface. In these cases the surface would be appreciably rougher than that of a glass cover.

If Rowley's plate dimensions and typical temperatures are substituted into equation 3.5 for natural convection then the value of 4.5 $Wm^{-2}K^{-1}$ is obtained. If the assumed radiative component of 4.0 $Wm^{-2}K^{-1}$ is subtracted from the value of the heat transfer coefficient obtained for glass under still conditions from equation 3.8 then the experimentally derived value for the natural convection coefficient is in excellent agreement with that predicted by the theory. By performing a similar exercise on the turbulent boundary layer equation 2.26, (it can be assumed that a turbulent boundary layer will have developed in the region of the test section due to the length of the proceeding tunnel wall) the following dimensional form is obtained.

$$h = 7.47\ V_{\infty}^{0.8}\ \ Wm^{-2}K^{-1} \qquad (3.10)$$

At first sight Rowley's experimental results may not appear to conform with this theory, his correlations being linear. However, by considering Figure 3.1 it can be seen that there is some general agreement between the linear relationship for a smooth glass surface and the turbulent theory power law. The cross over point between the turbulent theory and Rowley's results for glass, at approximately 2 ms^{-1}, could indicate that below this velocity natural convection effects become important. It will be recalled from Section 2.3 that this wind speed i.e. 2 ms^{-1}, is also given by Green [1980] as the speed at which the natural convection regime, over solar collectors, breaks down.

3.1.3 The work of Parmelee and Huebscher

The experimental results of Jurges [1924] and Rowley et al [1930 (a) and (b)] are limited to plates with heated lengths of 0.5m and 0.3m respectively. Parmelee and Huebscher [1946, 1947] examined the effect of both air velocity and surface length, on the convective heat transfer through a turbulent boundary layer, from a smooth surface to a parallel air flow.

Their experimental set-up consisted of a composite heater of four separate 0.26 x 0.26m elements placed vertically in the centre of a 0.41 x 0.76m wind tunnel. The plate was suspended on struts and the heat transfer surface was made of polished aluminium; this was in order to reduce radiative exchange to a minimum. Temperature and velocity measurements were made midway between the plate and the tunnel wall, about halfway along the plate length. Heat could be input to the four plates individually or in any combination. Thus it was possible for Parmelee and Huebscher to systematically vary the length of their heated surface.

The heat transfer coefficient was calculated by subtracting from the electrical power supplied to the plate or plates the calculated heat loss by radiation and conduction. The plate temperature was taken by five thermocouples embedded in each heated element and the mean of these temperatures was used in the assessment of the plate to air stream temperature difference.

The heat transfer coefficient was again found to be linearly dependent upon wind-speed, for a particular heated length, over the range considered (0-11 ms^{-1}). For example the two equations given below show the correlations for a 0.3 x 0.3m heated surface and for a 0.3 x 1.2m heated surface respectively.

$$h = 3.1\ V_\infty + 14.2 \qquad Wm^{-2}K^{-1} \qquad (3.11)$$

$$h = 2.4\ V_\infty + 9.6 \qquad Wm^{-2}K^{-1} \qquad (3.12)$$

As can be seen from the above, there was found to be a strong dependence of the heat transfer coefficient on the length of heated surface. The heated surface length effect becomes larger the greater the wind speed, i.e. the convection coefficient decreases the longer the heated surface. Parmelee and Huebscher present curves covering a range of heated plate lengths from 0.3 to 30m. Their experimental set-up, however, allowed them only to measure values of the heat transfer coefficient from plates with heated lengths of 0.3m to 1.2m. The equations presented below represent only experimental data and apply only to the range of heated length examined i.e. 0.3-1.2m.

$$h = 13.6 - 3.3\ x_1 \qquad Wm^{-2}K^{-1} \qquad (3.13)$$

$$h = 48.8 - 9.9\ x_1 \qquad Wm^{-2}k^{-1} \qquad (3.14)$$

where x_1 is the length of heated surface in meters. Equation 3.13 is for a mean wind speed of 2.2 ms^{-1} and equation 3.14 for a mean wind speed of 11 ms^{-1}.

This effect of surface length has been discussed by Gates [1962]. It arises because the ability of the air to cool a heated plate decreases with distance along the surface. This is due to the decreasing temperature difference between the air and the surface as the flow develops along the plate.

The dimensional form of the natural and forced turbulent equations 2.9 and 2.26 for Parmelee and Huebscher's plate of 0.3 x 0.3m are essentially the same as those of Rowley. It must be noted that their experimental work gives a value for the natural convection coefficient some 70% higher than Rowley's for glass, but an agreement on the slope of the lines to 15%

3.1.4 The work of Reynolds et al

Reynolds et al [1958 (a)] examined the local heat transfer from a 1.54 x 0.83m plate placed in a 2m diameter wind tunnel. The plate consisted of 24 separate heating elements. By controlling the heat input to each individual element the plate temperature was kept uniform to better than ± 0.5 K. Local Reynolds numbers in the range $10^5 < Re_x < 3.5 \times 10^6$ were examined with the flow over the plate being turbulent. A correlation between Nu_x, the local Nusselt number and Re_x was found to be given by:

$$Nu_x = 0.0296\ Re_x^{0.8} Pr^{0.6} \left[\frac{T_s + 251}{T_\infty + 251}\right]^{-0.4} \qquad (3.15)$$

This shows agreement to within 1% with the theoretically derived local Nusselt number relationship for turbulent flow i.e.

$$Nu_x = 0.0292\ Re_x^{0.8}\ Pr^{0.33} \qquad (3.16)$$

The difference in the exponents for the Prandtl number, and the correction factor involving T_s and T_∞, arise from the fact that in the theoretically derived relationship, the physical properties of the air are evaluated at the mean of the surface and air temperatures, whilst Reynolds evaluated these properties at the free stream air temperature T_∞.

By supplying different heat inputs to each element Reynolds et al [1958 (c)] were able to produce plates with non-uniform surface temperatures. This situation may, for reasons given in the introduction to this chapter, be of importance in the study of convective heat transfer from flat plate solar collectors.

One temperature distribution studied by Reynolds is of particular interest. This is the step-ramp wall temperature illustrated in Figure 3.2. This is a first approximation to the flow wise temperature distribution of the absorber plate of a flat plate solar collector. Reynolds calculated theoretically that the local Nusselt number for this temperature distribution, Nu'_x, would relate to the local Nusselt number for an isothermal plate, Nu_x, by the expression.

$$Nu'_x = \frac{1.134 + \Delta T_o/Mx}{1 + \Delta T_o/Mx} Nu_x \qquad (3.17)$$

where ΔT_o = the temperature difference at the leading edge of the plate k

M = the slope of the surface temperature, km^{-1}

x = distance from the leading edge of the plate, m.

Using his 24 heated elements Reynolds produced a plate with a step-ramp surface distribution having ΔT_o = 2.1 K and M = 8.5 Km^{-1}. He then evaluated the local Nusselt number at each element and compared it to that predicted by equation 3.17. The agreement was better than 2% in all cases.

3.1.5 The work of Wang

Wang [1982], like Reynolds, also studied the local convective heat transfer from a large flat plate in parallel flow. The main interest in this study, however, was convective heat transfer at low free-stream wind speeds.

The plate used by Wang was 1.2m long by 0.25m wide and the local heat transfer coefficient was evaluated at 18 evenly spaced stations along the plate length. The flow over the plate was laminar, and the relationship between the local Nusselt number Nu_x and the local Reynolds number Re_x was found to be

$$Nu_x = 0.295\ Re_x^{0.5} \tag{3.18}$$

This can be compared to the theoretically derived relationship for local heat transfer to a laminar boundary layer, i.e.

$$Nu_x = 0.332\ Re_x^{0.5}\ Pr^{0.33} \tag{3.19}$$

Excellent agreement is found between the two above equations as the value of $Pr^{0.33}$ in Wangs experiments was of the order of 0.89. Wang also studied the heat loss from the plate under still conditions and found that the local Nusselt number could be related to the local Grashof number Gr_x by:

$$Nu_x = 0.14\ Gr_x^{0.33} \tag{3.20}$$

This equation corresponds exactly to that given by McAdams [1954] (and given in section 2.3) for natural convection losses from square flat plates, thus confirming that this theoretical equation may be applicable to other flat plate geometries.

3.1.6 Summary

In this section the work of five authors who have dealt with the problem of heat transfer from a flat plate to a parallel air flow has been described and examined. It has been shown that the heat transfer coefficient under these conditions varies with surface temperature, surface temperature distribution, heated surface length, surface roughness and above all flow velocity. An inter-comparison of the work of Jurges, Rowley, Parmelee and Huebscher (i.e. those authors dealing with the overall heat transfer coefficient) is shown in Figure 3.3. It can be seen that most correlations between h and V_∞ are linear in form. Whilst this does not conform to the power law of the theory it has been shown earlier, see Figure 3.1, that the experimental results and the theoretical predictions are compatible to some extent.

The results of the work on smooth plates are all compatible and could be expressed by the single equation

$$h = 2.9\ V_\infty + 10.0 \qquad Wm^{-2}K^{-1} \qquad (3.21)$$

with a maximumum inaccuracy of $\pm$ 15%. This order of variation could be accounted for by the effect mentioned earlier, of the different distances away from the surface at which the air speeds were measured.

3.2 Forced Convective Heat Transfer from a Flat Plate in Non-Parallel Flow

As mentioned in the introduction to this chapter a solar collector is usually inclined to the horizontal, and may be subjected to wind flow from any direction. The rest of this section deals with the experimental investigation of convective heat transfer to a non-parallel air flow.

3.2.1 The work of Rowley et al

Some of the earliest work carried out to investigate the effects of wind direction on the convective heat transfer coefficient was again carried out by Rowley [1932]. His apparatus consisted essentially of a test piece 0.38m square with a 0.30m sharp ended extension piece fitted to its leading edge. This extension piece directed the wind over the surface and prevented disturbing eddy currents from the leading edge of the test plate.

The whole test plate was similar in construction and operation to that used by Rowley et al [1930] for work on parallel flow. The plate was placed on a rotatable support at the outlet of a duct 7.62m long and 0.76m in diameter. Wind speeds were measured close to, and parallel to, the heated surface and centrally within the duct at a distance 1.91m from the outlet. The mean plate - air temperature was maintained at 301.5 $\pm$ 3 K; from Rowleys previous work (Rowley [1930 (a) and (b)] the effect of this temperature variation was considered negligible. The radiative component of the surface conductance was assumed by Rowley to be 5.6 $Wm^{-2}K^{-1}$ at this mean temperature.

Wind incidence angles of 0-90° were examined in 15° increments, 0° corresponding to parallel flow. Wind speeds, as measured in the duct, of 0-13 ms^{-1} were investigated. For a plate glass surface it was found that for parallel flow the surface conductance was again linearly dependent upon the wind speed, the correlation being:

$$h = 3.7\ V_\infty + 8.5 \qquad Wm^{-2}K^{-1} \qquad (3.22)$$

In comparison with equation 3.8 for a similar surface placed flush with a duct side, it can be seen that for zero velocity the equations reduce to the same value for h, but as the velocity increases equation 3.22 gives slightly higher values of heat transfer for a given wind speed. This could be due to the fact that the wind speeds were measured at different distances away from the test surface or that some free stream turbulence was induced in the unconstrained flow from the duct outlet. Further consideration of the effect of free stream turbulence on heat transfer from flat plates will be given in Section 3.5. Figure 3.4 shows the variation of the convection coefficient with wind angle of incidence, for a glass surface at two duct wind speeds 5 ms^{-1} and 10 ms^{-1}. From this it can be seen that the dependence upon wind angle of incidence increases slightly with increasing wind speed, and that the value of the heat transfer coefficient decreases slightly for angles greater than 0°. At a wind speed of 10 ms^{-1} the maximum variation of h about its mean value of 36 $Wm^{-2}K^{-1}$ is approximately $\pm$ 5 $Wm^{-2}K^{-1}$ ($\pm$ 13%). Rowley considered this order of variation to be negligibly small as compared to the overall effect of the wind velocity.

One other important result to arise form this piece of work was, how the velocity parallel to the test surface, and close to it, varied with wind incidence angle. Figure 3.5 shows the ratio of the wind velocity parallel to the surface to that evaluated in the duct, averaged for all wind speeds measured. It can be seen that for angles of incidence in the range 0-45° the ratio is substantially constant

with a value of unity. Then with increasing angle the velocity parallel to the surface decreases. This could account for the generally lower rates of heat transfer at these angles of wind incidence, and may indicate that the heat transfer coefficient from an inclined surface is more closely linked with the wind velocity close to, and parallel to, the surface than one measured remote from it.

3.2.2 The work of Drake

Drake [1949] measured local heat transfer coefficients from a non-isothermal smooth plate, 2.54mm wide and 0.43m long, in laminar flow. He investigated wind incidence angles of 0-90° in 10° increments, 0° incidence being equivalent to parallel flow. The local Nusselt number at a distance x along the plate, Nu_x was found to be related to the plate Reynolds number Re_L, L = 0.43m, by the expression.

$$Nu_x = C_1\left(\frac{x}{L}\right)^{n_1} Re_L^{0.5} \qquad (3.23)$$

This dependence upon the square root of the Reynolds number is in general agreement with the laminar flow theory discussed in Chapter Two. The values of C_1 and n_1 were found to depend upon the angle of inclination of the plate. For example at 10° inclination C_1 = 0.652 and n_1 = 0.640, and at 90° inclination C_1 = 1.025 and n_1 = 1.000.

Equation 3.23 can be reduced to an expression for the local Nusselt number in terms of the local Reynolds number i.e.

$$Nu_x = C_2 Re_x^{0.5} \qquad (3.24)$$

The value of the constant C_2 varies with angle of inclination of the plate and also position along the plate, i.e. the ratio x/L. For instance, assuming that the plate has a 10° inclination to the wind flow, if x/L = 0.1 C_2 = 0.472 and if x/L = 1 then C_2 = 0.652. Both these constants are around 2-3 times as high as the theoretically derived constant for laminar flow over a flat plate, given in equation 3.19 assuming a value of Pr = 0.708. It must be noted that equation 3.19 implies no variation of the value of C_2 along the plate length.

3.2.3 The work of Coste et al

Coste et al [1981] performed a series of experiments on small heated square plates in ducts of circular cross-section. They examined the effect on the local heat transfer coefficient of:

(i) Flow velocity (5-20 ms^{-1})

(ii) Angle of wind incidence (0°-90°)

(iii) Plate size (20 x 20mm - 80 x 80mm)

(iv) Duct diameter (80mm and 120mm)

An expression for the Nusselt number in terms of the Reynolds number and the Prandtl number was developed thus.

$$Nu = C_3 Re^{n_2} Pr^{0.33} \qquad (3.25)$$

Where the values of the constants C_3 and n_2 depend upon the wind attack angle, the plate size, and the size of the duct. For example, for a 60 x 60mm plate inclined at an angle of 45° to the windstream the following applies.

$$Nu_x = 0.214\ Re_x^{0.6}\ Pr^{0.33} \qquad (3.26)$$

Figure 3.6 shows that the heat transfer coefficient was at a maximum in parallel flow (zero degrees wind incidence) decreased with attack angle till about 45° then increased again up to a local maximum at 90°. The curves show a similarity to those of Rowley et al (see Figure 3.4) but the increase of h at high angles of incidence is more pronounced.

In order to take into account the plate and duct dimensions two general correlations were developed.

When the plate was nearly parallel to the flow the Nusselt number is given by

$$Nu = 0.023\left[Re \left[\frac{\phi}{\rho}\right]^{1/2} \right]^{0.8} Pr^{1/3} \left[1 - \left[\frac{\phi}{\rho}\right]^{3/2} 0.079 \frac{\theta}{90} \right]^{0.8} \quad (3.27)$$

where ϕ = the diameter of the duct, m

ρ = half the plate length, m

θ = plate orientation relative to the flow

When the air flow is nearly normal to the plate the general expression for the Nusselt number is

$$Nu = k' \left[\frac{V\rho}{\nu} \left[\frac{\theta}{90}\right]^{1/2} \right]^{0.6} Pr^{1/3} \quad (3.28)$$

where V = flow velocity ms^{-1} and $0.230 < k' < 0.245$.

Thus, when the plate is orientated parallel to the flow, the heat transfer coefficient increases with the ratio of the diameter of the pipe to the characteristic length of the plate. In the same way

the reduction in the transfer coefficient when the angle of inclination increases becomes higher as the characteristic blockage ratio increases. Conversely when the plate is orientated normally or nearly normally to the flow, the heat transfer coefficient is independent of the blockage ratio. (The blockage ratio being defined as the area of the plate "seen" by the wind flow divided by the total area of the duct.)

3.3 Measurement of Convective Heat Transfer from Flat Plates via the Mass Transfer Analogy

In recent years several experiments have been performed to evaluate convective heat transfer losses from flat plates, using the mass transfer analogy. The transport of one constituent of a fluid solution, or volatile solid, from a region of higher concentration to a region of lower concentration is called mass transfer. This process is directly analogous to heat transfer in that both mass and heat are transferred in a direction which reduces an existing concentration gradient. In convection systems mass transfer occurs on a macroscopic level. For these cases it has been shown theoretically (e.g. see Bedingfield [1950]) that heat and mass transfer can be related by the dimensionless j-factor, where, for heat transfer

$$j = \left[\frac{Nu}{Re\ Pr}\right] Pr^{2/3} = \frac{h}{\rho\ C_p\ V_\infty} Pr^{2/3} \qquad (3.29)$$

and for mass transfer

$$j = \frac{K}{V_\infty} \left[\frac{\nu}{D}\right]^{2/3} \qquad (3.30)$$

where K = the average mass transfer coefficient, ms^{-1}

D = the diffusion coefficient, m^2s^{-1}

According to the heat-mass transfer analogy formulation, the j-factors of identical configurations should be equal under corresponding flow conditions. Hence heat transfer correlations can be obtained from mass transfer data.

Sogin and Providence [1958] determined the mass transfer rates from discs, to air streams flowing normal to their surfaces. They then compared the results, via the j-factor, to heat transfer data, obtained by Jakob et al [1950], for similar geometries and flow conditions. The 100mm diameter discs were made of napthalene and the mass was transferred by sublimation. For the wind speed range examined, 8-100 ms^{-1}, Sogin concluded that the heat and mass transfer results could be brought together for these conditions by the single equation

$$j = 1.08\ Re^{-0.5} \qquad (3.31)$$

which can be rewritten from equation 3.29 as:

$$Nu = 1.08\ Re^{0.5}\ Pr^{0.33} \qquad (3.32)$$

This is the correct form of correlation for heat transfer from flat plates in laminar flow. It compares well with the theoretical equation 2.16 but with the value of the constant being some 60% higher. Some discrepancy, however, is to be expected between theoretically derived relationship, and that evaluated experimentally here. In this case the air flow was normal to the plate surface, not parallel, and the plate was circular not rectangular. Equation 3.32 has a probable error of only $\pm$ 3% Thus the analogy between heat and mass transfer has been confirmed experimentally, for at least this type of flow condition and surface geometry.

Mass transfer experiments have been used to consider several of the differences between the theoretical case of Chapter Two and the situation under consideration here. However, for the sake of brevity and because of their unique nature all relevant mass transfer experiments will be considered in this section. They are being introduced at this stage because one of the initial parameters examined by mass transfer experiments was that of the effect of wind direction.

3.3.1 The work of Sparrow et al

Between 1977 and 1982, Sparrow et al conducted a protracted series of experiments to determine mass transfer rates from flat plates. The original impetus for undertaking the work was provided by a need to determine the heat loss from the upper surface of flat plate solar collectors, hence the possible importance of this work here. The mass transfer results were converted, by the afore-mentioned analogy, into heat transfer correlations.

Initially Sparrow et al [1977, 1979] reported on the heat/mass transfer from square and rectangular plates. They examined the effect of flow velocity, angle of inclination and yaw. The experiments were then refined so as to consider the effect of adiabatic co-planar extension surfaces (Sparrow and Lau [1981 (a)]), leeward orientations and elevating the plate above an adiabatic host surface (Sparrow et al [1981 (b), 1982]). In all cases the test surface was made of napthalene, and the mass transfer was by sublimation.

Sparrow states that this technique, with reasonable precautions, provides a well defined boundary condition on the transfer surface. This mass boundary condition is analogous to a uniform wall temperature in the corresponding heat transfer problem. Mass transfer measurements of this kind have an advantage over those dealing with heat transfer in that they are virtually free of the extraneous edge losses usually encountered in heat transfer experiments.

Most of the results in this series of experiments were presented as plots, and often correlations, between the j-factor and the Reynolds number. The usual form of the correlation is that also given by Sogin i.e.

$$j = C\ Re^{-n} \tag{3.33}$$

where C and n are constants, n invariably being equal to 0.5 and C variable with flow conditions and surface geometry, etc. The general simplicity of this equation, according to Sparrow, makes it a useful tool for design purposes.

Equation 3.33 can be reduced to a dimensional form. Using fluid properties of air at 300 K, the following equation is obtained.

$$h = 5.9\ C\ V_{\infty}{}^{0.5}\ x^{-0.5}\ \ Wm^{-2}K^{-1} \tag{3.34}$$

So it can be seen that the heat transfer coefficient varies directly with the square root of the wind speed and inversely with the square root of the characteristic dimension of the plate x.

This implies general agreement with the laminar regime theory developed in Section 2.5 and as already noted equation 3.33 can also be written in the form:

$$Nu = C\ Re^{0.5}\ Pr^{0.33} \qquad (3.35)$$

The dependence on surface length also shows some agreement with the earlier work of Parmelee and Huebscher, but it must be noted at this stage that the flow regime studied by Parmelee and Huebscher was turbulent, not laminar as in this case, and that Sparrow at no time undertook a specific examination of the effect of surface length on mass transfer rates from flat plates.

The experiments were carried out in a 3m long, open circuit low turbulence wind tunnel. It had a cross section of 305 x 610mm and was capable of producing velocities in the range 4.5 - 24.0 ms^{-1}. This implies that no investigation of natural convection was performed.

In all cases the essence of the experimental measurements were similar, as was the calculation of the j-factor. Only the geometry and positioning of the napthalene surface varied. Therefore it would seem adequate to describe the set-up and procedure for one series of experiments.

3.3.2 Experimental and calculational procedure used by Sparrow et al to determine the mass transfer from a square plate

A freshly made napthalene plate was used for each test run. In this case the plate was in the form of a 76.2mm square smooth napthalene surface surrounded by a 2.38mm metal frame. The frame was bevelled at an angle of 20°, in order to ensure that the oncoming flow would not be deviated by blockage by the plate.

The plate was housed in a stainless steel cassette, of which the aforementioned frame was an integral part. On the back face of the cassette was a connector. This enabled it to be fastened to a sting suspended from the ceiling of the wind tunnel. Hence the plate could be set at any angle of attack, α, or yaw, ϕ, with respect to the airflow. These angles are defined in Figure 3.7, the 20° bevelled angle is also illustrated.

The temperature of the napthelene plate was measured by two thermocouples. One was 13mm downstream of the leading edge of the plate, the other at its centre. Another thermocouple positioned just downstream and above the plate, facilitated the measurement of the air temperature.

Air velocities in the test section were measured using an L-shaped impact tube, in conjunction with a wall static tap positioned upstream from the plate. The tube was retracted during the mass transfer measurements, in order that its wake would not impinge upon the test surface.

At the start of the test run a napthalene plate would be cast, and the cassette fitted with a protective cap to prevent sublimation. A plate was then placed in the wind tunnel, which was set at the required velocity. Once it had reached thermal equilibrium with its surroundings, as sensed by the air and plate temperature thermocouples, the cassette was removed from the wind tunnel. It was then weighed and returned immediately to its required position for the test.

Now the cap was removed from the plate and a stop watch device activated. The end of the run, typically 40-75 min. depending on the wind velocity, was marked by the capping of the cassette and its immediate reweighing.

The j-factor for mass transfer was then evaluated in the following manner. The amount of napthelene sublimated during the test, M, was determined from the mass measurements. If t denotes the duration of the test and A the area of the test surface, then the average mass flux, $\dot{m}$, is given by:

$$\dot{m} = \frac{M}{At}, \text{ Kg m}^{-2}\text{K}^{-1} \qquad (3.36)$$

As the mass transfer is driven by the difference in concentrations of the napthelene vapour, between the plate surface and the free stream, the mass transfer coefficient, K, may be defined as:

$$K = m/(\rho_{nw} - \rho_{n\infty}) \qquad (3.37)$$

where ρ_{nw} = The wall concentration of napthalene vapour

and $\rho_{n\infty}$ = The free stream concentration of napthalene vapour = 0

ρ_{nw} can be determined using the perfect gas law and a knowledge of the temperature of the surface T_w and the vapour pressure at the surface P_{nw}. This vapour pressure was evaluated using the correlation presented by Sogin [1958]. i.e.

$$\text{Log}_{10} \; P_{nw} = 11.884 - \frac{6713}{T_w} \qquad (3.38)$$

The ratio of the kinematic viscosity, ν, to the napthalene - air mass diffusion coefficient, D, was evaluated. In all cases it was found to be within a percent of the value of 2.57. Thus with all the parameters on the right-hand side of equation 3.30 determined, the j-factor could be found.

In the cases where the j-factor was plotted against the Reynolds number, Re, the following definition was used.

$$\text{Re} = \frac{V_\infty \, x}{\nu} \qquad (3.39)$$

The characteristic dimension x being that defined in Section 2.2, i.e.

$$x = \frac{4\ L_1 L_2}{2(L_1 + L_2)} \qquad (3.40)$$

where L_1 and L_2 are the lengths of the sides of the plate in metres.

3.3.3 A description of the surface geometries used in mass transfer experiments by Sparrow et al

Using the basic working method described in Section 3.3.2, Sparrow et al were able to examine in detail several plate shapes and geometries. These are summarised below.

(I) A 76.2mm square plate.

(II) A 50.8 x 127mm rectangular plate.

(III) An originally square plate with various adiabatic co-planar extensions. These were produced by making sections of the plate inactive in the mass transfer process by covering them with tape.

(IV) A rectangular plate with adiabatic co-planar extensions.

(V) A 63.5mm square plate elevated above a host surface, being inactive in the mass transfer process. The active - inactive surface separation was varied between 4.2 and 12.7mm. The extension of the inactive surface beyond the active being varied between 0 and 12.7mm.

(VI) A 76.2mm square plate formed into one side of a roof shape of 45° pitch. The other side consisting of an inactive metal surface.

(VII) A similar situation to (VI) but with eaves attached to the roof, and the plate flanked by adiabatic co-planar extensions.

Table 3.1 presents the values of the angles of attack, α, and yaw, ϕ, studied in each case. It should be noted that in series II two plate orientations were examined, i.e. with the long side of the plate in the stream-wise direction and with the short side in the stream-wise direction. In series VI and VII the attack angle was fixed by the pitch of the roof.

Table 3.1 The Angles of Attack and Yaw Studied by Sparrow et al, for the Various Geometries Examined

Experimental Series	Angles of Attack, α	Angles of Yaw, ϕ
I	25°, 45°, 65°, 90°	0°, 22.5°, 45°
II	25°, 35°, 45°, 65°, 90°	-
III	25°, 55°, 90°	-
IV	25°, 90°	-
V	5° - 60°, 5° Increments	-
VI	45°	-
VII	45°	-

3.3.4 The results of the mass transfer experiments conducted by Sparrow et al

I. Square Plate (Sparrow [1977])

The heat/mass transfer coefficient was found to be relatively insensitive to both angles of attack and yaw, with the following correlations being presented. Again the dimensional form of the correlations are based on the properties of air at 300 K:

for α = 90° and 65°

$$j = 0.947\ Re^{-0.5} \tag{3.41}$$

$$\therefore \quad h = 5.58\ V^{0.5}\ x^{-0.5}\ Wm^{-2}K^{-1} \tag{3.42}$$

and

for α = 45° and 25°

$$j = 0.905\ Re^{-0.5} \tag{3.43}$$

$$\therefore \quad h = 5.34\ V^{0.5}\ x^{-0.5}\ Wm^{-2}K^{-1} \tag{3.44}$$

As the difference between the coefficients for each range of α is only 5%, a representative equation in terms of the more usual heat transfer parameters can be presented, i.e.

$$Nu = 0.926\ Re^{0.5} Pr^{0.33} \tag{3.45}$$

This agrees to within 16% of Sogin's data but is again some 40% higher than the theoretically predicted relationship. If the actual value of x is substituted into the above we obtain:

$$h = 19.79\ V^{0.5}\ Wm^{-2}K^{-1} \tag{3.46}$$

It seems strange, that despite a general reduction of the constant C with decreasing attack angle, Sparrow did not examine flow at zero incidence. This would have enabled him to compare his experiments more closely with both theory and previously conducted experiments in parallel flow.

II. Rectangular Plate - Two Orientations (Sparrow [1979])

When the plate was orientated with its short side to the stream-wise direction the heat transfer coefficient was found to be totally insensitive to variations of attack angle. A representative correlation being:

$$j = 0.939\ Re^{-0.5} \tag{3.47}$$

$$\therefore \quad h = 5.54\ V^{0.5}\ x^{-0.5}\ Wm^{-2}K^{-1} \tag{3.48}$$

However, when the plate was positioned with its long side to the stream-wise direction, a definite increase in the heat transfer coefficient was observed when the attack angle was increased. Hence

for $\alpha = 90°$

$$j = 0.939\ Re^{-0.5} \tag{3.49}$$

$$\therefore \quad h = 5.54\ V^{0.5}\ x^{-0.5} \qquad Wm^{-2}K^{-1} \tag{3.50}$$

and

for $\alpha = 25°$

$$j = 0.766\ Re^{-0.5} \tag{3.51}$$

$$\therefore \quad h = 4.52\ V^{0.5} x^{-0.5} \qquad Wm^{-2}K^{-1} \tag{3.52}$$

Therefore there is almost a 25% increase in h over the range of attack angles considered, i.e. 25° - 90°.

III. Square Plate - Adiabatic Extensions (framing)

(Sparrow [1981 (a)])

The value of C, the constant in equation 3.33, for each type of framing, illustrated in Figure 3.8, is given in Table 3.2. In this series of experiments the Reynolds number used in the correlations is based on the hydrodynamic dimensions of the plate, not on the dimensions of the area which is active in the mass transfer process.

From Table 3.2 it can be seen that the maximum sensitivity to attack angle occurs for configuration F, i.e. the case where the active surface is totally surrounded by an inactive extension surface. The variation of h, for a given wind speed, is $\pm$ 15% of its mean value over the attack angle range considered. It can also be seen that framing along the side edges has a greater effect in reducing h than framing along the leading and trailing edges.

Table 3.2 Values of C for Relation $j = C\,Re^{0.5}$ for Framing Types shown in Figure 3.8

(Sparrow [1981 (a)])

Framing Type	Attack Angle α		
	90°	55°	25°
A	0.884	0.841	0.823
B	0.839	0.830	0.879
C	0.803	0.837	0.887
D	0.825	0.783	0.791
E	0.807	0.835	0.885
F	0.701	0.980	1.031

IV Rectangular Plates - Adiabatic Extensions (framing)

(Sparrow [1981 (a)])

Two plate orientations were tested, as in Series II, only this time with narrow adiabatic extension surfaces on the streamwise edges. The lowest value of C in this, and the previous, series of experiments dealing with rectangular plates was found to occur for the long side streamwise orientation at $\alpha = 25°$. In this case C = 0.702. For this orientation there was a general increase in heat/mass transfer with increasing attack angle, whilst for the short side streamwise orientation the converse was found to be true.

V Square Plate Elevated above an Host Surface

(Sparrow [1981 (b)])

The results of this series are presented as plots of the ratio of the measured heat transfer coefficient, h, to the heat transfer coefficient determined for a similar, but unelevated, plate, h^*.

Conclusions were drawn as follows:

(a) There is a generally monatonic decrease of h with attack angle up to a given angle, say α'.

(b) The value of α' is mainly dependent upon the Reynolds number, it increasing slightly with this parameter.

(c) For attack angles greater than α', h/h^* is virtually insensitive to plate geometry and Reynolds number, its value being close to unity.

(d) Increasing the step height H (see Figure 3.9) gives rise to a greater enhancement of h at attack angles less than α'.

(e) Increasing the skirt width W (see Figure 3.9) increases both the enhancement of h and the value of α'.

(f) The maximum enhancement of h, therefore, occurs at large values of Reynolds number, step height and skirt width. A value of $h/h^* = 1.95$ was observed at

$Re = 70,000$

$H/L = 1/5$

$W/L = 1/5$

where L = The plate length, mm.

The enhancement of h can be explained, states Sparrow, in terms of the separated flow region which occurs at the leading edge of the elevated surface. This zone is illustrated in Figure 3.10. The separation region contains vigorously recirculating fluid of a turbulent nature. So in this zone there are higher local heat/mass transfer rates. Hence the larger this zone the greater the overall heat transfer coefficient.

The extent of the separation zone decreases with increasing attack angle, and at an angle roughly corresponding to α' disappears altogether. The extent of the separation zone shows basically the same dependence upon Reynolds number step height and skirt width as does the heat transfer enhancement. Therefore the conclusions above, can be readily understood in these terms.

VI 45° Pitch Roof

The aim of this series of experiments was to examine the difference in heat transfer coefficients, between a windward and leeward orientated roof shape. The original hope was that the leeward surface would offer shelter from the wind-flow, and therefore lead to lower heat transfer rates.

For the windward orientation the heat/mass transfer was found to follow the usual relationship in that

$$j = 0.97\ Re^{-0.5} \tag{3.53}$$

$$\therefore \quad h = 5.7\ V^{0.5}\ x^{-0.5}\ Wm^{-2}K^{-1} \tag{3.54}$$

In the leeward orientation the heat/mass transfer did not quite follow the well known relationship i.e. the 0.5 power law relationship did not hold, indicating that the flow over the plate in the leeward position was not laminar. The dependence on the Reynolds number of the j-factor decreased with increasing Reynolds number.

The results of the two orientations were compared. It was found that for Reynolds numbers less tha 6×10^4, the heat transfer coefficient was greatest for the windward orientation. For Reynolds numbers greater than 6×10^4, however, the heat transfer coefficient

was greatest for the leeward orientation. In both cases, the value of the j-factor for a given Reynolds number did not vary by more than ± 5%. Thus the hope of any major sheltering effect, according to Sparrow, is eliminated.

These results were interpreted in terms of the flow regimes around the roof. At low Reynolds numbers the leeward face is slightly shielded, but is still subjected to a recirculating flow. At higher Reynolds numbers this recirculation becomes more vigorous. Therefore, the heat transfer coefficient is enhanced above its corresponding windward value.

VII 45° Roof Pitch - Adiabatic Extensions (Sparrow [1982])

Experiments in this series were conducted with the same roof shape as described above. The effects of four types of adiabatic framing, on the heat/mass transfer, were examined. The first two types of framing were the same as A and D in series III, as illustrated in Figure 3.8. The third and fourth types of framing consisted of a narrow strip, applied first to the top edge of the active surface, near the roof ridge line, and then to the bottom edge. By comparing the heat transfer results to those of the unframed leeward surface results of series V, it was found that:

(a) Both the lateral framing cases, A and D, gave rise to increased heat transfer coefficients over the unframed case.

(b) The enhancement of h was larger for the wide framing case, with a maximum increase of 20% being observed.

(c) The effect of the enhancement decreased with Reynolds number.

(d) Both the top and bottom edge framing had no measurable effect on the heat transfer coefficient.

These conclusions can, again, be reconciled by a consideration of the flow characteristics on the leeward face of the roof pitch. A flow visualisation, using lamp black, was employed. These studies revealed a pair of parallel counter-rotating eddies whose axes are also parallel to the lateral edges of the roof surface. The flows in the outer portions of the two eddies collide as they approach the centre line of the surface. This gives rise to a stagnation line at this point. The effect of this is to increase the local heat/mass transfer in the centre portion of the roof.

Thus framing those areas, i.e. the edges of the roof, where there is a relatively low transfer rate, serves to increase the overall transfer rate. The top and bottom framing will have little effect as the transfer rate in those areas will be close to the average for the plate.

In this series the effect of eaves was also examined. It was found that eaves placed on the lateral edges of both the windward and leeward sides of the model had no significant effect on the heat/mass transfer rate.

3.3.5 Summary

The results of all the experiments described above, except series IV, and the leeward results of series VI can be reduced to a global correlation of

$$j = 0.86\ Re^{-0.5} \tag{3.55}$$

$$h = 5.1\ V^{0.5}\ x^{-0.5}\ \ Wm^{-2}K^{-1} \tag{3.56}$$

With an accuracy of $\pm$ 10% this includes all angles of attack and yaw considered. It would therefore appear that the value of C is universal under these conditions.

The j-factor is also equivalent to the dimensionless grouping Nu $Pr^{-1/3}$/Re. So the Nusselt number may be correlated with the Reynolds number as, using C = 0.86.

$$Nu = 0.86\ Re^{0.5}\ Pr^{1/3} \qquad (3.57)$$

This equation agrees in form with the laminar equation for a flat plate but the value of the constant is some 30% higher in the experimental case.

If equation 3.57 is dimensionalised by substituting in the properties of air at 300 K and a value of x typical for the series of experiments i.e. x = 75mm = 0.075m then we obtain

$$h = 18.6\ V^{0.5}\ \ Wm^{-2}K^{-1} \qquad (3.58)$$

This is compared to the average correlation for heat transfer results in parallel turbulent flows, equation 3.21, in Figure 3.11. The third line shows equation 3.57 dimensionalised using x = 0.5m, which is typical of the dimensions found in the experiments described in Section 3.1. As can be seen there is "order of magnitude" agreement between the data but a substantial percentage difference overall.

Despite the fact that Sparrow does not examine any scale effects, i.e. by varying the characteristic dimension (x), he applies his results to full size solar collectors which are two order of magnitude larger. He also applies the results to wind speeds lower than those studied experimentally and as these experiments do not take into account natural convective effects this type of extrapolation would seem unwise.

This, coupled with the facts that the mass transfer boundary conditions corresponds to a uniform surface temperature and that no real attempt was made, despite having the facilities to study the effect of yaw where it would probably have the most effect i.e. over the 45° roof pitch, still leaves doubt in this author's mind as to the total applicability of these results to heat loss from flat plate solar collectors. The most useful results, however, are probably those which relate most closely to the geometry of actual collectors i.e. series V - a plate elevated above an host surface. These indicate that for this type of surface the heat transfer will be enhanced above its nominal flat plate value.

3.4 Convective Heat Transfer from a Rectangular Body Submerged in a Two Dimensional Flow

3.4.1 Wind flow over a rectangular body

As mentioned in the discussion of the work of Sparrow et al, the flow over a plate of finite thickness is quite different to that over an infinitely thin plate or one with a stream-lined leading edge. Solar collectors represent such a bluff body. A brief study of the flow over rectangular plates is a pre-requisite to the understanding of the heat transfer from such a surface. Ota and Itasaka [1976] examined the two dimensional incompressible flow on a flat plate with finite thickness and a blunt leading edge. The flow configuration treated in this study is shown in Figure 3.12. As can be seen the flow separates at the leading edge of the plate, it then reattaches to the surface at a distance downstream from the leading edge. From this point it subsequently redevelops in the downstream direction.

It was found that flow reattachment occurred at about 4 to 5 times the plate thickness downstream from the leading edge and that the flow did not fully redevelop until about 20 times the plate thickness downstream.

The effect of angle of inclination, to the air flow, of a rectangular body was studied by Sam et al [1979]. At small angles of attack the flow pattern will be similar to that already discussed above. Increasing the angle of attack eventually results in a stagnation point at the upper corner of the plate. This is illustrated in Figure 3.13. At large attack angles the stagnation point (as shown in Figure 3.13) will be located on the upper surface of the plate. The flow will then separate from the leading and trailing edges of the plate.

For zero attack angle Sam et al concluded that the reattachment distance was 4.68 plate thickness downstream from the leading edge; this is in good agreement with Ota and Itasaka. This is despite the two plates used having widely differing aspect ratios, i.e. the ratio of plate thickness to plate length. For Ota and Itasaka this ratio was 1:26 which is similar to that found in solar collectors (as shown in the Introduction to this Chapter) and for Sam et al it was 1:6. This is actually within the range found for real collectors.

The variation of reattachment distance with angle of attack, α, was determined in the range $0° < \alpha < 10°$. The results were non-dimensionalised in terms of the plate thickness H and the plate length L.

$$(H/L)_{Reattachment} = 0.785 - 0.0991(\alpha) + 0.004(\alpha^2) \qquad (3.59)$$

Extrapolation of this equation beyond its limits would seem unwise, even though it would offer an approximation to the angle of attack at which the separation bubble does not occur. However, by considering the pressure distribution across the plate, and in particular the back-pressure, i.e. air movement opposite to the general flow direction, Sam concluded that separation ceases to exist at an angle of attack between 20° and 30°.

Because of these variations in flow regime over the plate the local heat transfer coefficient will also vary with position along the plate. Several workers have undertaken experiments to study the heat transfer from rectangular bodies in two-dimensional flows.

3.4.2 The work of Ota and Kon

Ota and Kon [1974] examined the heat transfer in the separated and reattached flow on a blunt flat plate, with the airstream blowing normally to the leading edge.

The experiments were carried out on a 20mm thick, 100mm long, 400mm wide plate placed in the two dimensional flow of a low turbulence wind tunnel. It was found that generally higher heat transfer rates existed near the leading edge of the plate. This is in agreement with the work of Sparrow et al [1981 (b)] described earlier. The maximum local heat transfer rate was found to exist at around 4 to 5 plate thicknesses downstream from the leading edge at a position, roughly corresponding to the reattachment point. The reason for these high rates of heat transfer in this region, typically twice those found in the redeveloped flow downstream, is that the flow is rapidly recirculating in the separation bubble.

Ota and Kon [1979] also examined the effect of nose shape on the heat transfer rates from a rectangular body. The reattachment distance was found to decrease with decreasing nose angle, its value being only a fifth of its blunt plate value for a nose angle of 60°. This implies that by streamlining the leading edge the separation zone and hence the overall heat transfer coefficient will be reduced. Of course if the leading edge is streamlined enough the plate will assume the properties of an infinitely thin flat plate.

3.4.3 The work of Test et al

Test and Lessmann [1980] examined the heat transfer from a rectangular body 34mm thick 203mm long which filled completely the width of a 775mm square wind tunnel. The plate was arranged so it could be rotated and thus a range of wind attack angles investigated.

It was found that the heat transfer rate decreased with increasing attack angle up to about an attack angle of 30°. Then the heat transfer was reasonably constant with any further increase of attack angle. This is to be expected as the separation bubble disappears at attack angles above this value and the rectangular body acts as a flat plate

Perhaps the most important piece of work to date performed to examine heat transfer from rectangular bodies (in relation to the study undertaken here) was carried out by Test et al [1981]. The experiments were performed in the natural environment using a plate with dimensions 1.22m (long), 0.81m (wide) and 0.2m (deep). Because the plate had a finite width it was necessary, in order to induce pseudo-two-dimensional flow conditions over the plate, to place side baffles along the streamwise edges of the plate. Several baffle

configurations were tested using a 1/8 scale model of the plate in a wind tunnel. Particular attention was paid to the effectiveness of each baffle arrangement in yaw. Two dimensional flow was found to be most closely simulated using baffle plates, each half the width of the plate, inclined at 45° to the plate surface. Side attachments of this type were fitted to the full scale plate.

The top surface of the rectangular box contained three rows of heating elements (each of area 150mm sq) with eight elements in each row. The middle row, corresponding to the streamwise centre line of the plate, was used for the heat transfer measurements. Heating elements in the outer rows acted as guards. The whole heated section of the plate was kept isothermal to $\pm$ 1.1 K during test runs using a rheostat.

In order to avoid any separation affects the plate was inclined at 40° to the horizontal. All measurements were taken at night in order to avoid any direct solar radiation inputs, and the heater surfaces were made of polished chrome so as to reduce the radiative exchange with the sky to a minimum.

Because the measurements were carried out in the natural environment, a crucial element of the experiments was the evaluation the wind flow past the plate. An anemometer consisting of a triaxial array of helicoid propellers, as described by Gill [1973] was placed 1m above the top edge of the test surface. It was calculated that the error in evaluating the mean wind speed over a run was of the order of $\pm$ 4%. In order to achieve this accuracy, and to ensure a greater degree of two-dimensionality of the flow over the plate, the test rig was always placed with the heated surface facing the mean wind flow direction.

Test runs were typically of the order of four hours and wind speeds in the range 2.2 to 5.6 ms^{-1} were encountered. The arithmetic average heat transfer coefficient was evaluated over the whole test surface and a linear regression gave:

$$h = (2.56 \pm 0.32)V + (8.55 \pm 0.86) \quad Wm^{-2}K^{-1} \qquad (3.60)$$

This is in excellent agreement with the work of Rowley et al on smooth glass surfaces placed flush with the sides of a wind tunnel (see equation 3.8). However, as compared to wind tunnel results on the small scale model of the plate the outdoor results were approximately twice as high. Test states that these variances could be due to either the lack of true two-dimensional flow over the test piece or the large levels of free-stream turbulence in the natural environment. The effect of free stream turbulence on the heat transfer coefficient will be examined in the next section.

Despite, as mentioned earlier, the general importance of this work, in that it deals with the heat transfer from a flat plate in the natural environment, care must be taken in assessing its suitability for predicting the convective heat transfer coefficient from flat plate solar collectors.

It must be remembered that the flow over an un-baffled plate is three-dimensional and that solar collectors do not always face the mean wind flow. Secondly the heat transfer measurements in this series of experiments were taken along a strip up the centre line of the plate and not over the entire surface. This is where the two dimensionality of the flow will be strongest and the rest of the plate acts as an adiabatic extension piece. Sparrow has shown that this type of framing can have some effect on the heat transfer

(see Section 3.3.4). Finally despite having some data at lower wind speeds than the range already mentioned, these points were not included in the correlation given in equation 3.60. These low wind speed values would help give a clearer indication of the true value of the natural convective component of the heat transfer coefficient.

3.5 The Influence of Turbulence on Heat Transfer from a Flat Plate

The theoretically derived relationships for heat transfer to laminar and turbulent boundary layers share the basic assumption that the free-stream was initially free from any turbulence. It is impossible to eliminate free-stream turbulence from any physical wind flow. It has already been suggested e.g. by Test et al [1981] that this turbulence may have some affect on heat transfer results. In order to assess whether this is true, it is necessary to derive a standard definition of turbulence intensity. By assuming that the mean velocity of the flow is V_∞ and that superimposed upon this velocity are three coplanar velocity fluctuations U', V' and W' (U' is usually taken as the fluctuation of the flow in the mean direction of the flow) the turbulence intensity T_u is defined as:

$$T_u = \sqrt{\frac{1}{3}(\overline{U'^2} + \overline{V'^2} + \overline{W'^2})}/V_\infty \qquad (3.61)$$

If, as is often the case, the velocity fluctuations become isotropic, i.e.

$$\overline{U'^2} = \overline{V'^2} = \overline{W'^2}$$

Then it is sufficient to define the turbulence intensity thus:

$$T_u = \sqrt{\overline{U'^2}}/V_\infty \qquad (3.62)$$

The numerator in the above expression is the root mean square of the velocity fluctuation and will be denoted by U* in this thesis.

The turbulence intensity in a wind tunnel can be varied by the introduction of screens at the entrance to the tunnel. These screens have the effect of churning the windflow in the desired fashion. The environmental windflow is naturally turbulent, and the turbulence intensity will vary with ground roughness and height. It is often more explicit to express the turbulence intensity as a percentage, i.e. the right hand side of equation 3.61 multiplied by 100. The turbulence intensity produced in wind tunnels is of the order of 5% whilst that measured in the outdoor environment is of the order of 20% - 30% (for example see Counihan [1965]) depending on height, etc.

3.5.1 A summary of experiments conducted to investigate the influence of free stream turbulence from a flat plate

Edwards and Furber [1956] undertook experiments to determine the influence of the free stream turbulence on the average coefficient of heat transfer from a flat plate provided with a round nose of very small radius. Two wind tunnel screens were used to promote turbulence intensities of 1.5 and 2.5% This investigation led to the conclusion that changes in free stream turbulence of this order had no effect on the rate of heat transfer across a laminar or turbulent boundary layer. However, it was noted that a higher turbulence intensity promoted transition, between laminar and turbulent boundary layers, at a lower Reynolds number.

Earlier Fage and Faulkner [1931] had performed experiments on a thin, electrically heated, platinum foil and found no influence of the free-stream turbulence intensity in the laminar range to which their measurements were confined.

The local coefficient of heat transfer from a flat plate to a turbulent air stream was measured by Sugawara and Sato [1958]. Their experiments showed no effect in the laminar region for intensities up to 1%, in agreement with Edwards and Furber. However, in the turbulent range they measured large increases is the local Nusselt number. Increases in the Nusselt number of up to 55% were observed for a variation in turbulence intensity from 1% to 8%

Kestin et al [1961] studied the influence on heat transfer from flat plates of turbulence levels in the range 0.7% to 3.8% and were again unable to find any major effect.

In the outdoor study made by Test et al [1981] mentioned in Section 3.4.3. heat transfer enhancement of around 300% was found over tests carried out on similar plate geometries placed in a low turbulence wind tunnel. The measured natural turbulence was of the order of 30% - 40%, whilst the wind tunnel turbulence intensity was around 3%

This spurred McCormick et al [1984] to make a systematic study of the heat transfer from rectangular bodies, in a two dimensional flow, as influenced by free-stream turbulence intensities. Experiments were carried out in a low speed open-circuit wind tunnel with a 0.77m square test section. The model had a rectangular cross-section and dimensions of 203mm by 51mm high. Thus giving it an aspect ratio of 1:4. The local heat transfer rates were measured at 16 stations in the span wise direction using small heated plates. These heaters were guarded in a similar manner as those of Test [1981], by heaters placed either side of the central line. By inclining the plate at 40° to the wind flow the stagnation point was located near the leading edge, thus eliminating any separation effects.

The presence of the model induced a free-stream turbulence level of about 5.5% Two further levels of turbulence were created by the positioning of slats upstream from the model. These turbulence intensities varied over the chord length of the model. The first varying from 45% at the leading edge to 17% at the trailing edge. A similar variation for the second level was 19% to 10%.

Turbulence intensity effects were observed. The overall heat transfer from the plate increased with free-stream turbulence levels. By taking the 5.5% turbulence intensity as the base increases of the order of 60% in the heat transfer were observed for the highest turbulence level and 20% for the intermediate level.

3.5.2 Summary

It can be seen therefore that there is conflicting evidence on the subject of turbulence effects, but in general it is thought that high levels of turbulence intensity, such as those found in the natural environment will lead to much higher rates of heat transfer than from similar geometries placed in a low turbulence wind tunnel. Therefore, care must be taken when comparing, seemingly identical, laboratory and outdoor data, and it is recommended that in wind tunnel tests turbulence levels similarto those found in the natural environment should be created.

3.6 Heat Transfer Experiments on Three Dimensional Bodies in a Simulated Natural Environment

The experimental data discussed so far in this Chapter has, in the main, been obtained from flat plates or bodies submerged in a two-dimensional flow, (the obvious exception being the work of Sparrow et al) which has a constant free stream velocity over the test surface.

However, this study is primarily concerned with solar collectors placed on dwellings in the outdoor environment. It is therefore necessary to consider experiments performed on three-dimensional bodies placed in three-dimensional flows. Especially those dealing with building shapes or closely related geometries. Several experiments have been carried out in wind tunnels adapted to simulate the natural environment. In order to understand this simulation it is necessary to examine first the nature of the earth's atmospheric boundary layer.

3.6.1 The earth's atmospheric boundary layer

The earth's atmosphere is always in motion and as the winds blow over the globe they maintain a "layer of frictional influence". This is known as the atmospheric boundary layer and extends to heights typically of the order of one kilometre. In this layer the mean wind velocity varies with height. This is similar to the boundary layer over a smooth flat plate with its increased depth being due to the general roughness of the earth's surface. So the boundary layer velocity profile is not constant but alters locally due to variations of surface roughness, i.e. the presence of buildings and trees, etc.

A full discussion on the variation of velocity with height for various terrain types is given in Counihan's [1975] classic review paper which examines and analyses wind data over the period 1880-1972. However for the purposes of this section it will be sufficient to note that a simple expression for the wind profile over a given terrain is given by:

$$\frac{V_1}{V_2} = \left[\frac{Z_1}{Z_2}\right]^{\alpha} \qquad (3.63)$$

where V_1 = The mean velocity at height Z_1

V_2 = The mean velocity at height Z_2

α = A constant depending upon the local terrain

A basic definition of terrain types and the associated values of α are presented in Table 3.3 after Counihan. Typical wind profiles are shown in Figure 3.14.

Table 3.3 Values of α to be used in Equation 3.63

After Counihan [1975]

Classification of Terrain Type	Terrain Description	α Range
Smooth	Ice, mud, snow sea	0.08 - 0.12
Moderately Rough	Short grass, crops rural	0.13 - 0.16
Rough	Rural/woods, woods suburbs	0.20 - 0.23
Very Rough	Urban	0.25 - 0.40

The simplicity of equation 3.63 however, leads to errors in the estimation of the wind speed, especially in the lower 30-50m of the boundary layer. As this work deals mainly with low rise dwelling then this failing cannot be ignored. For these cases it has been found that wind velocity data is better fitted by a log relationship of the form:

$$\frac{V_1}{V_*} = \frac{1}{k} \text{Ln} \left[\frac{Z_1}{Z_o}\right] \qquad (3.64)$$

where V_* = The friction velocity

Z_o = Roughness length, m

k = Von Karman's constant usually taken as 0.4

The friction velocity is defined by Flay et al [1982] as

$$V_*^2 = -\overline{UW}$$

where U = Wind velocity component parallel to the mean wind vector

W = Wind velocity component vertical to the mean wind vector

Flays measurements of the wind profile over a rural terrain gave values of V_* of approximately 0.6. Table 3.4 gives values for the roughness length Z_o for the various terrain types described in Table 3.3.

Table 3.4 Values of z_o to be used in Equation 3.64 for Various Terrain Classifications - After Counihan [1975]

Terrain Classification	Z_o Range
Smooth	0.01 - 20mm
Moderately Rough	1.0 - 200mm
Rough	1.0 - 1.5m
Very Rough	1.0 - 4.0m

It is not sufficient to characterise the natural wind by its velocity profile alone. The atmospheric boundary layer is highly turbulent and unlike the ideal case mentioned in Section 3.5 is non isotropic i.e. the values of U', V' and W' (longitudinal, lateral and vertical components of the turbulence) are not identical. Several workers have performed measurements of turbulence intensities in the

natural environment and many of these have been reported by Counihan [1975]. The general conclusion from this review paper is that for urban sites the longitudinal turbulence, based on local mean velocity, lies in the range 20-30% and that for sites with a rural terrain the corresponding range is 10-20%. A more recent experimental study by Flay et al [1982], has shown that for a very exposed site, the longitudinal turbulence intensity in the first 20m of the atmospheric boundary layer lies in the range 14-21%. The importance of Flay's work in relation to this current study lies in the fact that here the primary concern is with low rise dwellings. This type of building will be situated in the portion of the boundary layer in which Flay made his turbulence intensity measurements.

The usual method of rationalising the non-isotropic nature of the natural wind is to compare the root-mean-square values of the three velocity fluctuations, i.e. U^*, V^* and W^*. This is done by non-dimensionalising them in terms of the friction velocity V_*. Counihan gives the following, taken as an average for all the data he surveyed in his review paper.

$$U^* : V^* : W^* : V_* = 2.50 : 1.88 : 1.25 : 1.00$$

Flay's more recent work gives good agreement with these values, i.e.

$$U^* : V^* : W^* : V_* = 2.43 : 1.93 : 1.20 : 1.00$$

The longitudinal integral length of turbulence LU_x, is a measure of the dominant eddy size in the turbulence. Its value is a function of height above the ground. Whilst Kestin [1961] has shown that the effects of turbulence scale can be neglected with regards to convective heat transfer, it is still a relatively important parameter in defining the flow characteristics of the natural wind. In general

LU_x decreases with increasing surface roughness and increases with height up to around 200-300m, Counihan [1975]. Actual values of LU_x are given by Berman [1965] for various values of Z_o at a height of approximately 15m. These range from LU_x = 36m at Z_o = 1.00m to LU_x = 82m at Z_o = 0.01m

The final characteristic of importance when defining the flow of the natural wind is the Reynolds stresses. These shear stresses arise from the fluctuations in the velocity components parallel and vertically perpendicular to the flow U' and W'. For urban areas Smith [1970], quoted by Counihan, states that

$$0.003 < \frac{-U'W'}{V_g^2} < 0.0045 \qquad (3.65)$$

where V_g = the wind velocity at the top of the atmospheric boundary layer, i.e. free-stream, ms^{-1}

and the estimated range for rural sites given by Counihan is:

$$0.002 < \frac{-U'W'}{V_g^2} < 0.0045 \qquad (3.66)$$

Thus the natural wind can be evaluated in terms of the above five parameters i.e., α, Z_o, turbulence intensity, turbulence scale and Reynolds stresses. The next section deals with methods by which these characteristics can be adequately simulated using wind tunnels.

3.6.2 Laboratory simulation of the atmospheric boundary layer

The simulation of the natural boundary layer in wind tunnnels has been discussed by several authors, for example Cermak [1971] and Cook [1978]. The general concensus of opinion is that the best way to simulate the boundary layer is to use a wind tunnel of large cross-section. By introducing roughness elements on the tunnel floor

a thick boundary layer of the required form is produced. Roughness elements of various sizes are obviously required to simulate the various terrain types. The elements are usually made of small blocks of wood or foam rubber for the higher roughness terrain types and sand paper or a layer of gravel is often adopted for the smoother terrains.

Cook [1978] also discusses the scale factor to be adopted when simulating the natural wind as does Jensen [1958]. Jenson postulates a simple scaling law based on the roughness length and the model to full scale ratio. This is expressed as

$$\frac{Z_{oFS}}{Z_{om}} = \frac{D_{FS}}{D_m} \qquad (3.67)$$

where Z_{oFS} = Roughness length in nature

Z_{om} = Roughness length in the wind tunnel

D_{FS} = Linear measurement of the full scale

D_m = Linear Measurement of the model

This, states, Jensen is adequate to determine the scale factor provided the model is entirely immersed in the turbulent boundary of the tunnel.

3.6.3 The work of Iqbal and Khatry

Iqbal and Khatry [1977] examined the heat transfer from a heated copper model of a greenhouse. The model was 50.8mm long, 25.4mm wide and 25.4mm high; it had a roof pitch of 45°. The wind tunnel used was 24m long and had a cross section 2.4m square. By placing spires and blocks near the mouth of the tunnel and spreading corrugated cardboard throughout its length on the floor a wind velocity profile similar to that found in rural terrain was developed in the test section. The value of α for equation 3.63 was found to be 0.156; this is in the range of the power indices for rural terrain (see Table 3.3).

Free-stream wind velocities were varied between 4 and 18 ms^{-1}. The model was tested under four different wind directions i.e. 0°, 30°, 60° and 90° to its long axis. Thermocouples placed on the surface indicated almost no variation in temperature when the model was heated by an internal 50W heater. The average temperature of the model is not stated.

The overall heat transfer coefficient for the model was calculated and was found to depend on wind speed and to some extent on wind direction. The mean correlation for all wind directions was:

$$h = 17.9\ V_g^{\ 0.576} \qquad Wm^{-2}K^{-1} \qquad (3.68)$$

where V_g = The free-stream wind speed just outside the boundary layer ms^{-1}.

This shows excellent agreement with Sparrows global correlation for heat transfer from a small flat plate given by equation 3.58 i.e.

$$h = 18.6\ V^{\ 0.5}\ \ Wm^{-2}K^{-1} \qquad (3.69)$$

The agreement between the two equations is remarkable. Whilst the two geometries studied had similar linear dimensions i.e. of the order of 50mm, one was a flat plate placed in a uniform flow and the other was a 3-D body placed in a three-dimensional shear flow. This would seem to indicate that the most important parameter, after flow velocity, in the determination of the average heat transfer coefficient from any body, is its dimensions.

The wind direction effect was found to be only $\pm$ 5% over the range of directions tested. This lack of effect is probably due to the overall heat transfer being measured, local variations being averaged out.

The main problem in applying these results to heat loss from flat plate collectors is that the model here was heated all over its surface and no local effects were observable. This is quite clearly not the case for solar collectors, in that the heated surface will only constitute a small section of the roof structure.

3.6.4 The work of Kelnhofer and Thomas

By using a more sophisticated model and heater arrangement Kelnhofer and Thomas [1976] were able to measure local heat transfer coefficients from a cubical model placed both in uniform flow and in a simulated boundary layer.

The model was a cube of 127mm edge with 9 small heater units placed on one face. An energy balance on these heaters provided the local heat transfer results required. A complete distribution of the heat transfer coefficient over the model surface was obtained by rotating the model to position the heated surface at any angle in the horizontal plane. Heat transfer results were obtained from the top face of the cube by changing the heater plate to this location.

Two flow conditions were examined. A uniform flow of turbulence intensity of 0.1% or less, and a shear flow with a value of α in equation 3.63 of 0.33. The turbulence intensity in this flow varied with height, its value being between 2% and 10% over the model dimensions.

Considering the uniform flow condition first. The maximum heat transfer occurs close to the upper sides and edges of the forward face. The lowest at the centre of the front face and the bottom

leading corner of the face parallel to the wind flow. On the top surface the heat transfer increased steadily in the stream wise direction. This in direct conflict with the work of Ota and Kon, etc. described in Section 3.4.2, who found that for a rectangular body in two-dimensional flow the maximum heat transfer occurred at the leading edge. However, it must be realised that the flow conditions in these two experiments are different. For a wind velocity of 12 ms^{-1} the heat transfer coefficient over the model was in the range 52-97 $Wm^{-2}K^{-1}$ with an average value of 76 $Wm^{-2}K^{-1}$. The heat transfer coefficient on the back face was fairly constant only varying between 75 and 85 $Wm^{-2}K^{-1}$.

In the shear flow a similar pattern of the distribution of the local heat transfer was observed save for the fact that the roof values decreased in the stream-wise direction. Again, for a 12 ms^{-1} free-stream wind speed (outside the boundary layer), the range of h was found to be 45-83 $Wm^{-2}K^{-1}$ with a mean value of 61 $Wm^{-2}K^{-1}$. This mean value is some 20% less than the uniform flow condition and can be attributed to a reduction in the mass flux of fluid past the cube.

Wind direction effects were also examined, the wind angle, Θ, being defined as the angle between the mean wind direction and the normal to the surface under consideration. It was found that for the mid position on a vertical surface the heat transfer was a minimum at $\Theta = 90°$, increased to a maximum for $\Theta < 90°$, reaches a second minimum for $\Theta > 90°$, and increases again as Θ approaches 180°. The variation in h with wind angle was more prevalent for uniform flow than shear flow. The overall heat transfer coefficient is constant with a wind angle for shear flow and shows only minimal dependence for uniform flow.

The sheltering effect of neighbouring building models was also briefly studied. It was found that the reduction in the overall heat transfer coefficient becomes greater the larger and closer (to the heat transfer model) the protecting building. The presence of the sheltering building also had effects on the local heat transfer but these results were not presented in the paper.

It was found that dependence on the overall heat transfer coefficient of the wind speed could be described in terms of the mean Nusselt number, and the Reynolds number based on the length of the sides of the cube.

$$\overline{Nu} = C\ Re^{m} \tag{3.70}$$

where C and m are constants depending upon the flow conditions and, in the case of the presence of a sheltering building, the height ratio of the two models. Values of these constants are not presented directly; however, after some calculations on the basic data it was found that for a free standing building in shear flow that:

$$\overline{Nu} = 0.95\ Re^{0.5} \tag{3.71}$$

Hence assuming an air temperature of 300 K we have

$$h = 17.8\ V_g^{0.5}\ \ Wm^{-2}K^{-1} \tag{3.72}$$

This is in excellent agreement with equation 3.69 after Iqbal and Khatry [1977], and the global equation for flat plates by Sparrow et al. Equation 3.72 is only applicable to free-stream wind velocities in the range 5-18 ms^{-1} and it should be noted that this and equation 3.69 do not take into account any natural convective effects.

3.6.5 The work of Kind

Perhaps the most relevant, and certainly most recent, piece of work in this area has been carried out by Kind et al [1983]; because of this and its similarity to model studies conducted in this series of experiments, described in Chapter Six, it will be examined in some depth here.

In this work convective heat transfer coefficients were measured for a model collector array mounted on a model representative of a two-storey solar heated single family residence. The model was, of course, tested in a wind tunnel in which the natural characteristics of the wind were simulated.

The tunnel was of an open circuit type 1.7m wide x 12.6m long; the test section height was 1.2m at the model position. The flow approaching the model was made to simulate the natural environment by distributing roughness elements over the first 10m of the tunnel floor. Turbulence intensities of the order of 20% were produced in the model region and the velocity profile approximated to the log law of equation 3.64 with Z_o = 0.5mm. As the model used was to be of a scale of 1:32 then this value of Z_o satisfies Jensen's criterion, equation 3.67, for simulating a rural environment since, for this type of terrain, full scale roughness length values lie in the range 0.1-200mm.

A second set of roughness elements were introduced to produce a simulated urban environment wind structure. In this case the turbulence intensity in the region of the model was around 30%. No mathematical relationship is given for this velocity profile.

Wind speeds at a height of 140mm ranging from 3 to 15 ms^{-1} were used in these experiments. This height corresponds to the height of the middle of the model collectors above the ground, H. This corresponds to Reynolds numbers, based on the solar collector length L, ranging from 1.6×10^4 to 8.0×10^4.

A two view diagram of the model residential building is shown in Figure 3.15. The model represents at 1:32 scale, a single family residence with six flat plate solar collectors each 1.2m wide x 2.4m high installed on the roof top. By making the model of extruded polystyrene conduction heat transfer was reduced to a minimum. Six electrically heated strip heaters were used to simulate the solar collectors; these were instrumented with a total of 12 resistance thermometers with an accuracy of $\pm$ 0.1 K. Four additional resistance thermometers were installed 20mm behind the heaters in the polystyrene. Measurement of these temperatures under steady state conditions allowed the heat conduction from the back of the heaters to be determined. This and the estimated heat loss by radiation from the upper surface of the plates was subtracted from the overall electrical input to the plates. Hence with a knowledge of the plate and air temperatures the heat transfer coefficient could be calculated.

Plate temperatures were found to be uniform in still air conditions. Two different electrical power levels, 1.2 W and 5.4 W, could be supplied to each heater. At wind speeds above and below 8 ms^{-1} power settings of 5.4 W and 1.2 W, respectively, were used. Heater surface temperatures were typically about 328 K but ranged from 308 K to 353 K. The air temperature was always near 298 K. The run conditions, which were identical except for heater power, and hence plate temperature, gave values for the heat transfer coefficient which

agreed to within 2%. This indicates that the convection film temperature has little influence on the heat transfer over the range tested.

By assuming that natural convection effects were negligible over the range of wind speeds tested, the results were plotted in the form of the Stanton number St against the Reynolds number Re where

$$St = \frac{\bar{h}}{C\ V_H} \quad \text{and} \quad Re = \frac{V_H\ L}{\nu}$$

where $\bar{h}$ = The average heat transfer coefficient $Wm^{-2}K^{-1}$

and V_H = The velocity at the mid collector height, ms^{-1}

No mathematical relationship is offered between St and Re by Kind, and as no primary data is presented it is difficult to obtain any relationship of this type. However by careful examination of the presented graphical data it was possible to obtain the following relationship:

$$St = 0.613\ Re^{-0.459} \tag{3.73}$$

As the Stanton number is also the ratio Nu/Re x Pr the more usual correlation can be obtained i.e.

$$Nu = 0.613\ Re^{0.54}\ Pr \tag{3.74}$$

By substitution of Kind's characteristic model dimension, L, i.e. L = 76mm we obtain

$$h = 23.9\ V_H^{0.54} \qquad Wm^{-2}K^{-1} \tag{3.75}$$

This again shows excellent agreement with the work of Kelhnofer and Iqbal despite several physical differences between the three series of experiments, not least being the position of measurement of the "free-stream" velocity.

If equation 3.75 is expressed in terms of the free-stream velocity of the wind tunnel then the equation below is obtained i.e.

$$h = 19.9\ V^{0.54} \qquad Wm^{-2}K^{-1}$$

This brings it into even closer agreement with the work of Iqbal and Khatry, and Kelnhofer and Thomas.

From his dimensionless power law relationships (i.e. equations 3.74). Kind presents linear relationships of the mean heat transfer coefficient against wind speed for a full scale collector array of height, L = 2.4m. The highest heat transfer rates were found for a wind angle of 90° to the plate normal with:

$$\overline{h} = 2.2\ V_H + 4.0 \qquad Wm^{-2}K^{-1} \qquad (3.76)$$

The lowest for a corresponding angle of 135° with

$$\overline{h} = 1.3\ V_H + 4.0 \qquad Wm^{-2}K^{-1} \qquad (3.77)$$

It should be noted that the non wind speed dependent value of equations 3.76 and 3.77 is also an extrapolation beyond the range of Reynolds number considered.

Tests, using a hot wire anemometer placed close to plate surfaces, indicated that the internal boundary layer over the model was laminar but unsteady. Kind states that in full scale work the internal boundary layer would be expected to be turbulent. This along with the extrapolation method used above indicates some limits to the applicability to full scale collector plates. An urban profile was also examined. The results for the two simulated atmospheric boundary layers were essentially similar, the dimensional correlations of

equations 3.76 and 3.77 being based on the rural simulation case. The leeward values of the heat transfer coefficient are about 20% greater for urban boundary layer over that of the rural. The maximum and minimum values of $\overline{h}$ differed by a factor of 1.8 and 1.5 in the rural and urban boundary layers respectively, over the wind angles considered.

Kind also notes that his data agrees with that of Sparrow et al [1977] for square plates to within 25%. He draws the conclusion that heat transfer coefficient are therefore relatively insensitive to the turbulence level in the approaching flow and to geometry.

Variations in the heat transfer coefficient over the collector array was also examined. It was found that the variation was not large and in the main the average heat transfer coefficient adequately describes the convective heat transfer. The biggest variation was found for a wind angle of 135° and was $\pm$ 20% of the mean value, the largest coefficents being found in the generally down stream positions.

The addition of 14mm eaves all round the roof periphery edge produced only minimal changes in the heat transfer results - of the order of 5%. This is again in agreement with Sparrow's [1982] work on pitched roofs.

3.6.6 Summary

In this section work which has considered convective heat transfer from bluff bodies in three-dimensional flows has been described and discussed. It has been found that the results are compatible with each other and with work performed to evaluate the heat transfer from flat plates of similar linear dimensions. Extrapolation of the data to Reynolds numbers orders of magnitude higher than those studies also shows basic agreement with wind tunnel tests performed on large plates.

Whilst wind tunnel produced atmospheric boundary layers adequately simulate the important flow characteristics of the natural wind it is of interest to consider full scale convective heat transfer experiments conducted in the outdoor environment. The reason for studying this type of experiment is not, perhaps, that the results obtained will be applicable to the convective heat loss from flat plate solar collectors but more to gain an understanding of the special difficulties faced when making such measurements in the natural environment. Full scale measurements of the convective heat transfer coefficient are examined in the next section.

3.7 Full Scale Measurements of Forced Convective Heat Transfer from Buildings

With the notable exception of Test et al [1981] non of the work reported on so far in this Chapter has dealt with convective heat losses in the natural environment. Test, however, reported that the convective heat transfer from flat plates placed in the outdoor environment was substantially different to that from plates of a similar geometry placed in a wind tunnel. This effect was primarily attributed to the large amount of free-stream turbulence present in the natural wind. A full account of the effect of free-stream turbulence on convective heat transfer was given in Section 3.5.1.

One area in which full scale measurements of convective heat transfer have gained importance is in that of heat losses from high-rise buildings. Whilst this study is primarily concerned with convective heat losses from flat plate solar collectors, it is necessary to review this type of experiment in order to gain an understanding of the problems encountered in the measurement of convective heat transfer in the natural environment.

3.7.1 The work of Gerhart

Gerhart [1967] conducted experiments in 1967 to determine the convective heat transfer coefficient from the centre of the top floor of a building measuring 12 x 14 x 30m high. The impetus for Gerhart's work was to estimate the cooling effects of the wind for sizing air-conditioning plants.

The apparatus consisted of two heated aluminium plates, exposed to the external environment on one side and to heat meters and electrical heaters on the other. One plate was painted matt black and the other was left unpainted and polished. If both plates were maintained at the same surface temperature it would be possible to derive values for the convection coefficient, h. The method for calculating h involved the solving of two simultaneous heat balance equations for the two plates A (polished) and B (matt black).

These are:

$$q_A + \alpha_A I + \epsilon_A R_L = \epsilon_A \sigma T_s^4 + h(T_s - T_\infty) \qquad (3.78)$$

and

$$q_B + \alpha_B I + \epsilon_B R_L = \epsilon_B \sigma T_s^4 + h(T_s - T_\infty) \qquad (3.79)$$

where q = The heat flow from heaters, Wm^{-2}

α = The solar absorptance

I = The incident solar irradiance, Wm^{-2}

ϵ = The long wave irradiance, Wm^{-2}

R_L = The incident long wave irradiance, Wm^{-2}

σ = The Stefan-Boltzman constant, $Wm^{-2}K^{-4}$

Solving the above in terms of h gives

$$h = \frac{q_A + q_B + (\alpha_A + \alpha_B) I + (\epsilon_A + \epsilon_B)(R_L - \sigma T_s^4)}{2(T_s - T_\infty)} \quad ,Wm^{-2}K^{-1} \qquad (3.80)$$

Gerhart measured or estimated all the parameters on the right hand side of equation 3.80 and was, therefore, able to derive h. He attempted to correlate h with the prevailing wind speed and direction. These parameters were measured by a cup anemometer positioned 6m above the roof of the building. Gerhart assumed that at this height the wind flow would be undisturbed by the presence of the building. However, more recent wind tunnel work on model representative of a 84m high building by Evans and Lee [1980] suggests that building effects are still discernable at mast height of 8m.

Gerhart presents the results he obtained for wind directions normal and parallel to the building wall containing the heater plates. Each direction exhibits a roughly linear relationship between h and the roof top wind speed with parallel flow producing higher values of h for a given wind speed.

The scatter in the data is large. This is blamed by Gerhart on the sluggishness of his control equipment in trying to maintain equal surface temperatures on the two plates. Sharples [1981] however blames Gerhart's poor experimental design and indicates the following problems. The experiments were made during the daytime in the months of July and August, thus the rapidly fluctuating solar gains become difficult to control. The building facade containing the plates was facing south-west and hence the solar gain problem was further exacerbated. Finally, by using two heated plates with such different values of solar absorptance and long wave emittance, it is hard to imagine any control system which would be able to rapidly supply different amounts of heat to the plates to maintain an equilibrium in surface temperatures.

3.7.2 The work of Ito and Oka

In Japan during the mid-1960's a major project was undertaken to investigate wind effects in urban environments. Part of this project was a study of forced convective heat transfer from full scale building. The development and testing of a unit to perform these measurements is described by Oka et al [1967]

The unit consisted of an exposed copper plate, a heat meter thermopile, another copper plate, a heat unit and finally an aluminium plate backing. The entire system was sandwiched together and surrounded, with the exception of the exposed plate, by insulation.

After initial wind tunnel tests to examine the thermal characteristics of the unit, the apparatus was used to estimate forced convection coefficients in the natural wind. This work is described by Ito et al [1967]. Unfortunately the English translation of this paper does not make it clear whether the heat meter systems were located on a building facade or an exposed site.

In these field measurements Ito et al adopted the same approach to deriving h as Gerhart, with the exception that one experimental variable, the solar irradiance I, was removed by making measurements only at night. Despite having removed one of the major causes of scatter in Gerhart's work, the results of Ito's experiment do not show any clear relationship between h and the wind speed. Although a sloping line has been drawn through the data points presented in Figure 1 of the paper, there is no possibility of a significant correlation existing with the data as shown.

Despite the inconclusive nature of these early tests the Japanese workers went on to investigate systematically the forced convective heat transfer from a full scale building. The importance of this work, described by Ito et al [1972], lies in the fact that it represents the first attempt to study how wind speed, wind direction and location on a building facade interact to effect the convection loss from a building facade.

An important change in the experimental technique for this full-scale work was the use of two identical heat meter systems both painted matt black at their external surfaces. This means that the incident long wave radiation need no longer be measured, as an equal amount of radiation is absorbed by each plate. The only disadvantage to this method is that the plates need to be kept at slightly different temperatures in order to derive h. Nocturnal energy balances of the two identical plates A and B are given by:

$$q_A + \varepsilon R_L = \varepsilon\sigma T_A^4 + h(T_A - T_\infty) \qquad (3.81)$$

$$q_B + \varepsilon R_L = \varepsilon\sigma T_B^4 + h(T_B - T_\infty) \qquad (3.82)$$

Hence, assuming $T_A > T_B$

$$h = \frac{q_A - q_B - \varepsilon\sigma(T_A^4 - T_B^4)}{T_A - T_B} \quad ,Wm^{-2}K^{-1} \qquad (3.83)$$

This solution assumes that the difference between the two surface temperatures T_A and T_B is small enough to assign a common value of h to both plates. Ito does not state the temperature difference used. However, from the work of Rowley et al [1930], described in Section 3.1.3 it may be assumed that the heat transfer coefficient is relatively insensitive to small changes in surface temperature.

The air temperature near the surface and at roof level was recorded along with the local wind speed 300mm from the building surface and 8m above the roof. It must be recalled at this point that Houghten et al [1931] determined that wind velocity does not reach a uniform value until a distance of about 260 - 330mm away from a 3.05 x 1.84m smooth plate. With the increased friction effects caused by the roughness of the building surface and the general development of the boundary layer along the wall it may be expected that the wind velocity as measured at 300mm from the surface will not be free from the effects of the building facade.

Initially a site at the centre of the 6th (top) floor was investigated; later measurement were recorded at the centre and edge of the 3rd, 4th, 5th and 6th floors. These measurements were not made concurrently. No information regarding the surrounding terrain and building is provided.

Ito analysed his data by first reducing it to 15 minutes mean values and then examining the relationships between the convection coefficient, h, the roof top wind speed, V_R and the surface wind speed V_S. His conclusions were, that

(I) V_S was 0.25 to 0.33 times V_R when the surface was windward, but virtually independent of V_R when the surface was leeward.

(II) The $V_S - V_R$ relationship varied with surface location and wind speed

(III) The $h - V_R$ relationships varied with surface location and the data points exhibited a large scatter

(IV) The $h - V_S$ relationship was relatively independent of surface location and wind direction.

Table 3.5 shows best straight line fits by eye to Ito's data for the $h - V_S$ and $h - V_R$ relationships. These fits would be more appropriate for windward surfaces only, since Ito's data contains very few leeward wind directions. It must be again reiterated that the data points showed a large scatter. For example, with a roof wind speed of 4 ms^{-1} the data points exhibit a spread of $\pm$ 20% about the value derived from the best fit relationship. This is for the 3rd floor centre location and other locations exhibit a similar scatter.

Table 3.5 Best Straight Line Fits by Eye to the Data of Ito et al [1972]

Site Location	Roof Top Wind Speed V_R ms^{-1}	Surface Wind Speed V_S ms^{-1}
6th Centre (6C)	$h = 2.5\ V_R + 10.0$	$h = 9.7\ V_S + 2.5$
4th Centre (4C)	$h = 2.0\ V_R + 3.5$	$h = 8.6\ V_S + 3.2$
4th Edge (4E)	$h = 2.5\ V_R + 4.6$	$h = 7.7\ V_S + 4.6$
3rd Centre (3C)	$h = 0.8\ V_R + 5.8$	$h = 5.8\ V_S + 5.8$
3rd Edge (3E)	$h = 2.4\ V_R + 3.3$	$h = 8.5\ V_S + 3.6$
	$Wm^{-2}K^{-1}$	$Wm^{-2}K^{-1}$

It is apparent that Ito's measured values of h increased with height and distance from the centre line of the building. This implies that the highest rates of convective heat transfer should occur at the 6th floor edge site. This compares well with Kelnhofer and Thomas's [1976] work on a cubical model described in Section 3.6.4, despite the fact that Ito's building was of a unique open L-shaped plane. No data for this assumed maximum position is given by Ito.

A further limitation on Ito's work is that only a limited number of wind directions were examined, a large proportion of his data being for winds blowing nearly normal to the measuring surface. Consequently Ito did not have the range of wind speeds and directions to give definite statements on the influence of these parameters on h.

The heat meter plates used by Ito in this series of experiments were 0.3m square, thus they are comparable,in terms of the characteristic dimensions of the plates with the work of Reynolds [1930] and Jurges [1924] as described in Section 3.1.2 and 3.1.3. Figure 3.16 illustrates the correlations of these two earlier pieces of work with the extremes of the data presented in this section. From this figure it can be seen that the work conducted on flat plates in wind tunnels is very similar to the outdoor heat transfer data when it is correlated with the roof top wind speed, V_R. There is, however, little agreement with the full scale data when it is correlated with the local surface wind speed, V_S. This indicates, perhaps, that a better indication of the free stream wind speed about the building is given by that measured 8m above the roof as opposed to that measured 300mm away from the building facade.

3.7.3 The work of Sturrock

Sturrock [1971] made full-scale, nocturnal measurements on a 26m high building in Liverpool. The building was sheltered to the North so the test points were located on the more exposed southern facade.

The heat meter system Sturrock used consisted of short strips (50 and 100mm long) of nicrome wire, 12mm wide, which were warmed by resistive heating. This means that the heat source and heat meter are, essentially, combined into one unit. The ribbons were heated directly by passing an electric current through them. Knowledge of the current and ribbon resistance allowed the resistive heating of the elements to be calculated. Surface temperatures were measured by copper-constantan thermocouples spot welded to the underside of the ribbons.

One disadvantage of this system is its small size. As mentioned in the introduction to this section forced convective heat transfer is an important process on building elements only when those elements have a very rapid thermal response to climatic perturbations. The predominant building element with this feature is the window. In winter a window will normally appear as a warmer surface than a wall due to its more rapid response to the effect of internal room temperatures.

The average forced convection coefficient of a heated surface, as shown by Parmelee and Hubscher [1946], is a function of its length. Therefore, while it is very difficult to produce and mount heat meter systems of several square meters, it is desirable to have a unit with dimensions of the order of those that might be found for a window. This is obviously not the case in this series of experiments.

A second disadvantage of this system concerns the assumptions which were made about the radiative, conductive and natural convective losses from the heater unit.

For a unit length of the ribbon Sturrock gives the heat balance equation as:

$$I_c^2 r = h.A.\Delta T. + E \qquad (3.84)$$

where

I_c = the heater current, amps

r = the resistance, per unit length, ohms m^{-1}

h = the forced convection coefficient, $Wm^{-2}K^{-1}$

A = the exposed surface surface area, m^2

ΔT = the air-surface temperature difference, K

E = the remaining heat losses from the surface by natural convection, conduction and radiation, W.

E was determined by placing the heater element in a "draught free area" (a non-operating wind tunnel section), applying several different power inputs to obtain different values of ΔT and then using equation 3.84 with h set at zero. The range of ΔT was approximately 5 to 25 K.

The value of E thus derived was then assumed to be constant for the heating element after it was removed from the test section and attached to the building. Values of h were then derived from equation 3.84 by measurement of I_c and ΔT.

It is difficult, however, to imagine that E will remain constant when exposed to the environment. There are several reasons for this. It is derived from measurements within an enclosure which could be taken approximately as an isothermal black body. Under exposed conditions the radiative environment

seen by the element will be much different and more variable. E will also be affected by the change in the total radiative emittance of the ribbon which will inevitably occur as its surface tarnishes. Finally the natural convection component of E may be affected by the length of wall, the wall temperature, the temperature step occurring at the edge of the heated ribbon and the wind velocity - especially at the lower end of the range.

Measurements were made on a wall forming part of a roof top structure and half way up the main wall of the building. Wind speed and direction were recorded on a mast - mounted cup anemometer on the top of the building.

Sturrock's main conclusion was that the convection coefficient was as much a function of wind direction as wind speed. The highest rates of heat transfer occurred when the heat meters were windward. However, as the building under test was sheltered by other structures to the north, only winds from this direction, which would put the heat meters leeward, would be likely to have a diminished impact. A brief discussion of the sheltering effects of other buildings on heat transfer from cubical models was given in Section 3.64, due to Kelnhofer and Thomas [1976].

From his measurements Sturrock suggests two relationships:

for an exposed surface

$$h = 6.1\ V_R + 11.4 \qquad Wm^{-2}K^{-1} \qquad (3.85)$$

for an average surface

$$h = 6.0\ V_R + 5.7 \qquad Wm^{-2}K^{-1} \qquad (3.86)$$

It must be noted at this stage that these correlations give much larger values of h for a given roof wind speed than for those of Ito presented in Table 3.5, though there is some agreement between the non-wind speed dependent values.

There are two main possibilities for these differences. Firstly, the buildings and surroundings in the two experiments might be sufficiently unalike to produce extremely different flow regimes about the test site. This could imply that any full-scale measurements of this nature may only be applicable to the particular situation under consideration. It therefore highlights the irrationality of applying one set of results to a wide variety of physical situations.

Secondly, the very small size and high working temperatures of Sturrock's heat monitoring system probably led to unrealistically high values of convection coefficients.

3.7.4 The work of Nicol

Nicol [1977] conducted full-scale measurements of the convective heat transfer coefficient from at Inuvick, Canada. The site was at a latitude of 68°N and air temperatures as low as 219 k were recorded during the experiment. Nicol pointed out that this type of climate "enhances the energy lost through the window surface".

Nicol's experimental technique was simple and different from those previously described. He used the energy balance equation for a window given by

Heat flow conducted through glass	=	external surface radiation exchange	+ external surface convective heat flow	(3.87)

to derive h indirectly. The external and internal surface temperatures of a window, T_{go} and T_{gi} respectively, together with the external air temperature T_∞ and the net radiative exchange R_L were measured. The balance equation may now be written as:

$$\frac{k_g(T_{gi} - T_{go})}{\Delta x} = h(T_{go} - T_\infty) + \Delta R_L \qquad (3.88)$$

where k_g = the thermal conductivity of the glass $Wm^{-1}K^{-1}$

Δx = the thickness of the glass, m.

Hence

$$h = \frac{k_g(T_{gi} - T_{go}) - \Delta x\, \Delta R_L}{\Delta x(T_{go} - T_\infty)} \qquad Wm^{-2}K^{-1} \qquad (3.89)$$

For this type of analysis to yield correct results it must be assumed that the window is in steady state (i.e. T_{gi}, T_{go} and ΔT are fairly constant) and that the glazing heat storage capacity is small compared to the total energy flows. Nicol gives data which shows that the outside glass temperature varied only by $\pm$ 1.5K over a 3 hour period.

Mean hourly values of h derived from equation 3.89 were correlated with wind speeds recorded on the roof of the laboratory where the measurements were being made. The derived regression equation was:

$$h = 4.35\, V_R + 7.55 \qquad Wm^{-2}K^{-1} \qquad (3.90)$$

for a roof top wind speed $\leq$ 5.0 ms^{-1}. The height and location of Nicol's test window was not given.

Whilst Nicol's work may at first sight seem less thorough than previously reported in this section it is important if only for one reason. In order to evaluate the convective heat transfer coefficient using a heated element it is obvious that the element must be raised to a temperature above that of the ambient air. Ito et al and Sturrock utilised temperature differences of the order of 30 K. Whilst it is true that under conditions of high solar irradiance certain building elements will reach temperatures far above those of the surrounding air, this is not necessarily true for glazed areas, glass being near transparent to solar radiation. Therefore it is a gross assumption to model the convective heat loss from a window by replacing it with a large heated plate. However, the fact that Nicol's work gives correlations which are similar to those experiments performed under this assumption shows that this is a valid method for conducting this type of convective heat loss evaluation.

3.7.5 The work of Sharples

During the late 1970's Sharples [1981 and 1984] conducted experiments to measure the convective heat transfer coefficient from the north facing facade of a large building, rectangular in plan, measuring 20 x 36 x 78m high. Measurements were made at central sites on floors 6, 14 and 18 and at an edge site on floor 18 only. The measurements were correlated with wind speeds measured 1m from the building surface, V_s, 6m above the building roof, V_R, and at a local weather station, aproximately 400m to the south west of the building, V_{10}.

Heat meters and calculation methods similar to those of Ito et al [1972] were used to evaluate the heat transfer coefficient h.

All parameters (except the weather satation data) were recorded simultaneously at 1 minute intervals for a 12 hour period on a data logger. Data reduction to 15 minutes mean values was performed on a main frame computer. A total of 100 nights recording were made at the four sites, thus making it the most systematic and comprehensive study of this type to date.

The inter-relationships between h, V_S, V_R and V_{10} were examined using a linear least-squares curve fitting technique. Data was classified as windward if the angle of incidence between the normal to the monitored facade and the wind direction was less than $\pm$ 90° and leeward for all other directions.

Sharples presents linear regression lines for the following pairs of parameters, h v V_s, h v V_{10}, h v V_R, V_s v V_R and V_s v V_{10}. The spread in the data presented is again quite high with correlation coefficients based on the least squares method being found to be in the range 0.163 - 0.894.

The correlations between h and V_R are presented here (see Table 3.6) in order to compare this study with the work previously performed in this field. It can be seen from this that Sharples' results are generally much lower than those found by other experimenters and that for certain correlations (e.g. 6 C leeward) the heat transfer coefficient becomes zero for a non zero value of the wind speed. This must be considered as an anomaly due to the fitting of a straight line to the raw data rather than an actual physical phenomenon.

Table 3.6 Correlations Between Heat Transfer Coefficient, h, and Roof top Wind Speed, V_R, After Sharples [1984]

Site	Wind Direction	Regression Equation $h - Wm^{-2}K^{-1}$	Correlation Coefficient
18th floor centre, 18C	Windward	$0.7\ V_R + 5.3$	0.631
	Leeward	$0.9\ V_R + 0.1$	0.622
18th floor edge, 18E	Windward	$2.0\ V_R - 0.6$	0.719
	Leeward	$0.9\ V_R + 1.9$	0.627
14th floor centre, 14C	Windward	$1.1\ V_R + 0.9$	0.829
	Leeward	$0.8\ V_R - 0.8$	0.662
6th floor centre, 6C	Windward	$1.2\ V_R - 1.6$	0.536
	Leeward	$1.3\ V_R - 2.4$	0.743

One of the most significant aspects of this work is the fact that the heat transfer data is correlated with the meteorological 10m wind speed V_{10}. This 10m wind speed is the most widely available wind statistic in the UK. As this wind speed is measured, ostensibly, at a site which is free from the influence of surrounding structures, it offers an accessible means for evaluating the wind environment at a particular location. Because this wind speed is evaluated at many sites in the UK it also offers a means of generalising full scale convective heat transfer results performed at a particular site. The correlations obtained between h and V_{10} by Sharples are presented in Table 3.7.

Table 3.7 Correlations Between Heat Transfer Coefficient, h, and 10m Meteorological Wind Speed, V_{10}, for Four Sites on a Tall Building. After Sharples [1984]

Site	Wind Direction	Regression Equation h - $Wm^{-2}K^{-1}$	Correlation Coefficient
18th floor centre, 18C	Windward	$1.4\ V_{10} + 6.5$	0.670
	Leeward	$1.4\ V_{10} + 4.4$	0.829
18th floor edge, 18E	Windward	$2.9\ V_{10} + 5.3$	0.592
	Leeward	$1.5\ V_{10} + 4.1$	0.599
14th floor centre, 14C	Windward	$1.6\ V_{10} + 3.3$	0.834
	Leeward	$1.5\ V_{10} - 1.0$	0.657
6th floor centre, 6C	Windward	$0.5\ V_{10} + 3.8$	0.163
	Leeward	$1.4\ V_{10} + 1.7$	0.654

From Tables 3.6 and 3.7 it can be seen that Sharples' results, whilst being generally lower than those of Ito et al [1972], confirm the findings of the earlier Japanese work i.e. that generally the heat transfer coefficient increases with height and closeness to the edge of the building.

3.7.6 Summary

This section has examined the work of five authors who have conducted full scale convective heat transfer studies on high rise buildings. Figure 3.17 shows a comparison between some of the results obtained in each case. Although there is an order of magnitude agreement between the results, and indeed with the fundamental wind tunnel results given in Section 3.1 (see Figure 3.16) there is still enough difference between them to warrant a further discussion on these experiments.

It must not be thought that these differences indicate any basic fault in any one particular series of experiments, rather that it reflects the fact that there is no one true general correlation between the convective heat transfer from a building and the wind speed. The buildings considered in each study were all of different shapes and dimensions thus the local flow regimes round each building will be unique to that building. The wind speeds to which the heat transfer results were related, although in general measured at some given height above the roof, were evaluated at various heights above the roof and at different positions on it.

A final point to consider when assessing the value of these experiments is this; the evaluation of the convective heat transfer from a large building facade (e.g. the building facade used by Sharples measured 36 x 78m) using a relatively small heated element, 0.25 x 0.25m in the case of Sharples, is analogous to the measurement of the local convective heat transfer coefficient rather than the average or overall convective heat loss, from the building. Thus, taking these points into consideration, a unique relationship between the convective heat transfer measured at a particular location on a given building facade and the wind speed measured at a particular position is not surprising.

Perhaps the most useful results to arise out of this section are those due to Sharples for h v V_{10} in that they are probably more generally applicable to other situations and are based on widely available wind speed data.

3.8 The Use of Experimentally Derived Convective Heat Transfer Relationships for Predicting the Convective Heat Loss from the Upper Surface of Flat Plate Solar Collectors

Several experimentally derived correlations between the convective heat transfer and wind speed for flat plates and associated geometries have been suggested as being relevant to the situation of convective heat loss from flat plate solar collectors.

Duffie and Beckman [1980] in their classic book on solar energy quote the results of both Sparrow et al [1977] and Jurges [1924] without being decisive as to which set of results should be applied.

Klein [1975], in his paper on the theoretical evaluation of the total heat loss from a flat plate solar quotes and uses, unequivocably, the earliest experimental data available, i.e. that of Jurges [1924].

Watmuff et al [1977] give their own radiatively corrected forms of the correlations obtained by Rowley [1930 (a) and (b)] and Jurges [1924] but conclude that "considerable work is required to obtain realistic experimental knowledge of this heat loss term".

Agarwal and Larson [1981] in their paper, which has similar objectives to that of Klein, state that the work of Jurges is of questionable validity as applied to solar collectors but do not offer any alternative suggestion.

By analysing the performance of four flat plate solar collectors, using convective heat transfer coefficients determined by the correlations obtained by Jurges and Sparrow, Ramsey and Charmchi [1980] concluded that the relationship due to Sparrow was more appropriate.

Green et al [1981] used a solar simulator and computer models to reach the conclusion that if the 10m wind speed is known then the correlation obtained by Sparrow et al [1977] could be used by making a direct substitution for the velocity at the centre of the wind tunnel duct with the meteorological wind speed. If, however, the velocity parallel to the surface is known then the equation proposed by Jurges should be used but with a term added to take into account natural convection. This new equation is given as:

$$h = 7.4\ V_p^{0.5} + 3.0 \qquad Wm^{-2}K^{-1} \qquad (3.91)$$

where V_p = The velocity parallel to the surface, ms^{-1}

The meaning of the 10m wind speed is readily understood. However, its direct substitution for a wind speed obtained at the centre of a wind tunnel duct is slightly less than axiomatic. The concept of a wind speed parallel to the surface of a collector is even more nebulous. The wind speed parallel to any surface, as shown by Houghten [1931] is a function of the distance away from the surface at which it is measured.

Oliphant [1980] measured the wind speeds at 9 positions 100mm above the surface of two solar collectors mounted on a frame placed on a flat roof. He compared these speeds with those measured by an anemometer mounted on a mast 6m above the plates. He concluded that the wind speed measured just above the plate was always less than the "free stream" velocity. It was also found that the wind pattern across the collectors was a function of wind direction and that it was not valid to take a single wind speed measurement either near the collector or at a height of several metres above it and expect this value to give an accurate indication of the average wind speed over the collector.

These anomalies, together with those already discussed in this chapter, seem to render the application of any of the previous experimentally obtained convective heat transfer correlations to the heat loss from the upper surface of a solar collector, due to the wind, unwise.

Conclusion

In this chapter the experimental analysis of convective heat transfer from flat plates and associated geometries has been described and discussed. It has been confirmed to some extent that the theoretical predictions of Chapter Two adequately describe the convective heat transfer process for the simple case of a flat plate in a two dimensional flow.

However it has also been shown that the convective heat transfer from a surface is affected, often greatly, by its geometry, dimensions and surface roughness. The temperature of the surface, and the properties of the flow around it, can also affect the rate of convective heat transfer from it.

The measurement of the average convective heat transfer coefficient has been performed both in wind tunnels and in the natural environment. The surface geometries examined can also be split into two broad categories according to their linear dimensions. These are; small - with linear dimensions of the order of 100mm or less and large - with linear dimensions of the order of 500mm or more.

All the work described in the small plate, wind tunnel tested, category can be adequately described by the global equation presented by Sparrow i.e.

$$h = 18.6\ V_{\infty}^{0.5} \qquad (3.92)$$

where V_{∞} = the free stream velocity in the wind tunnel.

The value of the multiplying constant in these experiments ranges from 17.8 - 19.9 and the exponent from 0.5 - 0.58 (see Sections 3.3 and 3.6). Equation 3.92 can be de-dimensionalised. By assuming a characteristic dimension of 75mm and that the properties of air are to be evaluated at 300k the following is obtained.

$$Nu = 0.77\ Re^{0.5} \qquad (3.93)$$

This is in remarkably good agreement with the laminar parallel flow theory given in Chapter Two, i.e.

$$Nu = 0.664\ Re^{0.5} Pr^{0.33} \qquad (3.94)$$

considering the wide range of surface geometries to which it is applicable. It must be noted that this type of equation takes no account of natural convection and that it has been confirmed experimentally only within the range $1.9 \times 10^4 < Re < 1.2 \times 10^5$. Solar collectors situated in the natural environment represent Reynolds numbers in the approximate range, $0 < Re < 10^6$, and Kind [1983] states that the flow over a full scale collector may be expected to be turbulent not laminar.

The general expression for experiments carried out with large plates in a wind tunnel environment has already been given in Section 3.17 as.

$$h = 2.9\ V_\infty + 10.0 \qquad Wm^{-2}K^{-1} \qquad (3.95)$$

This equation takes into acount natural convection effects and has been tested in the range $0 < Re < 10^6$. The dimensionless form of this equation, arrived at by assuming a characteristic dimension of 0.5m and evaluating the properties of air at 300k is, given by.

$$Nu = 1.73 \times 10^{-3}\ Re + 191 \qquad (3.96)$$

For the work conducted on large buildings in the outdoor environment comparison even between the results obtained is difficult, because of the factors mentioned in Section 3.7.6.

However representative equations may be given as

$$h = 1.1\ V_R + 0.9 \qquad Wm^{-2}K^{-1} \qquad (3.97)$$

for an averagely exposed site for windward data, and

$$h = 0.8\ V_R + 0.8 \qquad Wm^{-2}K^{-1} \qquad (3.98)$$

for an averagely exposed site for leeward data. It must be noted that the work of Sturrock [1971] gave correlations significantly different to this i.e.

$$h = 6.0\ V_R + 5.7 \qquad Wm^{-2}K^{-1} \qquad (3.99)$$

This, as pointed out earlier is probably due to the small size of his heat meter apparatus.

Thus it can be seen that the heat transfer coefficient is effected by a wide variety of parameters and often, especially in the outdoor environment, the position of their measurement (especially the "mean" wind speed). Despite these facts the convective heat transfer coefficient from the upper surface of a flat plate solar collector is still evaluated using equations derived from experiments performed in wind tunnels. This would seem inadequate, if only for the problems encountered in relating a given wind speed in the natural environment to that at the centre of a wind tunnel duct.

Therefore, the best method of approach in order to gain a deeper understanding of the convective heat losses from a solar collector would be to evaluate experimentally the convective heat transfer coefficient from a heated surface possessing the geometry and dimensions of a real flat plate solar collector. A description of an experimental set up for performing such a procedure is described in the next chapter.

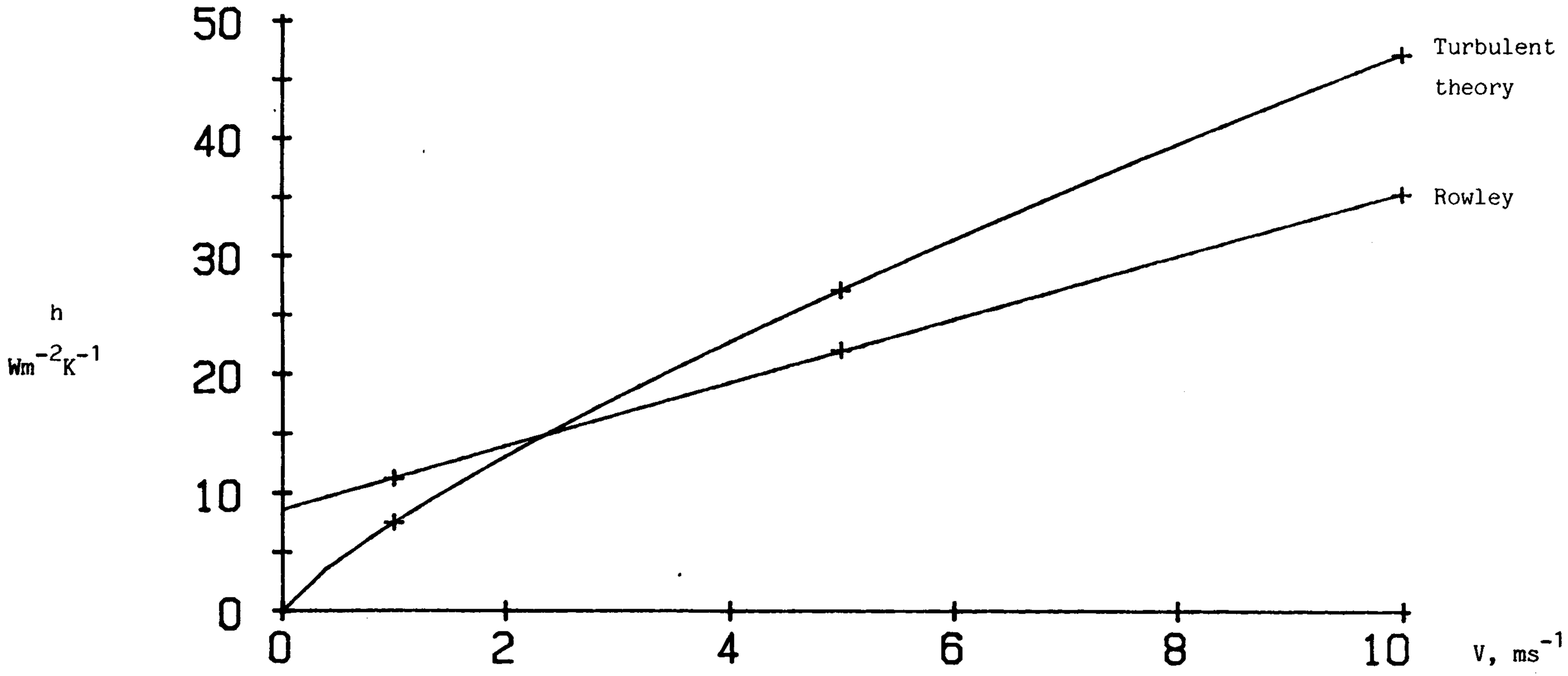

Figure 3.1 Comparison between the experimental results of Rowley [1930] and the theoretical "turbulent flow" equation for a plate with the same dimensions

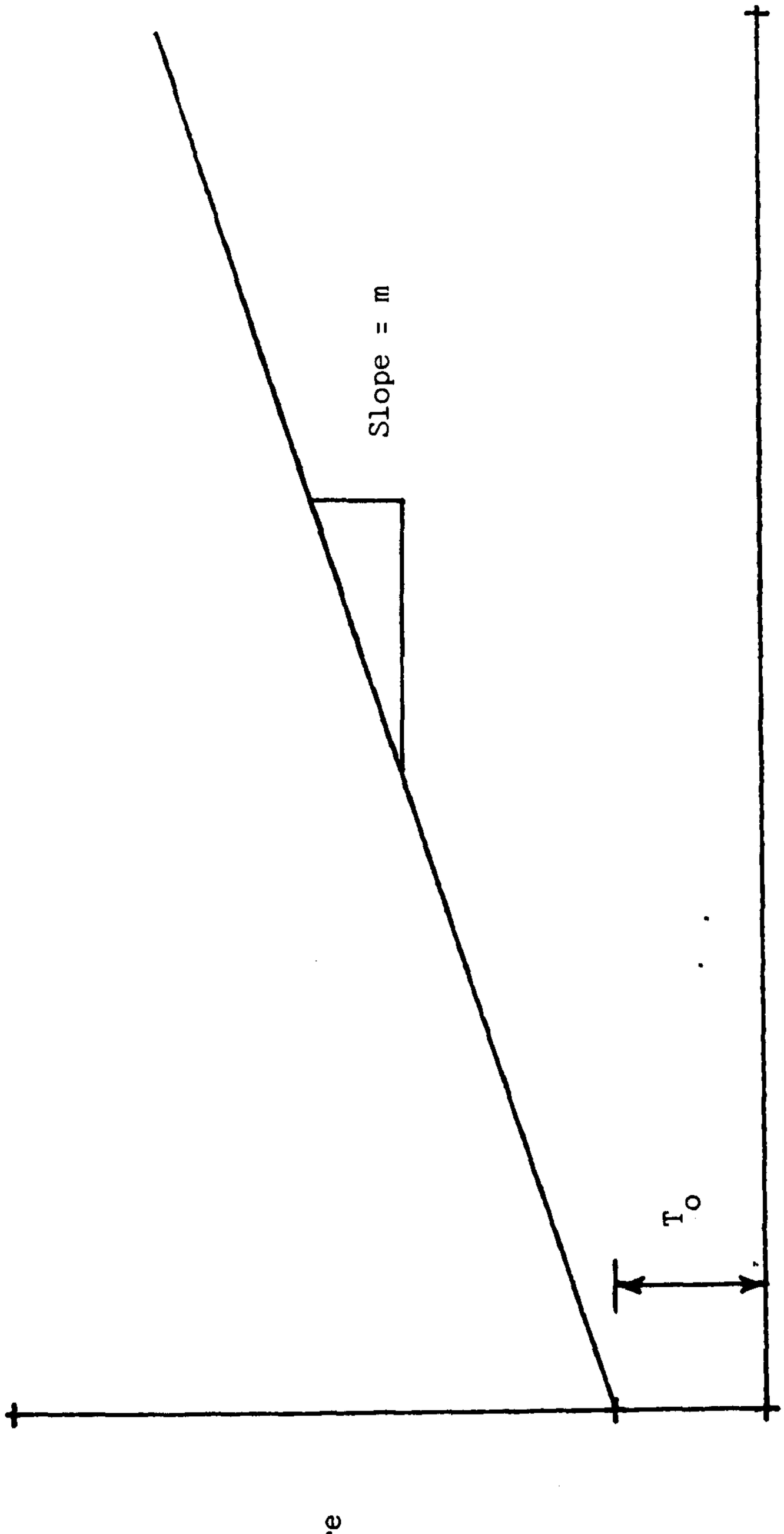

Figure 3.2 Step-ramp wall temperature distribution as examined by Reynolds [1958(c)]. This is a first approximation to the flow-wise temperature distribution of a solar panel

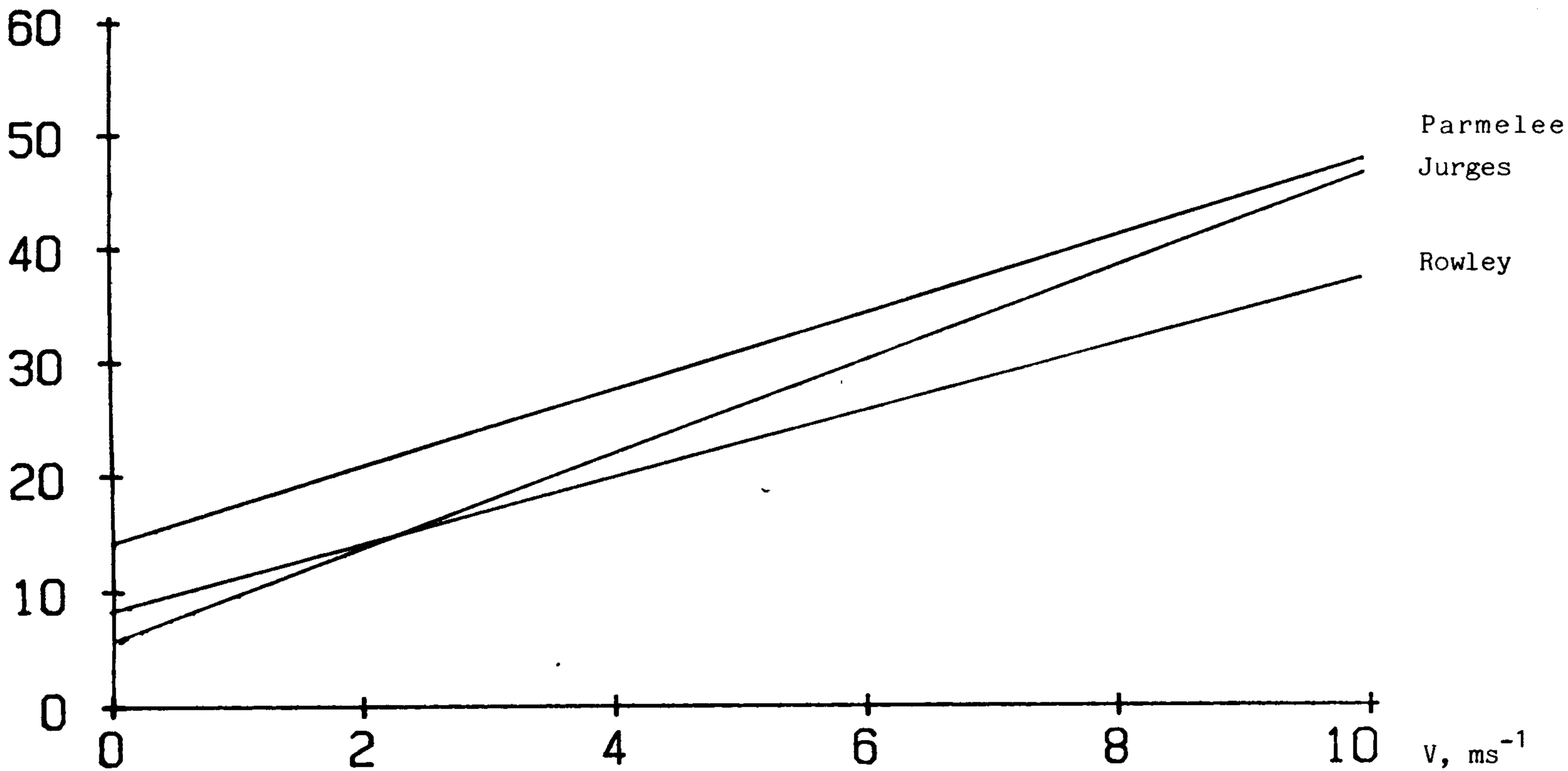

Figure 3.3 Comparison between the work of Jurges [1924], Rowley [1930] and Parmelee and Huebscher [1946]

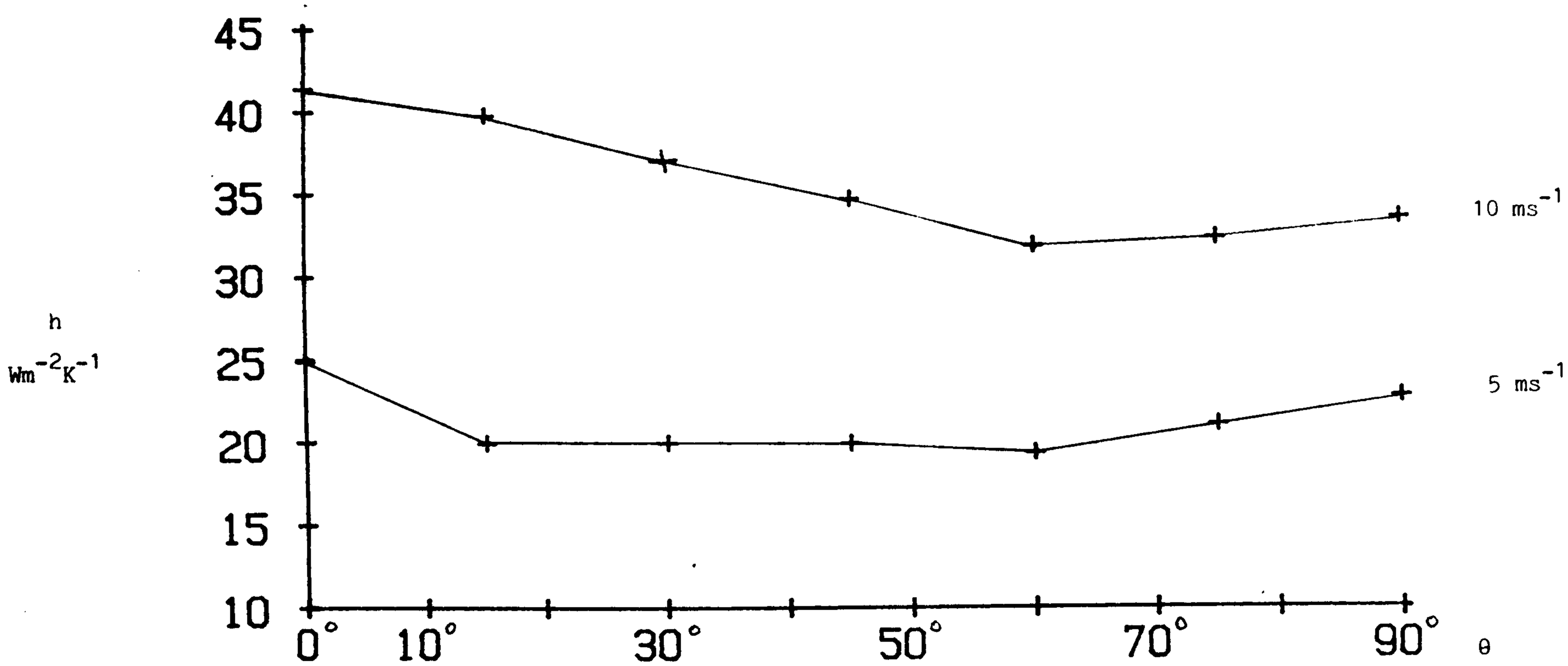

Figure 3.4 Convection coefficient, h, against wind incidence angle, θ, after Rowley [1932], 0° = parallel flow

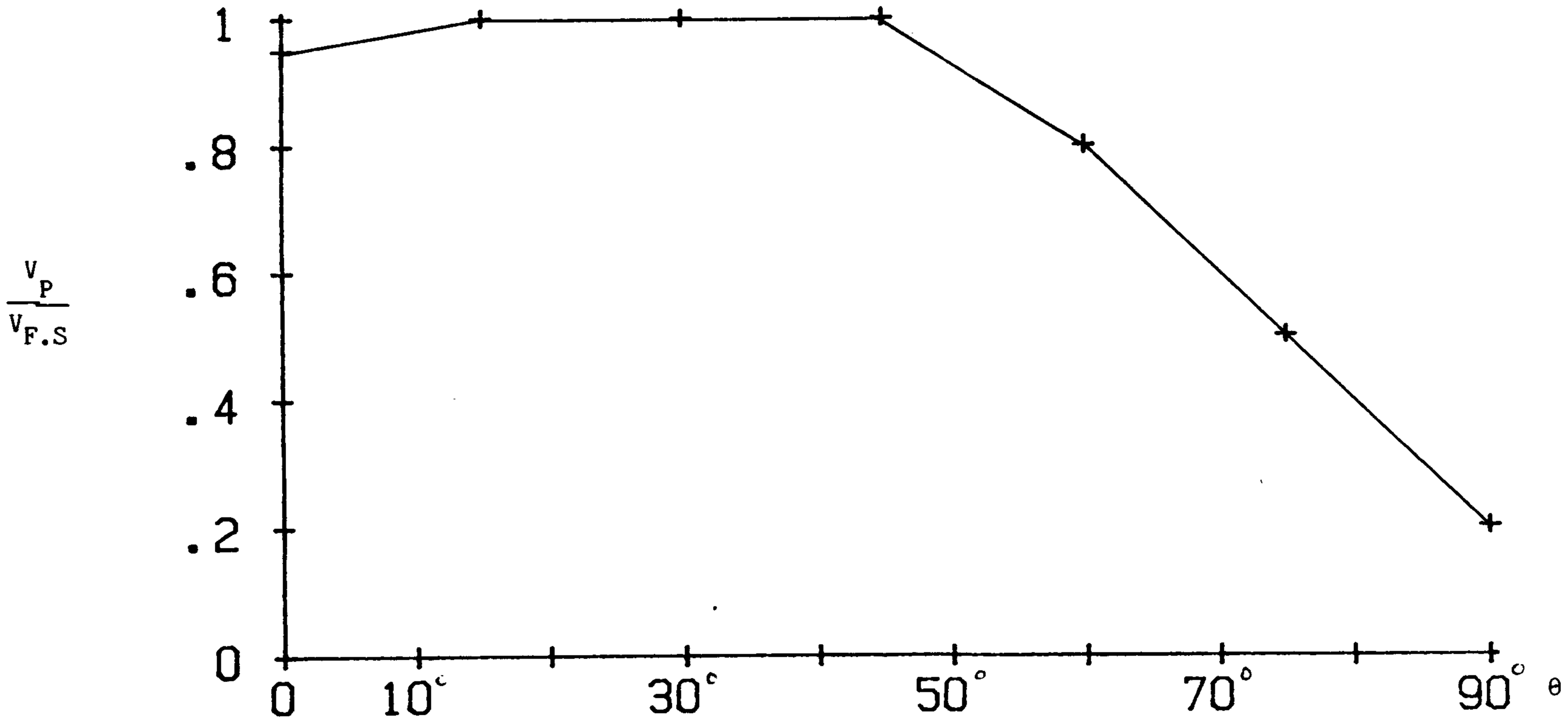

Figure 3.5 Ratio of velocity parallel to a surface, V_p, to velocity in the free stream $V_{F.S.}$. After Rowley [1932]. 0° = Parallel incident flow.

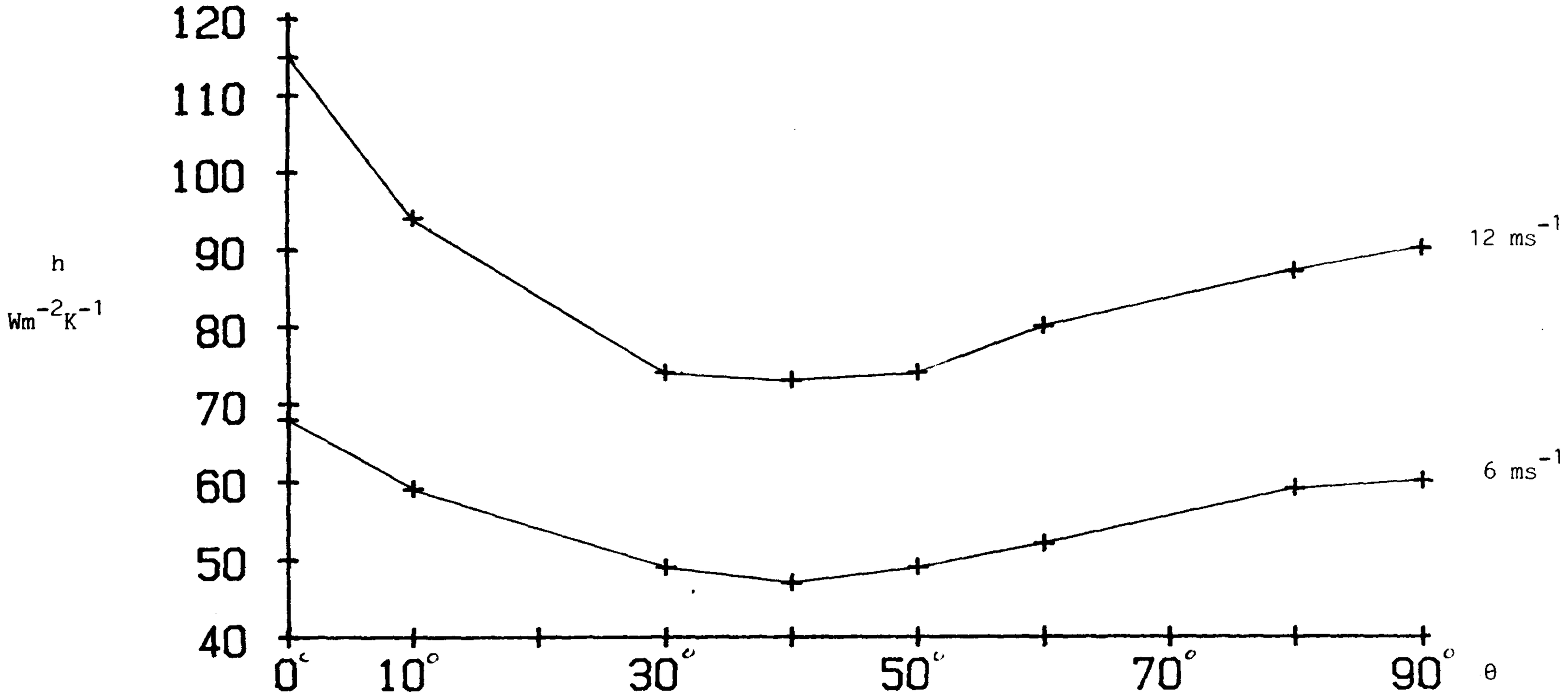

Figure 3.6 Convection coefficient, h, against wind incidence angle θ. After Coste et al [1981]

0° = Parallel flow

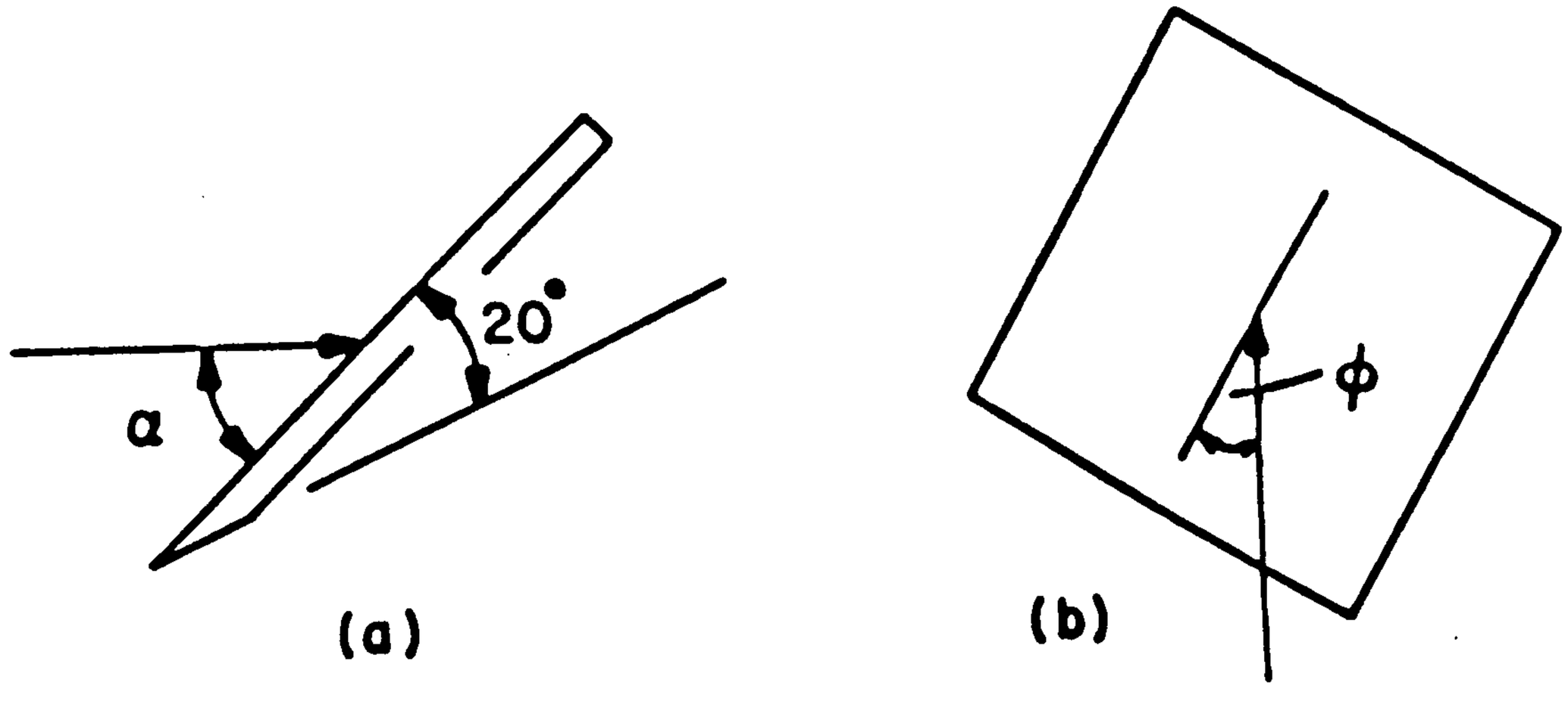

Figure 3.7 Angles of attack, α, and yaw, ϕ, as defined by Sparrow [1977], 20° plate bevel also illustrated

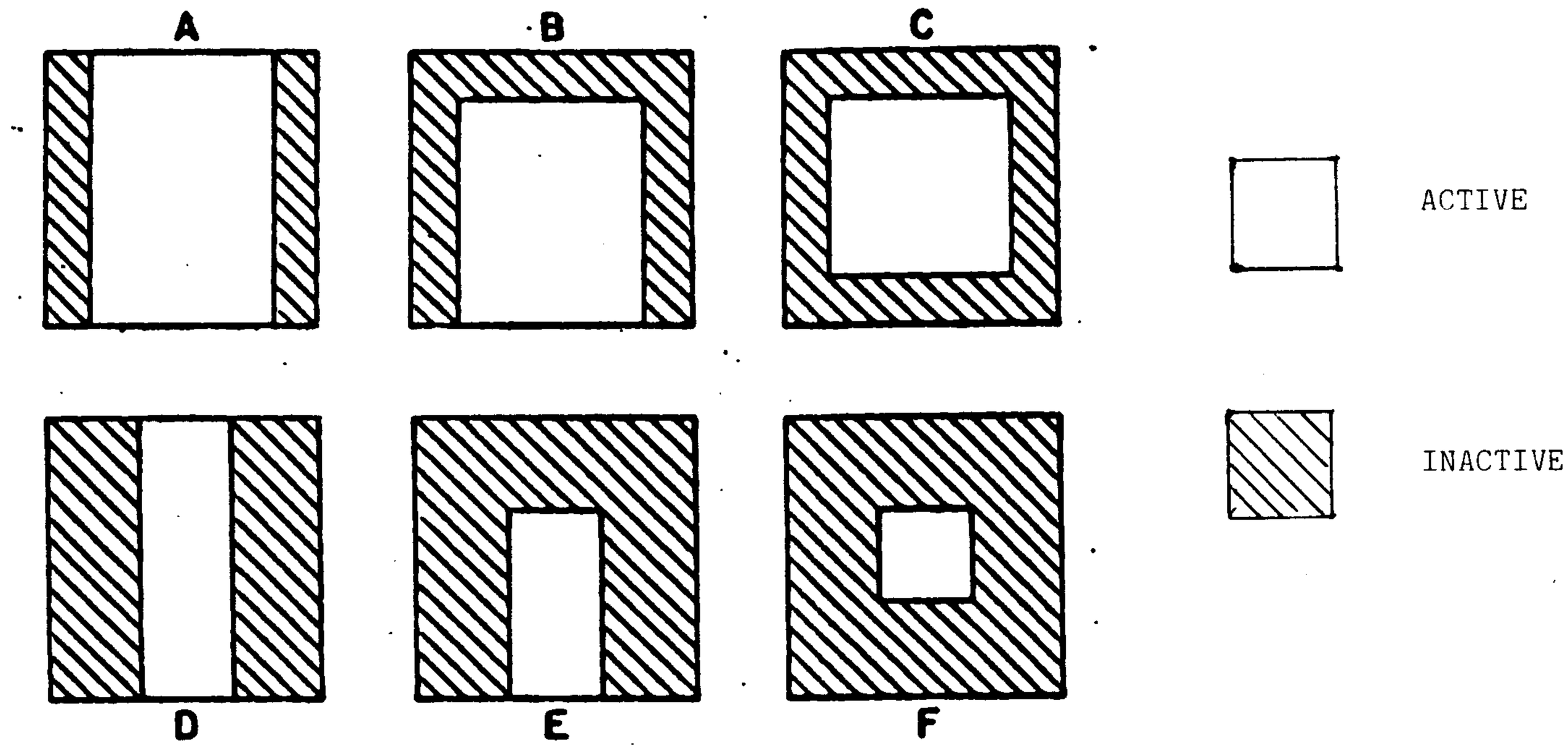

Figure 3.8 Adiabatic framing configurations for Sparrow's series III square flat plate experiments (Sparrow [1981], see also Table 3.2)

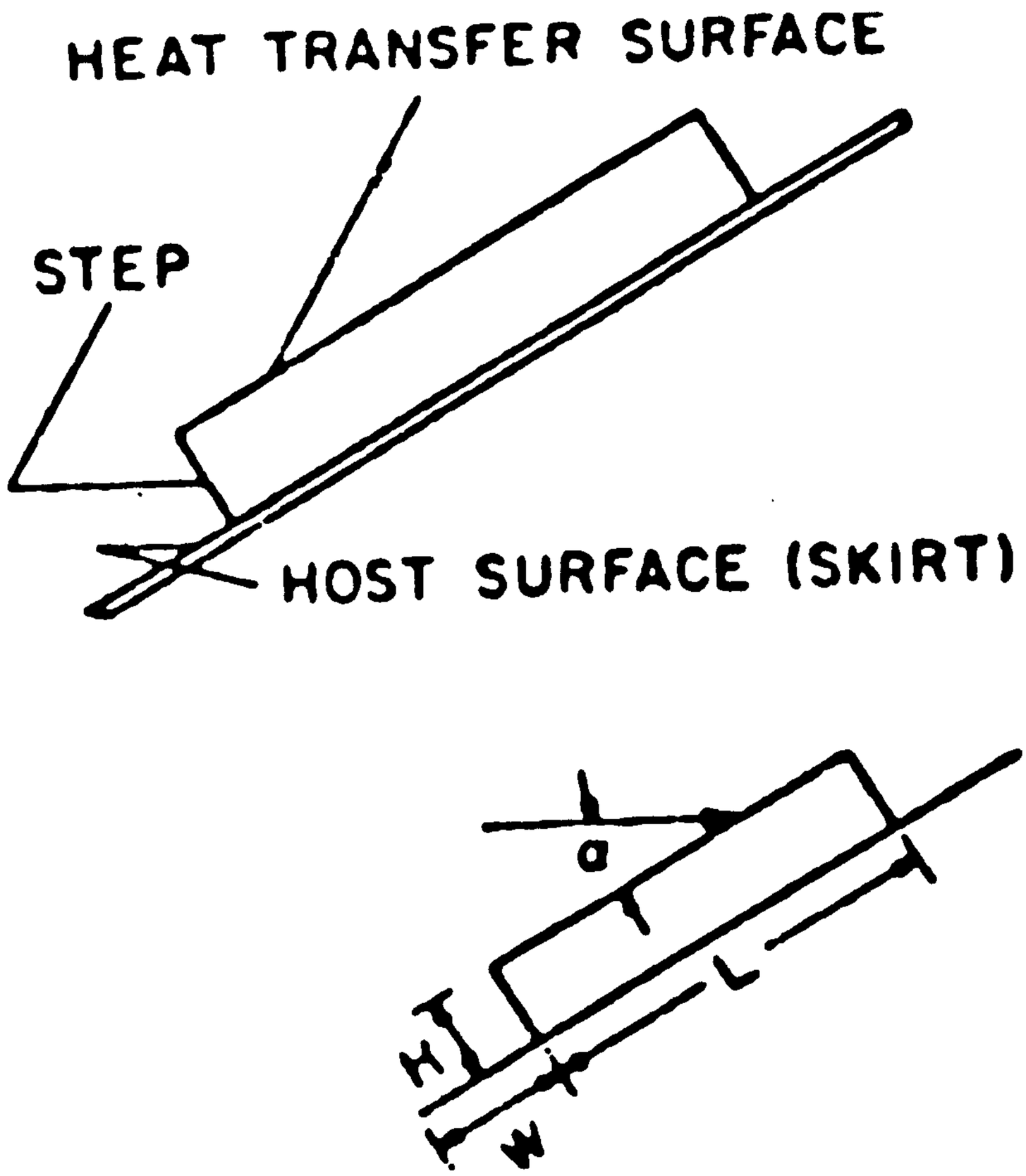

Figure 3.9 Illustration of step height, H, skirt width, W, and plate length, L, for Sparrow's series V experiments (Sparrow [1981(b)])

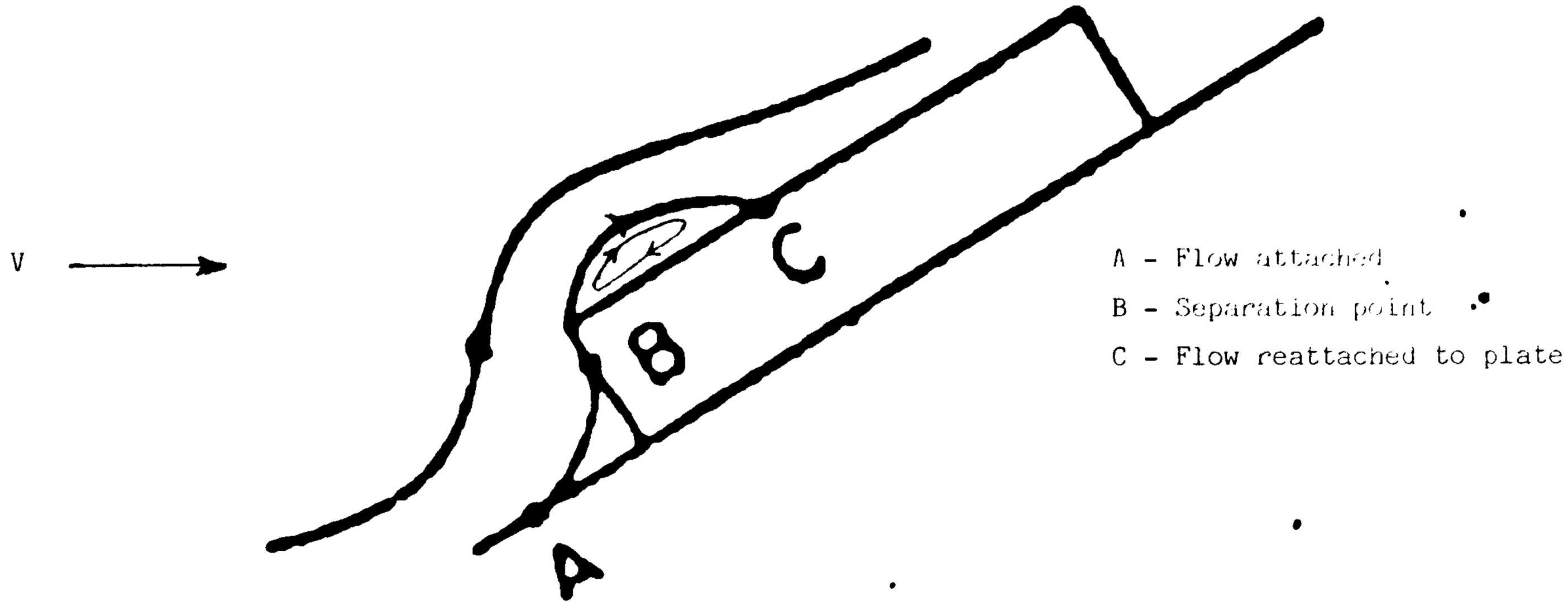

Figure 3.10 Illustration of the separation region over an elevated surface which contains a rapidly recirculating flow giving rise to enhanced mass/heat transfer (Sparrow [1981(b)])

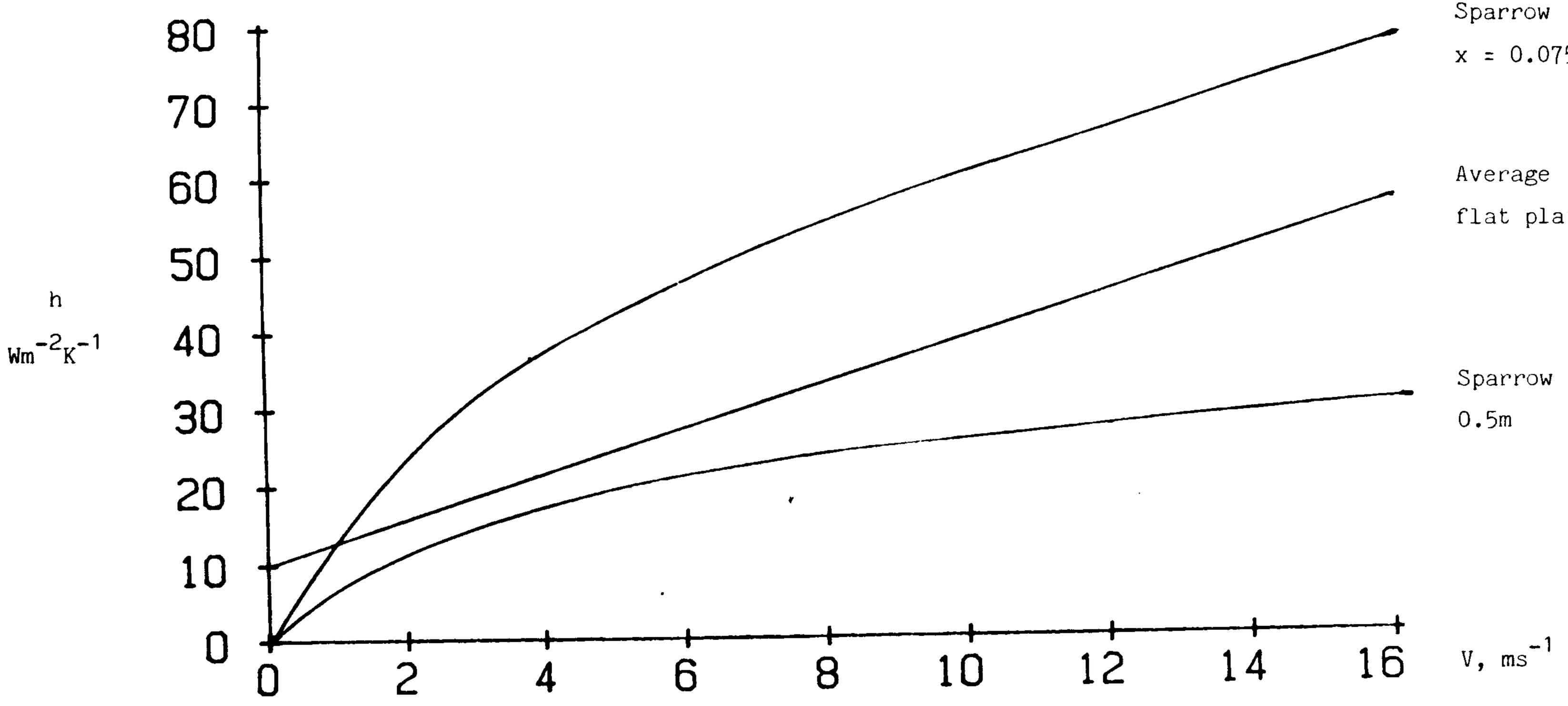

Figure 3.11 Comparison between the average flat plate equation (Equation 3.21) and Sparrow's global equation for two characteristic dimensions

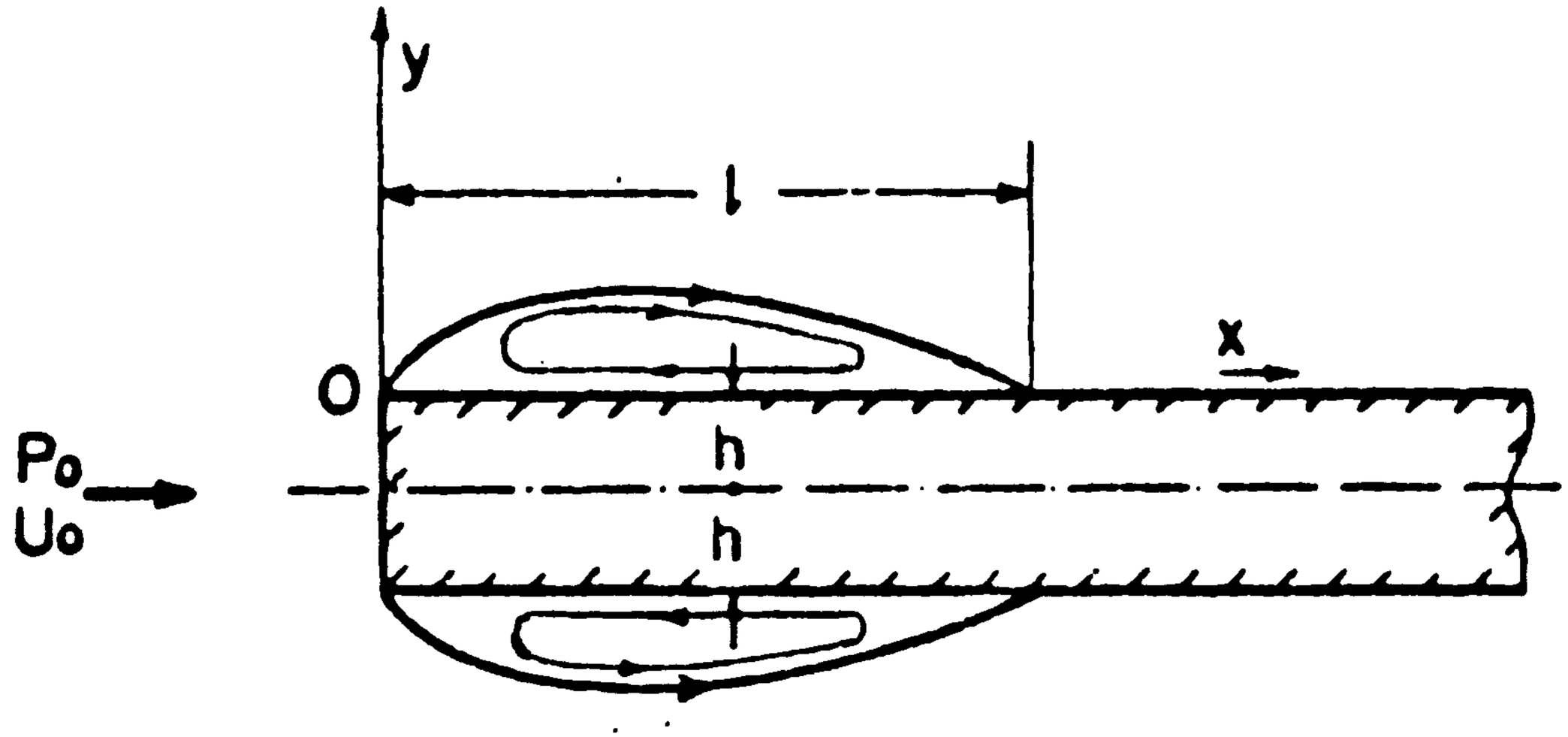

Figure 3.12 Flow conditions studied by Ota and Itasaka [1976] see Section 3.4.1

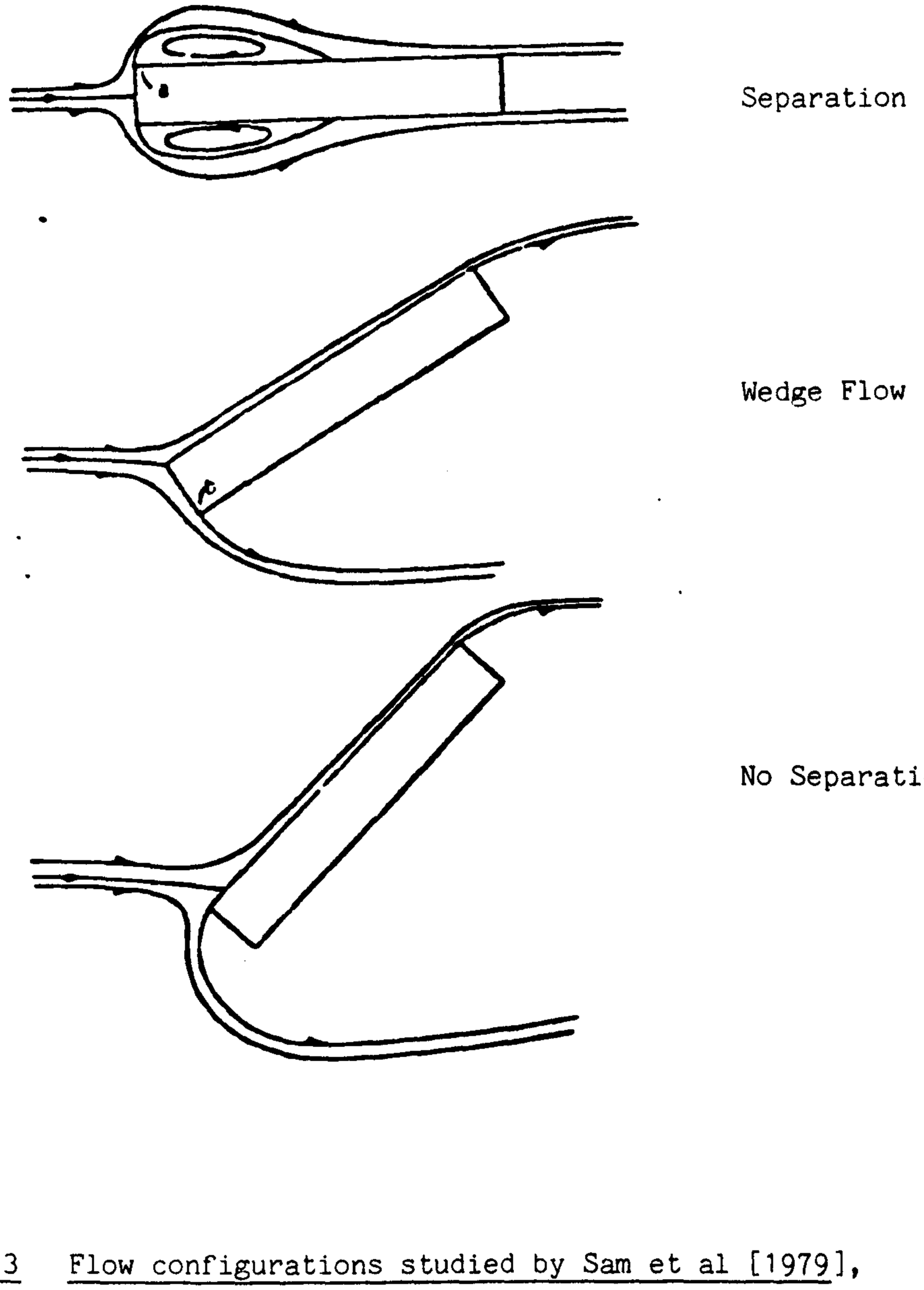

Figure 3.13 Flow configurations studied by Sam et al [1979], See Section 3.4.1

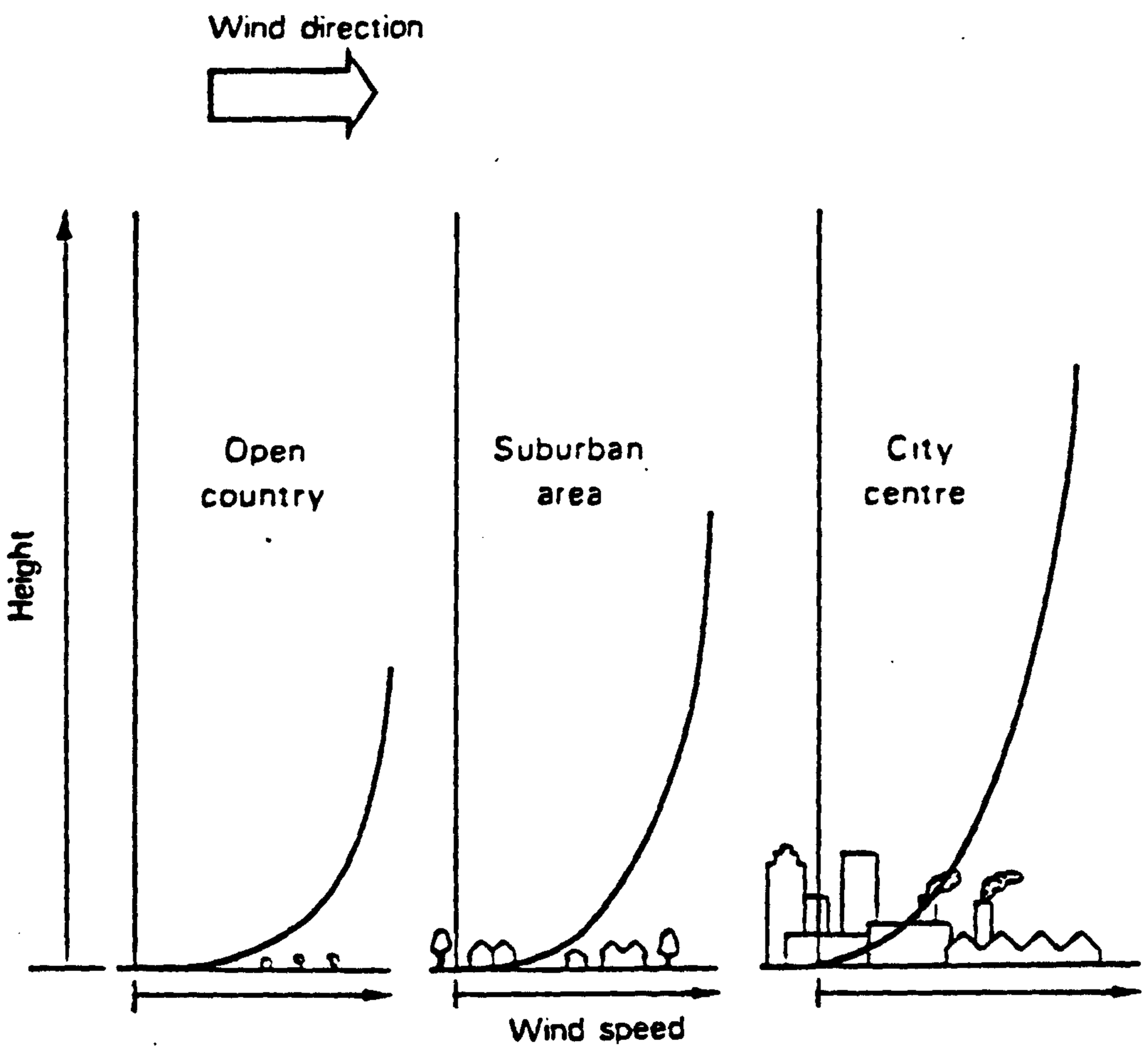

Figure 3.14 Typical wind velocity profiles over three terrain types. After Penwarden and Wise [1975]

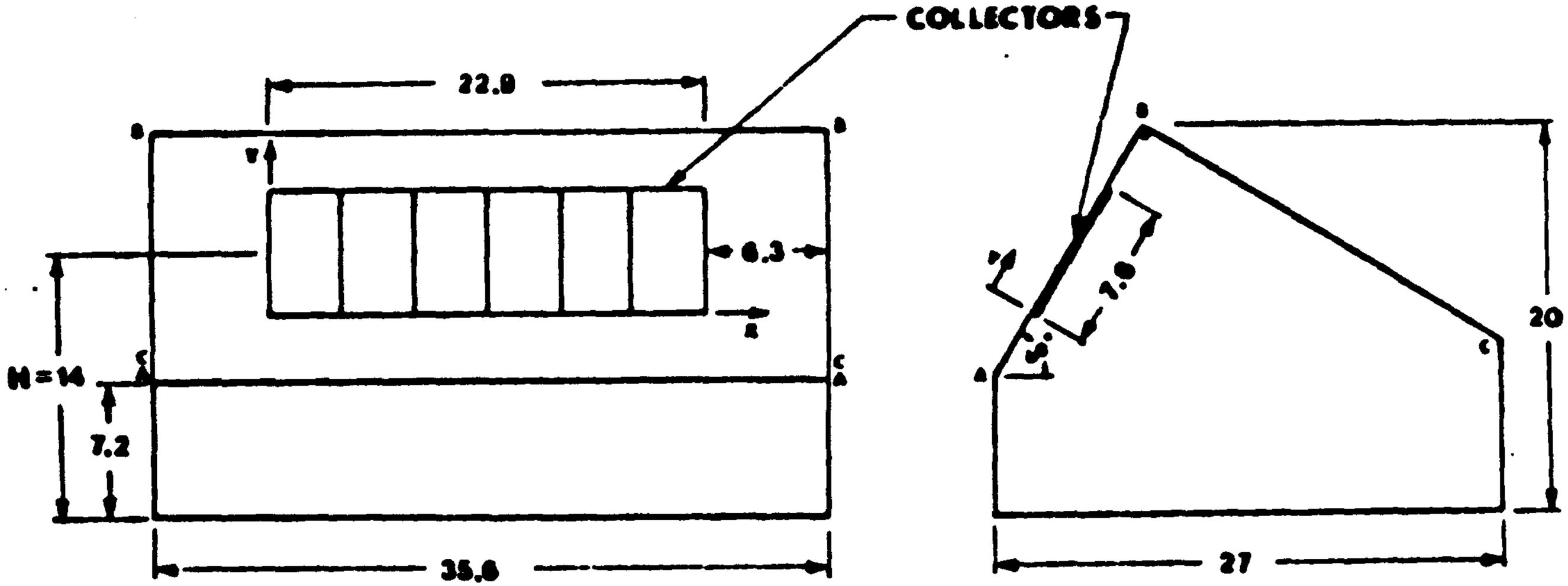

Figure 3.15 Two view diagram of model house with heater plates as examined by Kind et al [1983]
Dimensions in cms

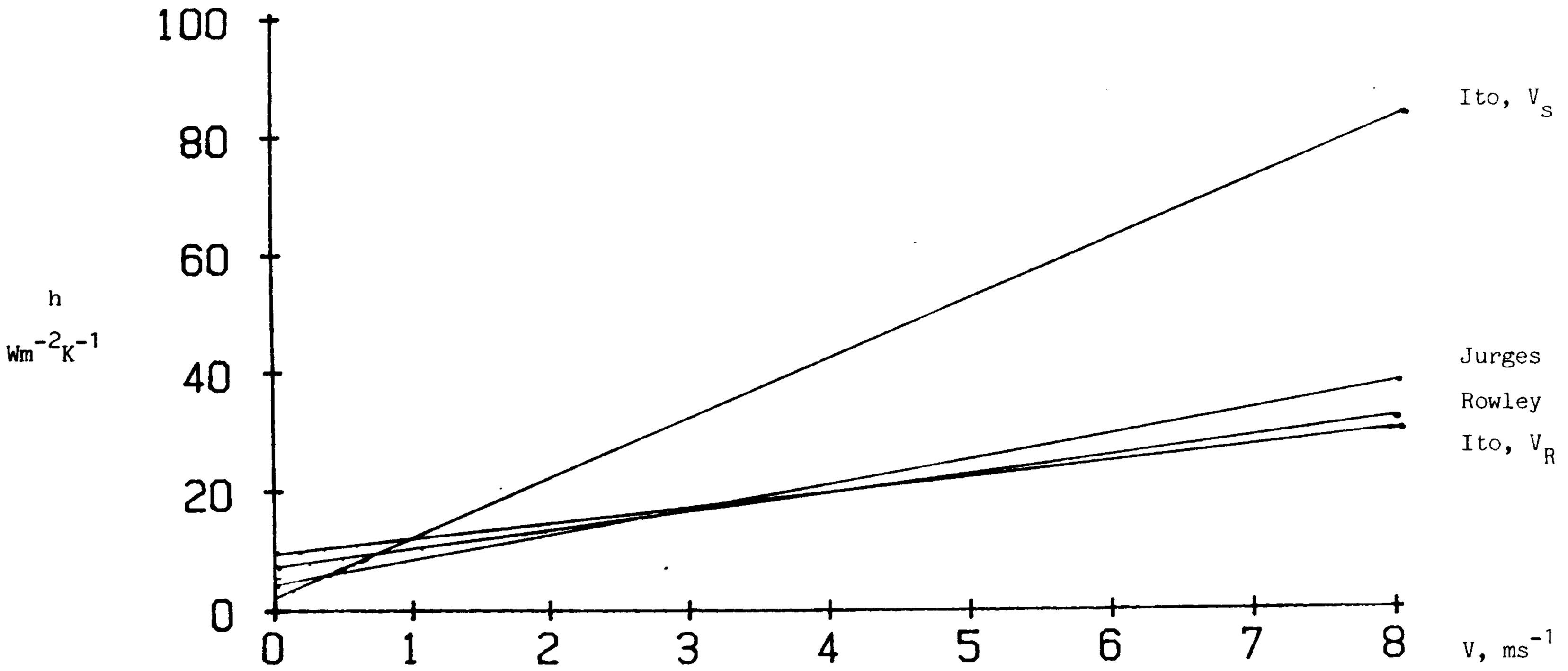

Figure 3.16 Comparison of the wind tunnel work of Jurges [1924] and Rowley [1930] with the full-scale outdoor tests of Ito et al [1972]

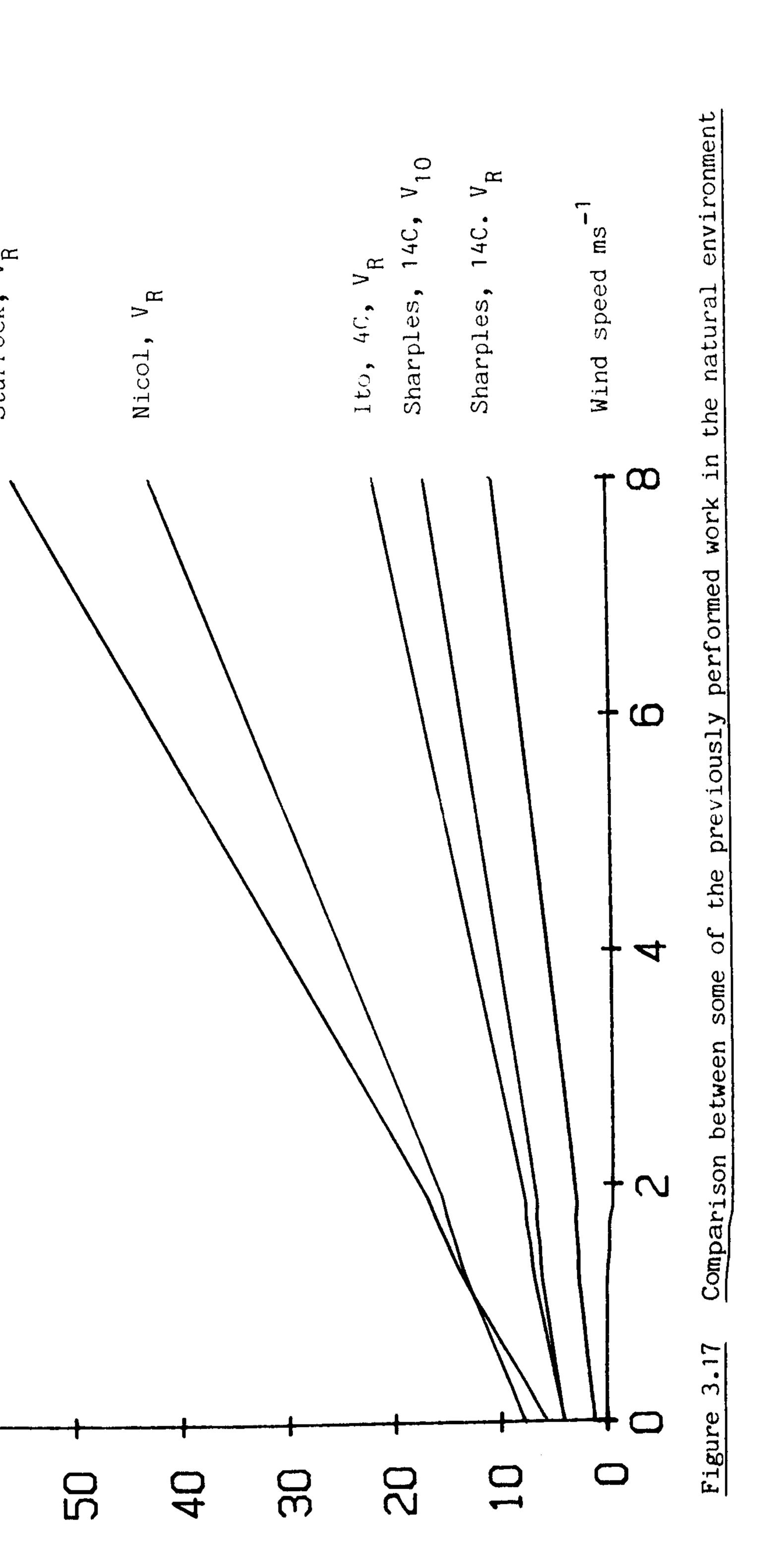

Figure 3.17 Comparison between some of the previously performed work in the natural environment

REFERENCES

Agarwal, V.K. and Larson, D.C. [1981]
Calculation of the top loss coefficient of a flat-plate collector.
Solar Energy, Vol. 27, pp. 69-71.

Agarwal, V.K. and Larson, D.C. [1983]
Erratum to Agarwal and Larson [1981]
Solar Energy, Vol. 30, No. 1, p. 86.

Angstrom, A. [1915]
A study on radiation of the atmosphere.
Smithsonian Miscellaneous Collection, Vol. 64, pp. 57-69.

Bedingfield, C.H. Jnr. and Drew, T.B. [1950]
Analogy between heat transfer and mass transfer - a psychrometric study.
Industrial and Engineering Chemistry, Vol. 42, pp. 1164-1173.

Berman, S. [1965]
Estimating the longitudinal wind spectrum near the ground.
Q.J.R. Met Soc. Vol. 91, pp. 302-317.

Blasius, H. [1908]
Grenzschichen in flussigkeiten mit kleiner reiburg.
Zeitschr Math U Phys., Vol. 56, No. 1.

Bradshaw, P. [1971]
An introduction to turbulence and its measurement.
Pergamon Press, Oxford, England.

British Standards Institute - Code of Practice [1972]
CP 3, Chapter 5, Part 2.

Brownlee, K.A. [1953]
Industrial experimentation,
Chemical Publishing Co., INC., New York, USA.

Burns, A.P. [1976]
An experimental study of heat transfer from a bluff body to a turbulent free-stream as applied to building heat loss.
Ph.D. Thesis, University of Glasgow.

Cermak, J.E. [1971]
Laboratory simulation of the atmospheric boundary layer.
A.I.A.A. Journal, Vol. 9, No. 9, pp. 1743-1754.

Chapman, A.J. [1974]
Heat Transfer, 3rd Edition,
MacMillan, New York.

Chatfield, C. [1970]
Statistics for technology,
Penguin Books Ltd., England.

Colburn, A.P. [1933]
A method of correlating forced convective heat transfer data with fluid friction.
Trans. A.I.Ch.Eng. Vol. 29, pp. 174-210.

Cole, R.J. [1976]
The longwave radiative environment around buildings.
Building and Environment, Vol. 11, pp. 3-13.

Cook, N.J. [1978]
On simulating the atmospheric boundary layer in wind tunnels.
Building Research Establishment - Current Paper BRE/CP - 71/78.

Cooper, P.I. [1981]
The effect of inclination on the heat loss from flat plate solar collectors.
Solar Energy, Vol. 5, pp. 413-420.

Coste, G., Renaud, M. and Charuel, R. [1981]
Expressions de correlation du coefficient de transfert thermique local sur une plaquette dons un ecoulment d'incidence variable (Correlation equations for the local heat transfer coefficient to a plate in a variable incidence flow)
Chemical Engineering Journal, Vol. 22, pp. 203-212.

Counihan, J. [1973]
Simulation of an adiabatic urban boundary layer in a wind tunnel.
Atmospheric Environment, Vol. 7, pp. 673-689.

Counihan, J. [1975]
Adiabatic atmospheric boundary layers: A review and analysis of data from the period 1880-1972.
Atmospheric Environment, Vol. 9, pp. 871-905.

Cunningham, M.J. [1981]
Measurement errors and instrument inaccuracies.
J. Phys.E.Sci. Instrumentation, Vol. 14, pp. 901-908.

Department of Energy (Energy Paper No. 39) [1979]
Energy Technologies for the UK.
HMSO Publication, London, England.

Deris, N. [1961]
Optimum angle of inclination - new chart for solar collector pin-points.
Air Conditioning, Heating and Ventilating, August, pp. 57-60.

Dhawan, S. [1952]
Direct measurement of skin friction.
NACA Tech. Note 2567.

Dickinson, W.C. and Cheremisinoff, P.N. [1980]
Solar Energy Technology Handbook, Part A, Engineering Fundamentals.
Dekker, New York.

Digest of UK Energy Statistics [1984]
Publication of the Government Statistical Service.
HMSO, London, England.

Dixon, A.E. and Leslie, J.D. [1979]
Solar Energy Conversion.
Pergamon Press, Oxford, UK.

Gates, D.M. [1962]
Energy Exchange in the Biosphere.
Harper and Row Monographs,
New York

Drake, E.M. [1949]
Investigation of the variation of point unit heat transfer coefficient for laminar flow over an inclined flat plate.
Applied Mechanics, March Issue, pp. 1-8.

Duffie, J.A. and Beckman, W.A. [1980]
Solar Energy Thermal Processes.
J. Wiley and Sons Inc., New York, 1980.

Eaton, K. and Mayne, J.A. [1974]
The measurement of wind pressures on two-storey houses at Aylesbury.
BRE Current Paper CP 70/74.

Edwards, A. and Furber, B.N. [1956]
The influence of free-stream turbulence on heat transfer by convection from an isolated region of a plane surface in parallel air flow.
Proc. Inst. Mech. Eng. Vol. 170, pp. 941-948.

Evans, R.A. and Lee, B.E. [1980]
Some observations on the problem of defining mean wind speeds representative of flow over urban and suburban terrain.
Department of Building Science, University of Sheffield - Internal Report No. BS 52.

Evans, R.A. and Lee, B.E. [1983]
The evaluation of wind speeds over roof mounted solar collectors.
Department of Building Science, University of Sheffield - Internal Report No. BS 73.

Fage, A. and Faulkner, U.M. [1931]
Relation between heat transfer and surface friction for laminar flow.
Aeronautical Research Committee Reports and Memoranda, No. 1408.

Flay, R.G.J., Stevenson, D.C. and Lindley, D. [1982]
Wind structures in a rural atmospheric boundary layer near the ground.
J. Wind Engineering and Industrial Aerodynamics, Vol. 10, pp. 63-78.

Fujii, T. and Imura, H. [1972]
Natural convection heat transfer from a plate with arbitory inclination.
Int. J. Heat Mass Transfer, Vol. 15, pp. 755-767.

Fussey, D.E. and Warneford, I.P. [1976]
An analysis of laminar free convection from upward facing flat plates.
Letters in Heat and Mass Transfer, Vol. 3, pp. 443-448.

Gerhart, K. [1967]
Modellversuche uber die verteilung des konvektiven warmeuberganges an gebaudegassaden.
(Model experiments on the local variation of convection heat transfer processes at building facades.)
Kaltetechnik - Klimatisierung, 19 Jahrgang, Heft 5.1967, pp. 122-128.

Gill, G.C. [1973]
The Helicoid Anemometer.
Atmosphere, Vol. 11, No. 4, pp. 145-155.

Gosset, W.S. [1908]
The probable error of a mean.
Biometrika, Vol. 6, pp. 1-25.

Green, A.A. [1979]
The influence of environmental parameters on flat plate collector performance.
UK-ISES Conf. Proc. C18 "Meteorology for solar energy applications", London.

Green, A.A., Kenna, J.P. and Rawcliffe, R.W. [1981]
The influence of wind speed on flat plate solar collector performance.
Solar Energy Unit, University College, Cardiff, UK.
(Publication)

Hewlett-Packard - Operator's Handbook [1981]
3054 DL Data Logger
Operators Handbook
Hewlett-Packard, Loveland, Colorado, USA.

Holman, J.P. [1981]
Heat Transfer - 5th Edition
McGraw-Hill, New York.

Hottel, H.C. and Woertz, B.B. [1942]
Performance of flat-plate solar-heat collectors.
Trans. Am. Soc. Mech. Engrs. Vol. 64, 91.

Hottel, H.C. and Whillier, A. [1958]
Evaluation of flat-plate collector performance.
Trans. Conf. on the use of Solar Energy, Vol. 2, Part I, p. 74
University of Arizona Press, 1958.

Houghten, F.C. and McDermott, P. [1931]
Wind velocity gradients near a surface and their effect of film conductance.
Trans. ASHVE, Vol. 37, pp. 301-322.

Iqbal, M. and Khatry, A.K. [1977]
Wind induced heat transfer coefficients from glasshouses.
Trans. ASAE, pp. 157-160.

Ito, N., Sato, A., Oka, T. and Kimura, K. [1967]
Convective heat transfer from the external wall surfaces of buildings in natural wind.
Trans. Architectural Inst., Japan. Paper No. 3038, p. 522.

Ito, N., Kimura, K. and Oka, J. [1972]
A field experiment study on the convective heat transfer coefficient on the exterior surface of a building.
Trans. ASHRAE, Vol. 78, pp. 184-191.

Jakob, M. and Kerzios, S.P. [1950]
Defrosting and ice prevention.
Final report 1950, Illionois Inst. of Tech.
Contract No. W33-038ac-16808.
Illinois, USA.

Jenson, M. [1958]
The model-law for phenomena in natural wind.
Ingenioren - International Edition Vol. 2, No. 4, pp. 121-128.

Johnson, H.A. and Rubensin, M.W. [1949]
Aerodynamic heating and convective heat transfer - a summary of literature survey.
Trans. ASME, Vol. 71, pp. 447-456.

Jurges, W. [1924]
Der wormeubergang on einer ebenen Wand
(Heat transfer at a plane wall)
Beih 2, Gesundh-Ing, Series I, Vol. 19.

Kelnhofer, W.J. and Thomas, C.J. [1976]
External convection heat transfer coefficients on a building model.
ASME Paper No. 76-WA/FE-30
ASME Annual winter meeting (1976).

Kestin, J., Maeder, P.F. and Wang, H.E. [1961]
Influence of turbulence on the transfer of heat from plates with and without a pressure gradient.
Int. J. Heat Mass Transfer, Vol. 3, pp. 133-154.

Kind, R.J., Gladstone, D.H. and Moizer, A.D. [1983]
Convective heat losses from flat plate solar collectors in turbulent winds.
J. Solar Energy Engineering, Vol. 105, pp. 80-85.

King, L.V. [1914]
On the convection of heat from small cylinders in a stream of fluid.
Phil. Trans. Royal Society, A214/373.

Klein, S.A. [1975]
Calculation of flat plate collector loss coefficient.
Solar Energy, Vol. 17, pp. 79-80.

Kreith, F. [1976]
Principles of heat transfer, 3rd Edition.
Harper and Row, London.

Lacy, R.E. [1977]
Climate and building in Britain.
HMSO London.

Lee, B.E. [1977]
The simulation of atmospheric boundary layers in the Sheffield University 1.2 x 1.2m boundary layer wind tunnel
Department of Building Science, University of Sheffield - Internal Report No. BS 38.

Lee, B.E. [1982]
Force and Pressure Measurements in Wind Tunnels - A prepared critique.
Proc. Int. Workshop on Wind Tunnel Modelling for Civil Engineering Applications.
US Nat. Bureau of Standards, Washington, USA.

Lee, B.E. and Evans, R.A. [1984]
The measurement of wind flow patterns over building roofs.
Building and Environment, Vol. 19, No. 4, pp. 235-241.

Loudon, A.G. [1965]
In discussion on Lumb [1964]
Quart. J. Roy. Met. Soc. Vol. 90, (386), pp. 439-495.

Lumb, F.E. [1964]
The influence of cloud on hourly total amounts of total solar radiation at the seas surface.
Quart. J. Roy. Met. Soc. Vol. 90, (383), pp. 43-56.

McAdams, W.H. [1954]
Heat transmission, 3rd Edition.
McGraw-Hill, New York.

McCormick, D.C., Test, F.L. and Lessmann, R.C. [1984]
The effect of free-stream turbulence on heat transfer from a rectangular prism.
J. Heat Transfer, Vol. 106, pp. 268-275.

Meinel, A.B. and Meinel, M.P. [1976]
Applied Solar Energy.
Prentice-Hall, New York.

Nicol, K. [1977]
The energy balance of an exterior window surface, Inuvick, N.W.T., Canada.
Building and Environment, Vol. 12, pp. 215-219.

Nicholls, P. [1924]
Measuring heat transmission in building structures and a heat transmission meter.
Trans. ASHVE, Vol. 30, pp. 65-104.

Norris, D.J. [1974]
Calibration of Pyranometers in inclined and inverted positions.
Solar Energy, Vol. 16, p. 53.

Oka, T., Sato, A., Ito, N. and Kimura, K. [1967]
Construction and characteristics of an apparatus for measurement of exterior heat transfer rate.
Trans. Architectural Inst. Japan. Paper No. 3037, p. 521.

Oka, T. and Kon, N. [1974]
Heat transfer in the separated and reattached flow on a blunt flat plate.
J. Heat Transfer, Nov. Issue, pp. 459-462.

Oka, T. and Itasaka, M. [1976]
A separated and reattached flow on a blunt flat plate.
J. Fluids Engineering, March Issue, pp. 79-86.

Oka, T. and Kon, N. [1979]
heat transfer in the separated and reattached flow over blunt flat plates - effect of nose shape.
Int. J. Heat Mass Transfer, Vol. 22, pp. 197-206.

Oliphant, M.V. [1980]
Measurement of wind speed distributions across a solar collector.
Solar Energy, Vol. 24, p. 403.

Ower, E. and Pankhurst, R.C. [1977]
The measurement of air flow.
Pergamon Press, Oxford, England.

Parmelee, G.W. and Heubscher, R.G. [1946]
Forced convection heat transfer coefficients along a flat surface.
Heating Piping and Air Conditioning - ASHVE Journal, May Issue, pp. 112-116.

Parmelee, G.W. and Huebscher, R.G. [1947]
Forced convection heat transfer from flat surfaces - smooth surfaces.
Trans. ASHVE, Vol. 53, pp. 245-284.

Penwarden, A.D. and Wise, A.F.E [1975]
Wind environment around buildings.
BRE Report, C1/SfB 9 (E7). Department of the Environment - HMSO, London, England.

Pohlhausen, E. [1921]
Der warmeaustaugh zurischen festen korpern und flussig - keiten mit kleiner keibung un kleiner warmeleitung.
Zeitscher fur Angew. Math. und Mech., Vol. 1, p. 115.

Ramsey, J.W. and Charmchi, M. [1980]
Variances in solar collector performance predictions due to different methods of evaluating wind heat transfer coefficients.
J. Heat Transfer, Vol. 102, pp. 766-768.

Reynolds, O. [1874]
On the extent and action of the heating surface for steam boilers.
Proc. Manchester Lit. Phil. Soc., Vol. 14, pp. 7-12.

Reynolds, W.C., Kays, W.M. and Kline, S.J. [1958(a)]
Heat transfer in turbulent incompressible boundary layer.
I, Constant wall temperature.
NASA Memorandum 12-1-58W, Washington, USA.

Reynolds, W.C., Kays, W.M. and Kline, S.J. [1958(b)]
Heat transfer in turbulent incompressible boundary layer.
II, Step wall-temperature distribution
NASA Memorandum 12-2-58W, Washington, USA.

Reynolds, W.C., Kays, W.M. and Kline, S.J. [1958(c)]
Heat transfer in turbulent incompressible boundary layer.
III, Arbitary wall temperature and heat flux.
NASA Memorandum 12-3-58W, Washington, USA.

Rowley, F.B., Algren, A.B. and Blackshaw, J.L. [1930(a)]
Effects of air velocities on surface coefficients.
Transactions ASHVE, Vol. 36, pp. 123-136.

Rowley, F.B., Algren, A.B. and Blackshaw, J.L. [1930(b)]
Surface conductances as affected by air velocity temperature and character of surface.
Transactions ASHVE, Vol. 36, pp. 429-446.

Rowley, F.B. and Eckley, W.A. [1932]
Surface coefficients as affected by direction of wind.
Trans. ASHVE Vol. 38, pp. 33-45.

Sam, R.G., Lessmann, R.C. and Test, F.L. [1979]
An experimental study of flow over a rectangular body.
J. Fluids Engineering, Dec. Issue, pp. 443-448.

Sharples, S. [1981]
Forced convective heat transfer from building facades.
Department of Building Science, University of Sheffield.
Ph.D. Thesis.

Sharples, S. [1984]
Full-scale measurements of convective energy losses from exterior building surfaces.
Building and Environment, Vol. 19, No. 1, pp. 31-39.

Smith, F.B. [1970]
The profile of shearing stress in the boundary layer of the atmosphere.
Unpublished note. Met. Office.

Sogin, H.H. and Providence, R.I. [1958]
Sublimation from discs to air streams flowing normal to their surfaces.
Trans. ASME. Jan. issue, pp. 61-69.

Sparrow, E.M. and Tien, K.K. [1971]
Forced convection heat transfer at an inclined and yawed square plate - Application to solar collectors.
J. Heat Transfer, Vol. 99, pp. 507-512.

Sparrow, E.M., Ramsey, J.W. and Mass, E.A. [1979]
Effect of finite width on heat transfer and fluid flow about an inclined rectangular plate.
Journal of Heat Transfer, Vol. 101, pp. 199-204.

Sparrow, E.M. and Lau, S.C. [1981(a)]
Effect of adiabatic co-planar extension surfaces on wind related solar collector heat transfer coefficients.
J. Heat Transfer, Vol. 103, pp. 268-271.

Sparrow, E.M., Somie, F. and Lau, S.C. [1981(b)]
Heat transfer from a plate elevated above a host surface and washed by a separated flow induced by an elevation step.
J. Heat Transfer, Vol. 103, pp. 441-447.

Sparrow, E.M., Nelson, J.S. and Tao, W.Q. [1982]
Effect of leeward orientation, adiabatic framing surfaces, and eaves on solar collector related heat transfer coefficients.
Solar Energy, Vol. 29, No. 1, pp. 33-41.

Streed, E.R. and Waksman, D. [1981]
Uncertainty in determining the thermal performance of liquid heating flat-plate solar collectors.
J. Solar Energy Engineering, Vol. 103, pp. 126-134.

Sturrock, N.S. [1971]
Localised boundary layer heat transfer form external building surfaces.
University of Liverpool, Ph.D. Thesis.

Sugawara, S., Sato, T. Komatsu, H. and Osaka, H. [1958]
The effect of free-stream turbulence on heat transfer from a flat plate.
N.A.C.A. Tech. Memo. No. 1441.

Surridge, A.D. [1982]
On the measurement of atmospheric winds.
Boundary Layer Meteorology, Vol. 24, pp. 421-428.

Swinbank, W.C. [1963]
Longwave radiation from clear skies.
Quart. J. Roy. Met Soc., Vol. 89, pp. 339-348.

Szokolay, S.V. [1975]
Solar energy and building.
The Architectural Press, London, 1975.

Test, F.L. and Lessmann, R.C. [1980]
An experimental study of heat transfer during forced convection over a rectangular body.
J. Heat Transfer, Vol. 102, pp. 146-151

Test, F.L., Lessman, R.C. and Johary, A. [1981]
Heat transfer during wind flow over rectangular bodies in the natural environment.
J. Heat Transfer, Vol. 103, pp. 262-267.

Von Karman, T. [1939]
The analogy between fluid friction and heat transfer.
Trans. ASME, Vol. 61, pp. 705-710.

Wang, X.A. [1982]
An experimental study of mixed forced and free convection heat transfer from a flat plate to air.
J. Heat Transfer, Vol. 104, pp. 139-144.

Watmuff, J.H., Charters, W.W.S. and Proctor, D. [1977]
Solar and wind induced external coefficients for solar collectors.
Comples - International Review D'Helio Technique, Vol. 2, p. 56.

Wozniak, S.J. [1979]
Solar heating systems for the UK: design, installation and economic aspects.
Department of the Environment, HMSO, 1979.